How to find a geothermal reservoir

temperature focus – some stress

(modelling and geophysical techniques)

GEOPHYSICAL EXPLORATION

Geophysics provides an undirect evidence (an “image”) of certain features of the underground, like bio-medical images

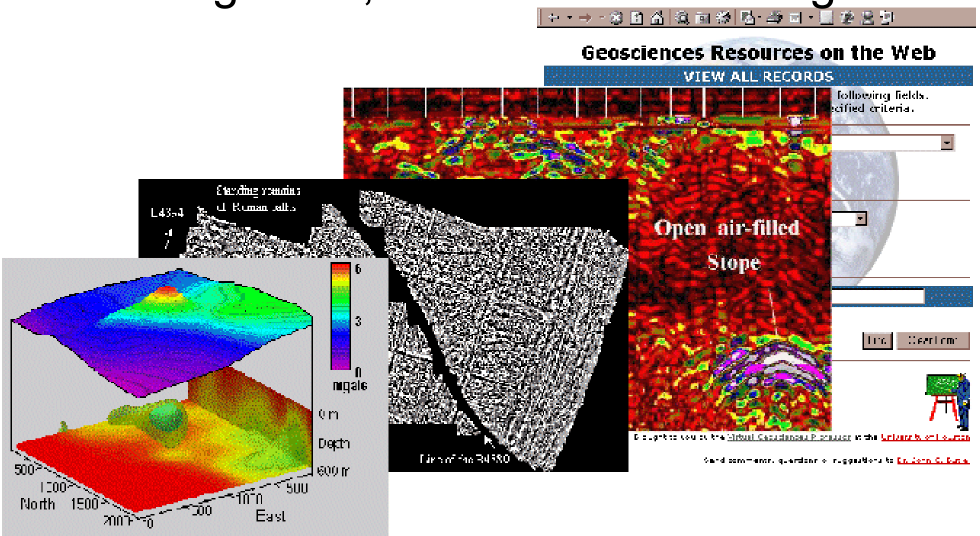

This is obtained by measuring the response of the medium under investigation to the passage of a certain “energy field”:

natural → passive tests or artificially induced → active tests

GEOPHYSICAL EXPLORATION

It is not wise to define a particular sequence of geophysical surveys as being applicable to all potential reservoirs:

Degree to which the measured property is related to the property of interest.

PHYSICAL PROPERTY

TARGET

	Density	Magnetic Susceptibility	Electrical Resistivity	Dielectric Permittivity	Seismic Velocity
Porosity (pore,fracture)	strong	none	strong	moderate	moderate
Permeability	none	none	weak	weak	weak
Water content	moderate	none	strong	strong	moderate
Oil content	moderate	none	strong	strong	moderate
Water quality	none	none	strong	none	none
Clay content	weak	none	strong	weak	moderate
Magnetic mineral content	moderate	strong	weak	none	none
Metallic mineral content	strong	none	strong	none	moderate
Metallic object	strong	strong	strong	none	moderate
Mechanical properties	moderate	none	moderate	weak	strong
Subsurface structure	moderate	moderate	moderate	strong	strong

strong	moderate	weak	none

Degree of relationship

GEOPHYSICAL EXPLORATION

A geothermal system generally causes inhomogeneities in the physical properties of the subsurface, which can be observed to varying degrees as anomalies measurable from the surface.

Changing physical parameters:

temperature (*heat flow survey*)

electrical conductivity (*electrical and electromagnetic survey*)

elastic properties influencing the propagation velocity of elastic waves (*seismic survey*)

density (*gravity survey*)

magnetic susceptibility (*magnetic survey*).

Content

- Geothermal gradients – introduced by Pierre
- Plate tectonics – covered by Pierre
- Convective controls: A closer look at Mantle dynamics
- Conductive controls: Lithosphere composition and differentiation
- Regional and local temperature assessment
  - Conductive (predictable →
    - **Use temperature data and models**
  - vs advective (magmatic, partially predictable)
    - Global (heat flow –tectonic analysis)
    - Local (**geophsyical exploration techniques** probing deeper temperature)

Temperature gradients in the upper crust

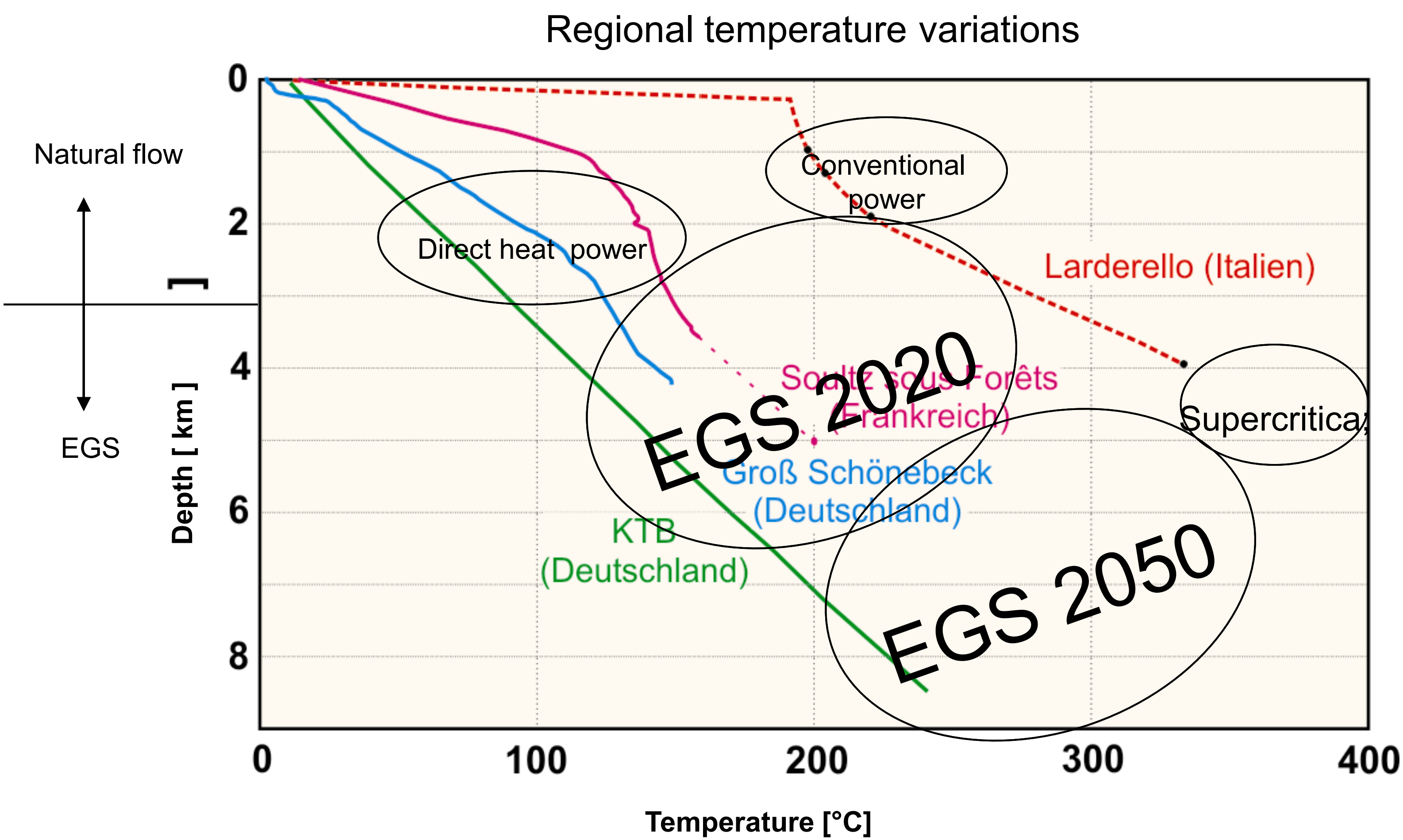

Soultz - Fluid circulation appears to play an important role in enhancing shallow heat flows at the expense of diminishing heat flow at deeper levels

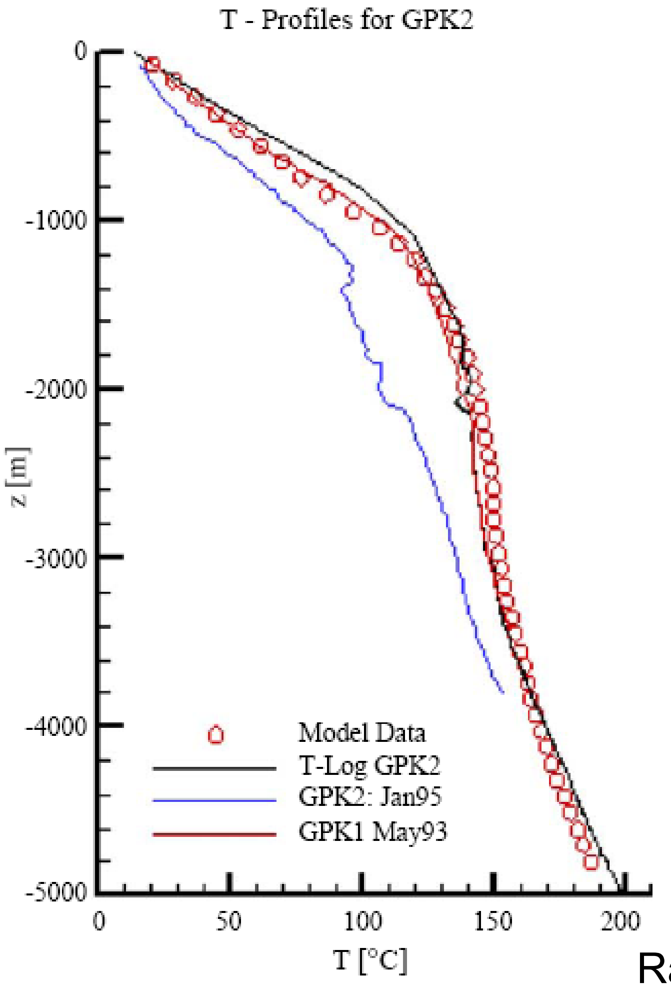

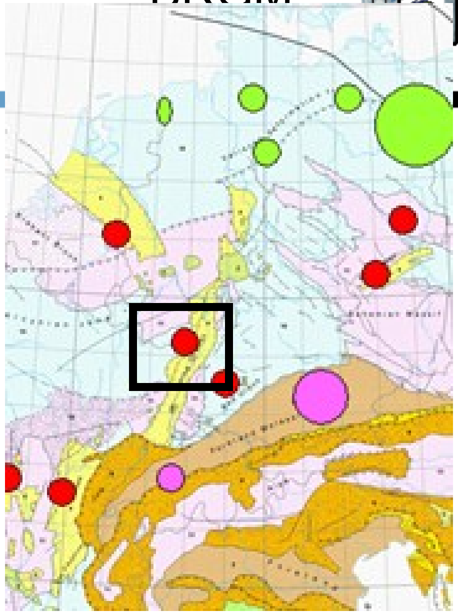

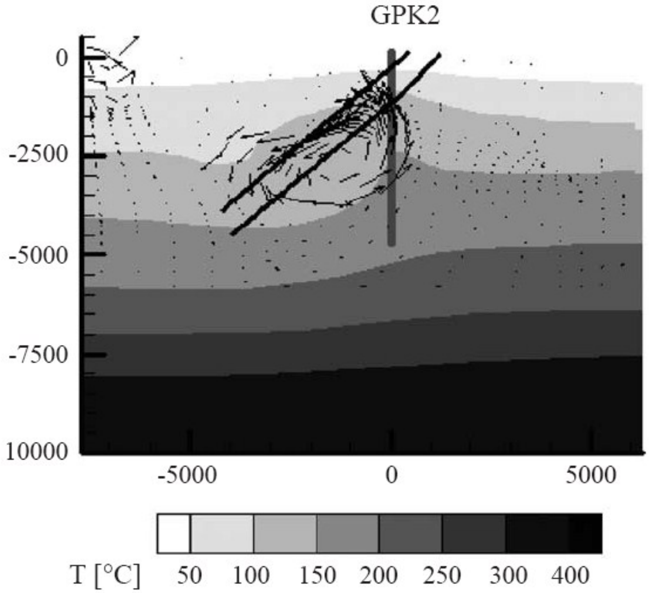

Ranalli and Rybach, 2005

Temperature is reconstructed using a steady state geotherm (conductive approach)

- **Heat flow q** [mW/m^{-2}] is an important boundary condition in basin modeling. It determines the temperature gradient in sediments in conjunction with **rock conductivity k** [$W\ m^{-1}\ C^{-1}$]

$$\frac{dT}{dz} = q / k$$

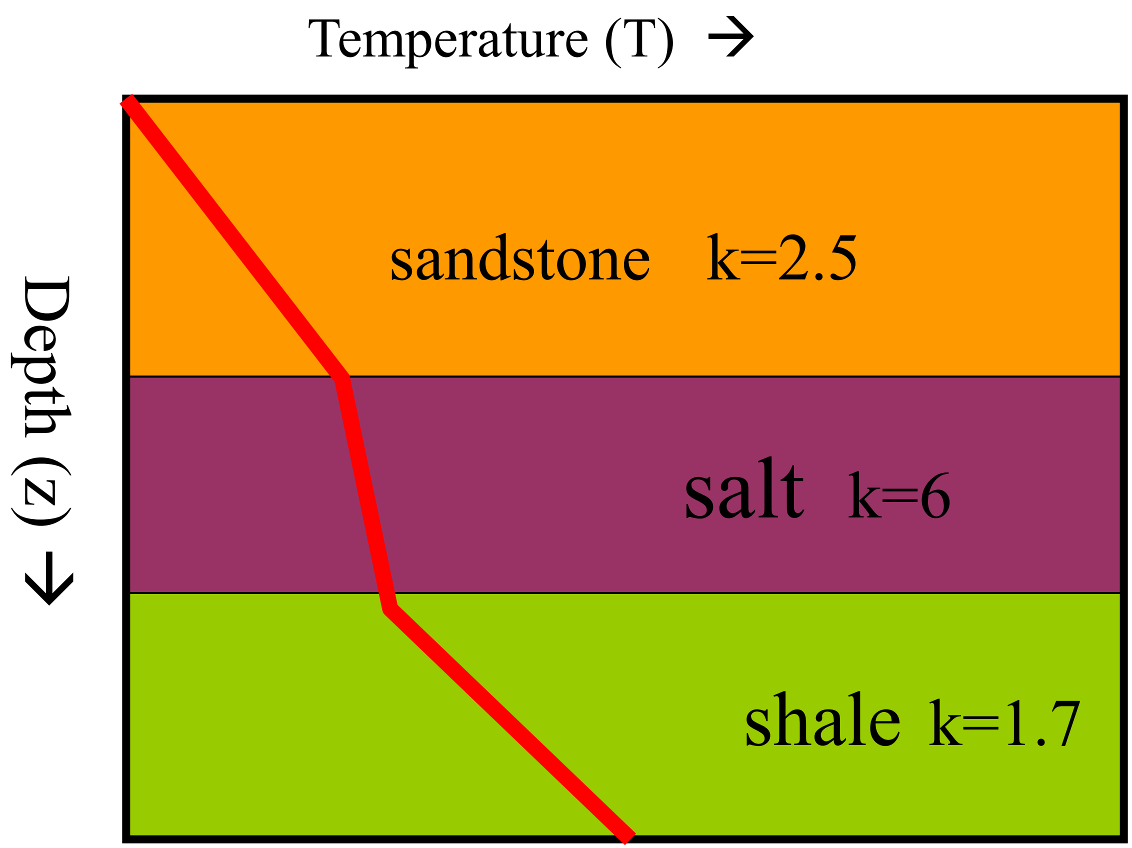

Geotherm
q=60

Heat Flow map of Europe

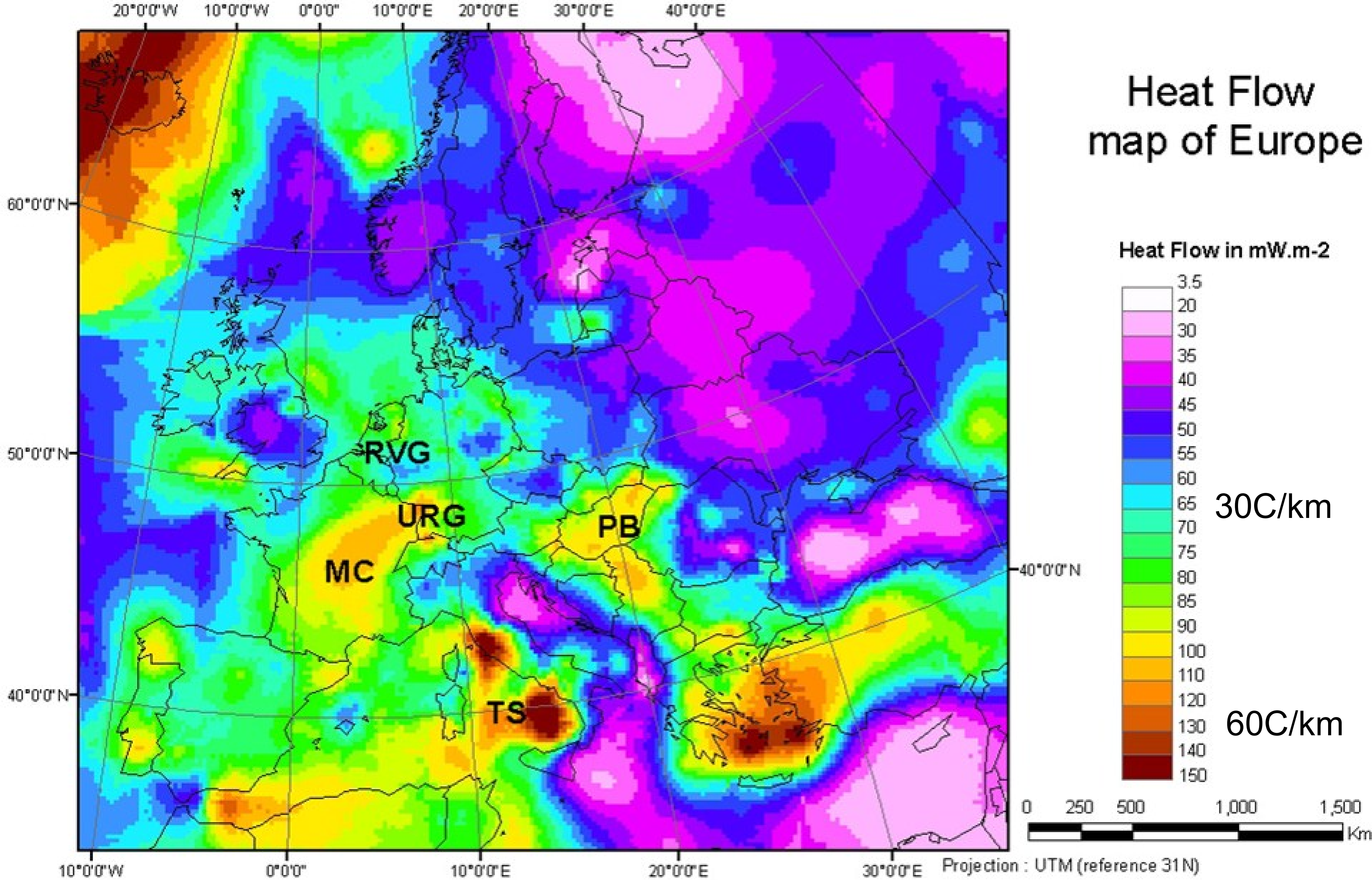

Cloetingh et al., 2010, Earth Science Reviews, in press

Content

- **Convective controls: A closer look at Mantle dynamics**
  - Lithosphere vs astenosphere
  - Cooling plate
  - Not so simple
  - Phase transitions
  - Smaller scale phenomena
- Conductive controls: Lithosphere composition and differentiation

Geotherm and geothermal gradient

Geotherm = temperature as a function of depth

Geothermic gradient = rate of change in temperature with increasing depth

- gradient varies depending on location
- surface gradient is average 20-30 oC/km
- Surface gradient is much higher than in mantle and core

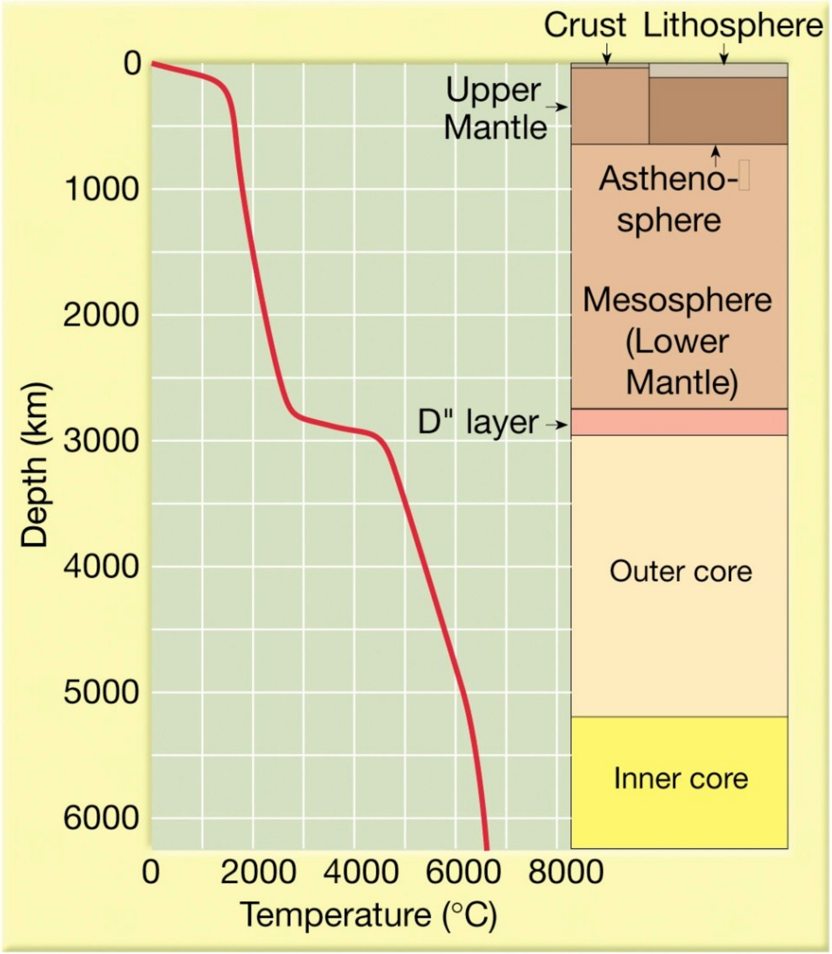

Heat flow at Earth's surface

Continental lithosphere: heat flow is heterogeneous as a consequence of thickness variations, composition and thermal

age

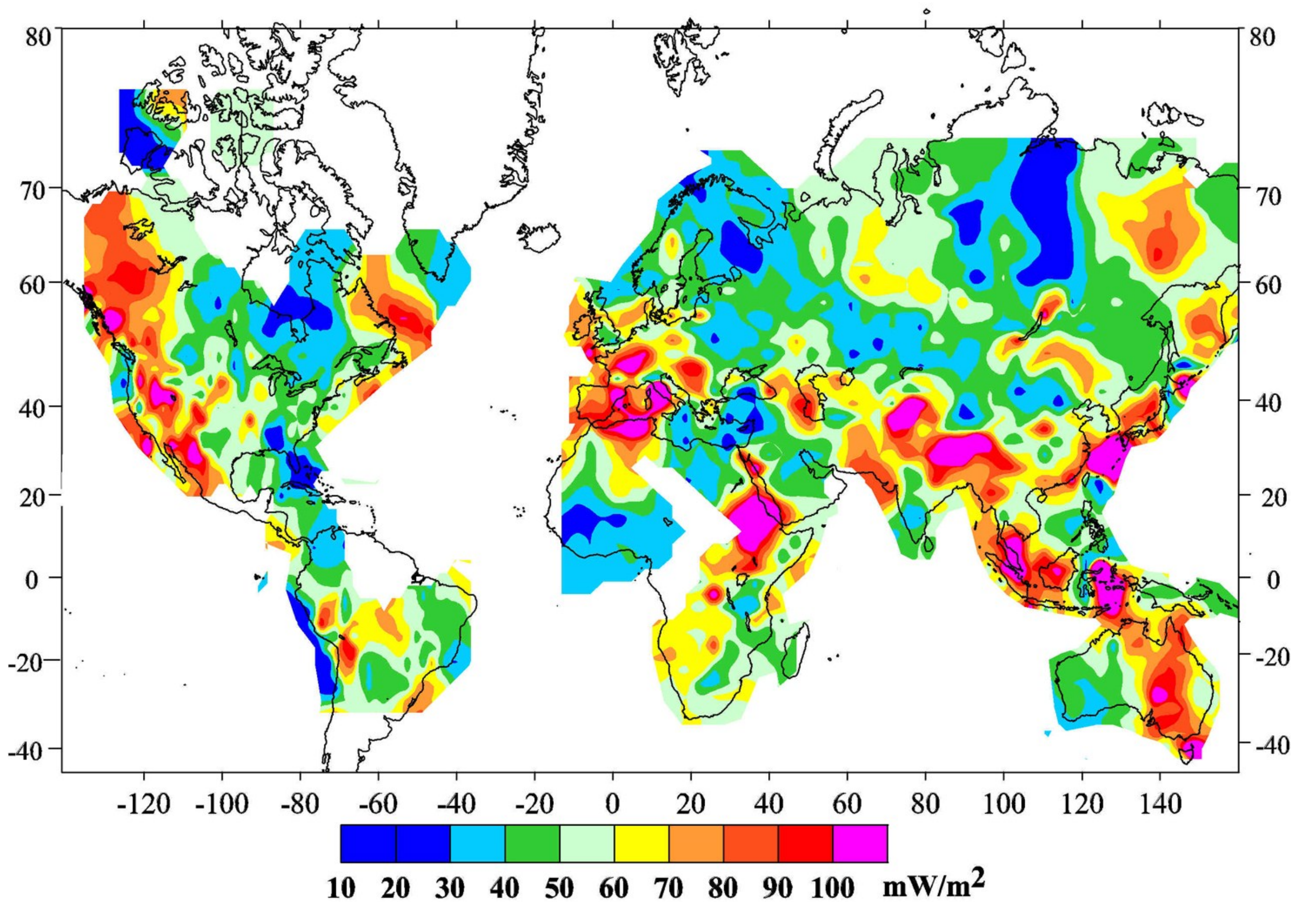

Lithosphere thickness

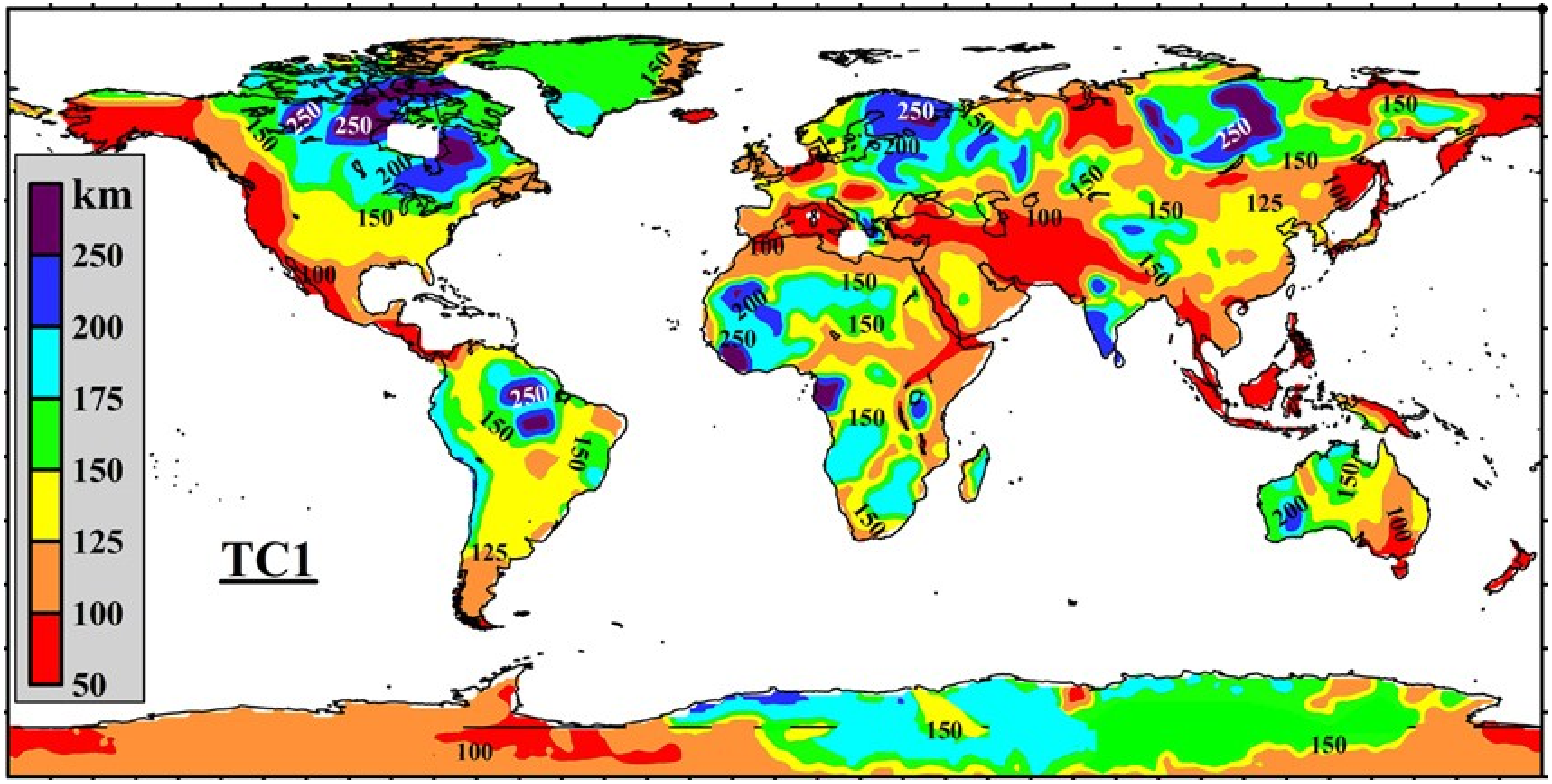

Seismic tomography

Seismic wave velocity is a function of temperature:

- Warm → slower
- Cold → faster

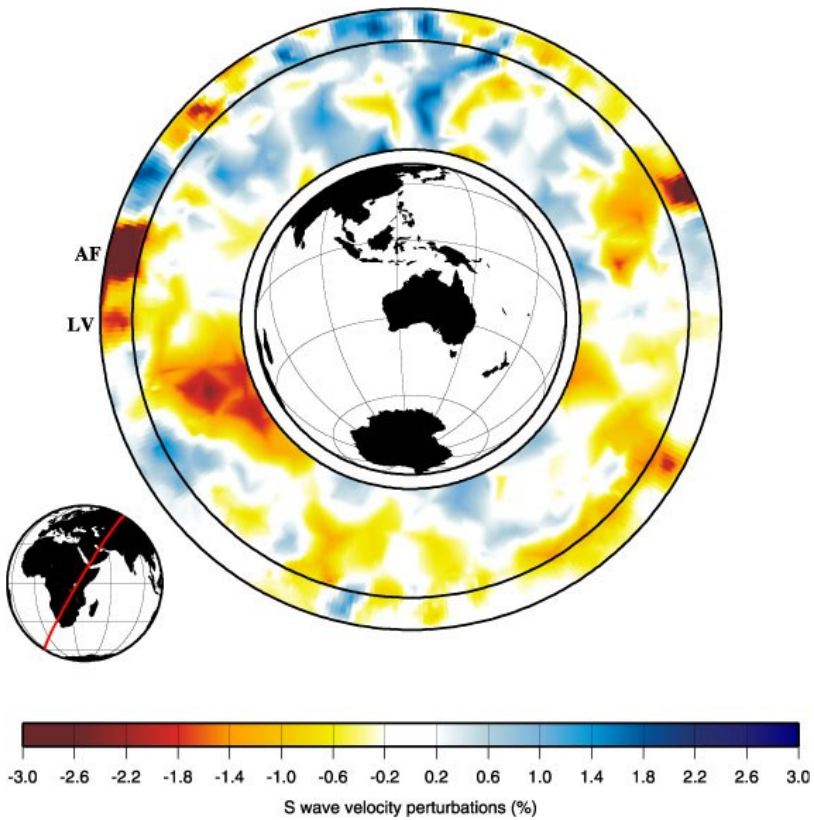

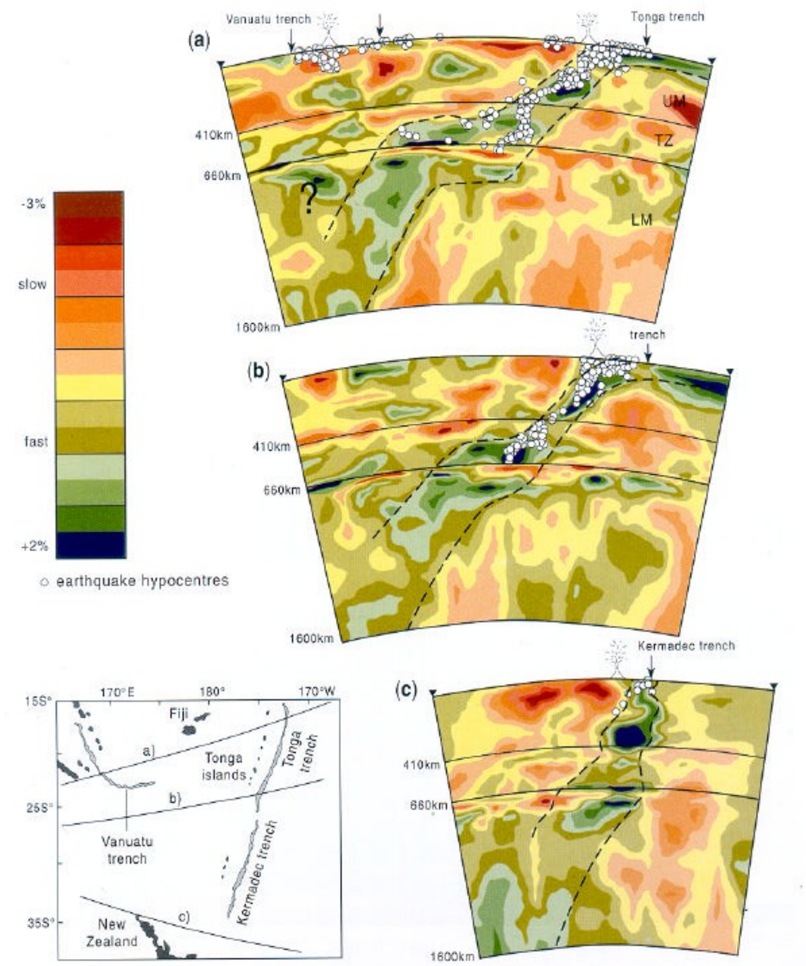

Seismic tomography

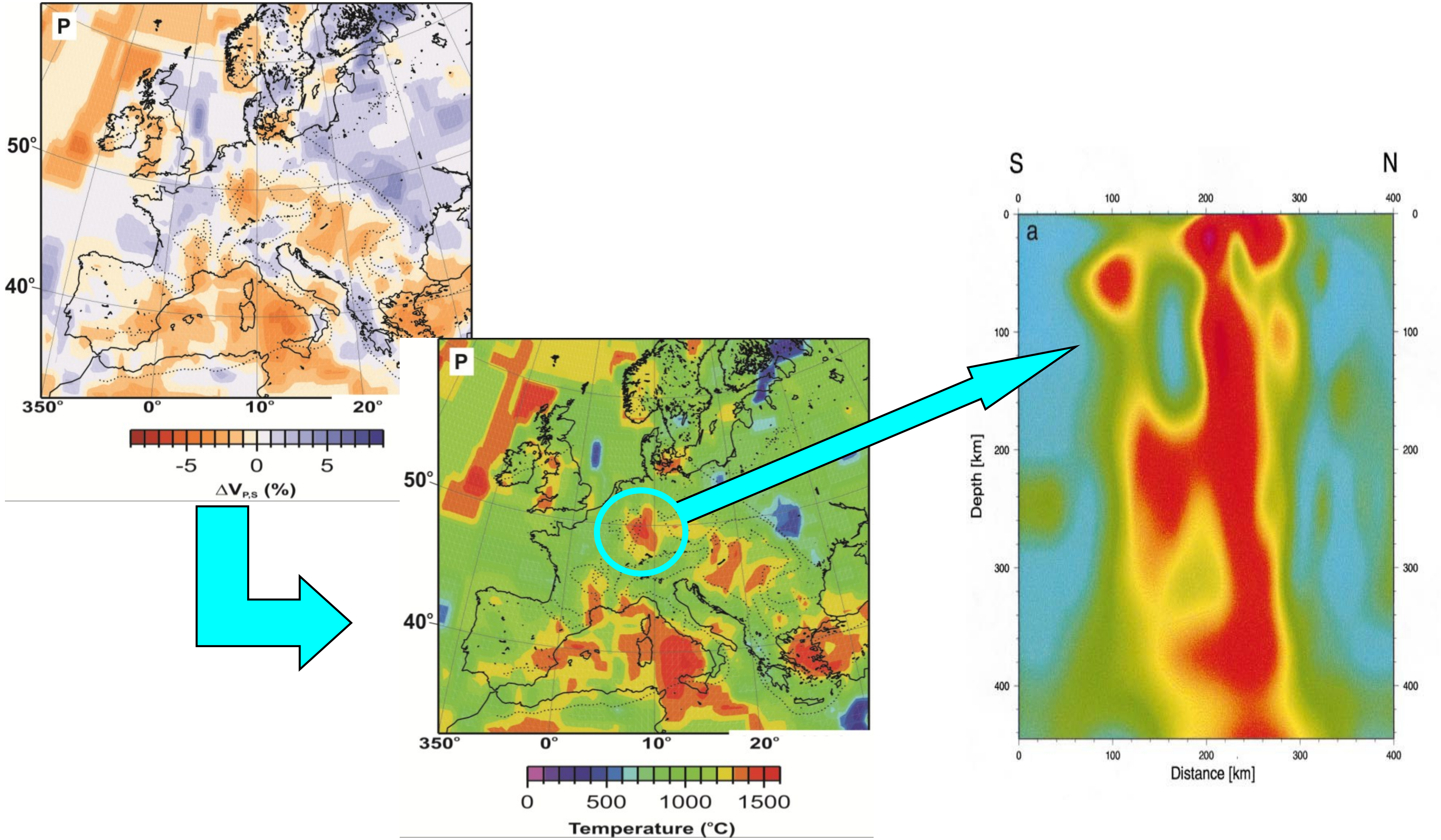

Conclusions

- Strong differentiation in heat flow at base of the lithosphere due to convection/advection
- Can explain heat flow variations to some degree
- Kinematic response at surface convective forcing more

Content

- Geothermal gradients, power-EGS and the conductive earth
- Plate tectonics
- Convective controls: A closer look at Mantle dynamics
- **Conductive controls: Lithosphere composition and differentiation**

Crustal thickness

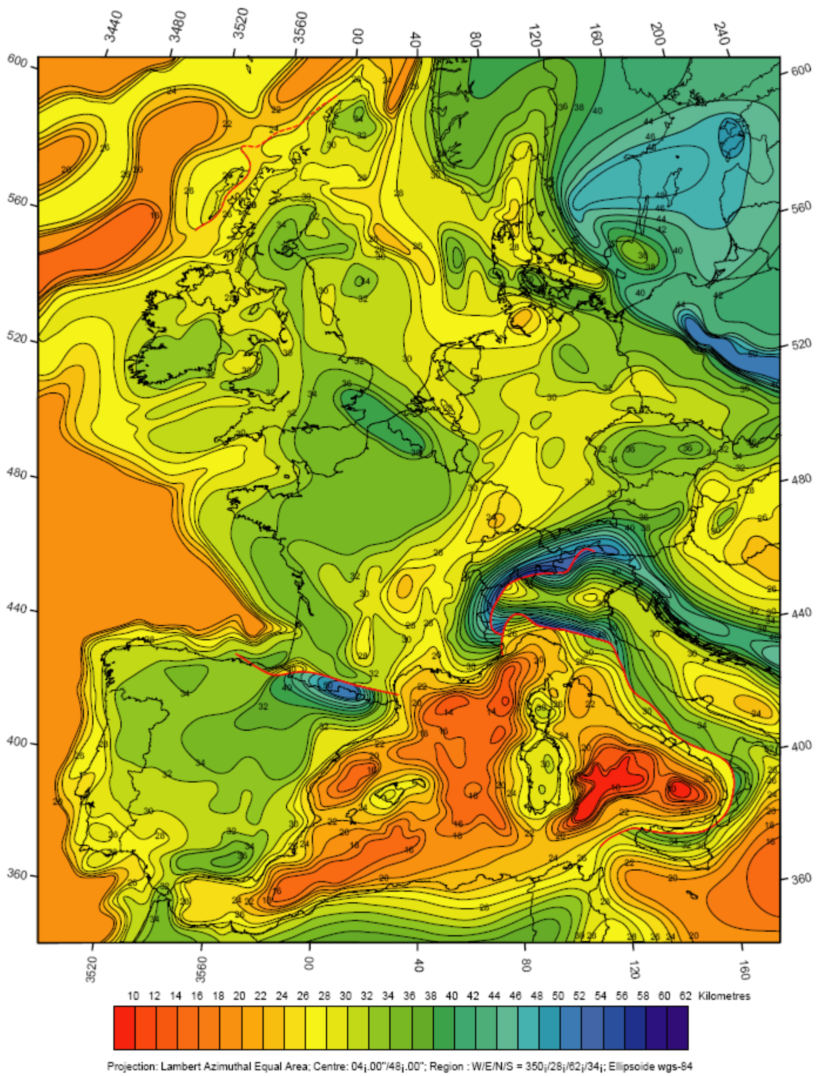

Radiogenic heat generation A **[μW m^3] is a function of relative abundance of radiogenic minerals in rock. It influences the steady state geotherm**

$$\frac{dT}{dz}(z) = q_s / k - Az / k$$

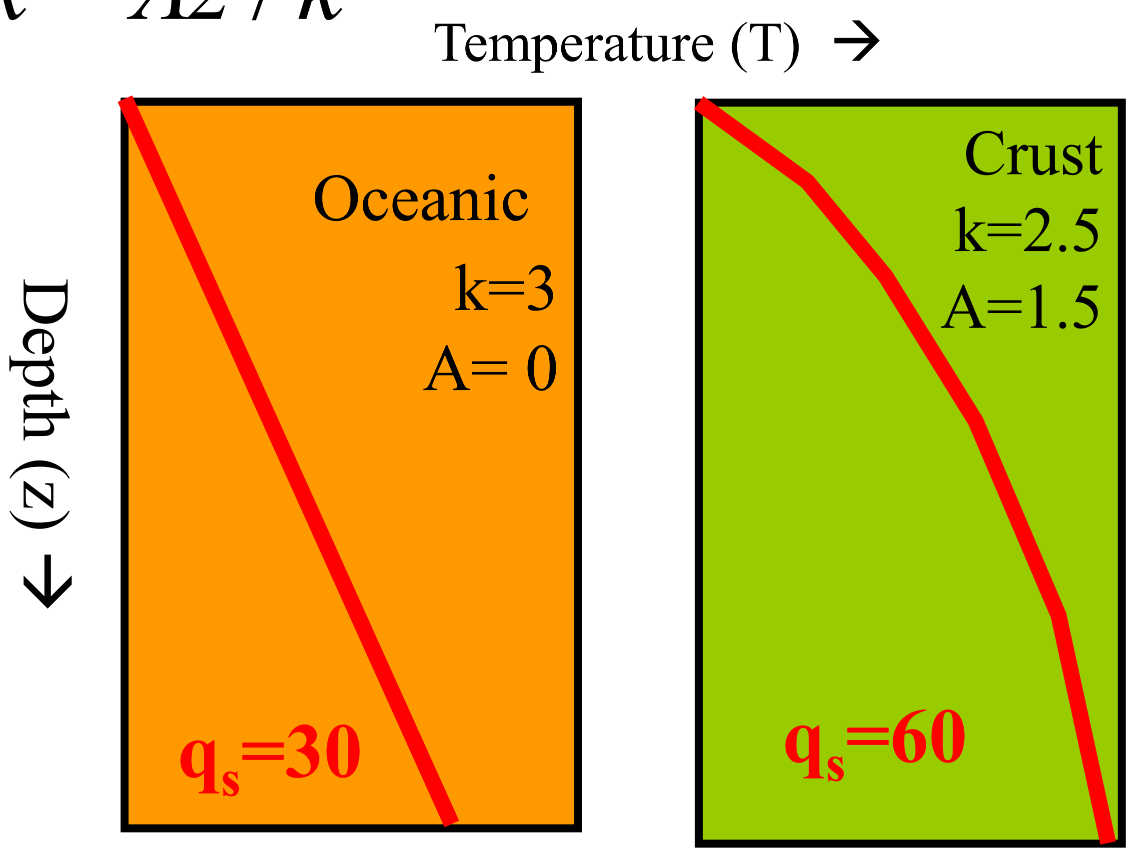

Crustal heat production and geothermal gradients

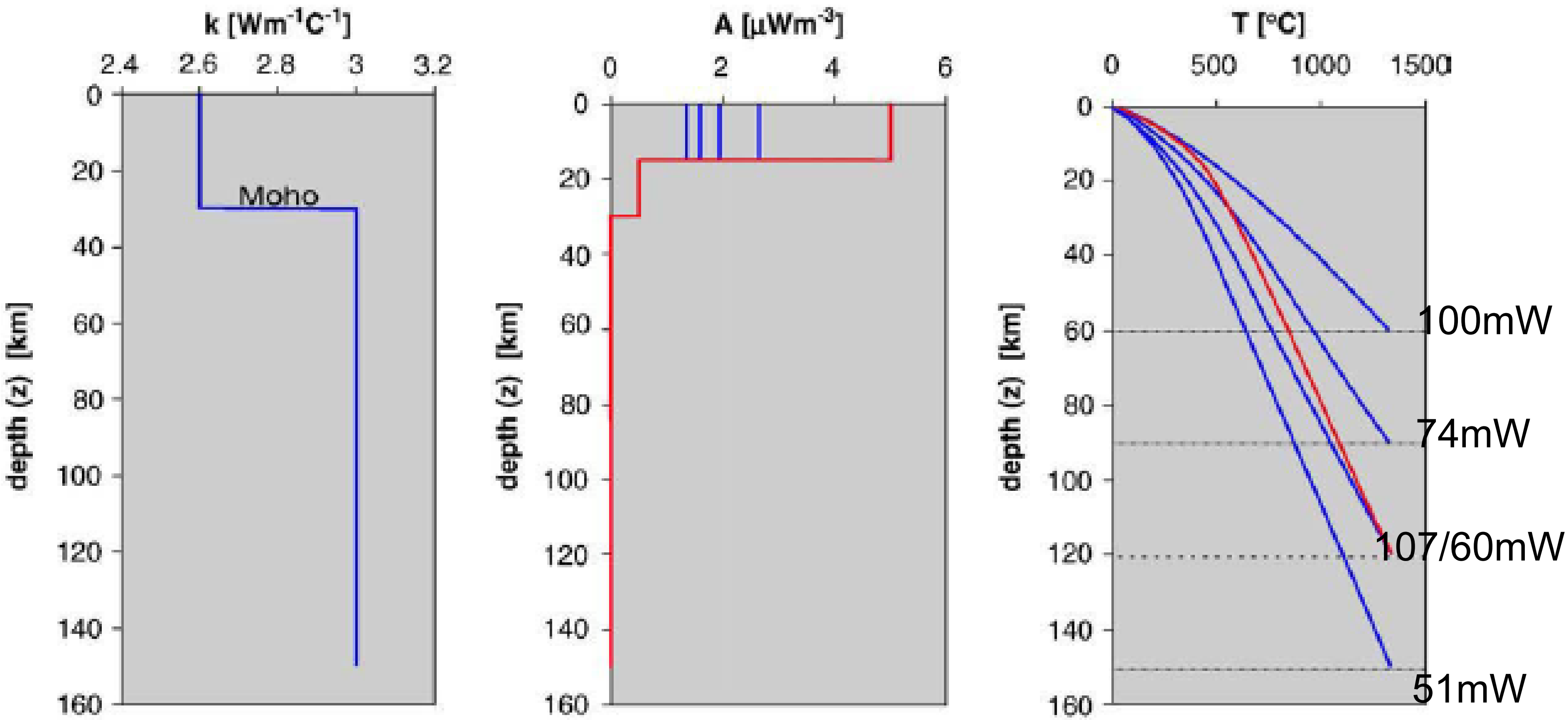

FAULT SYSTEMS

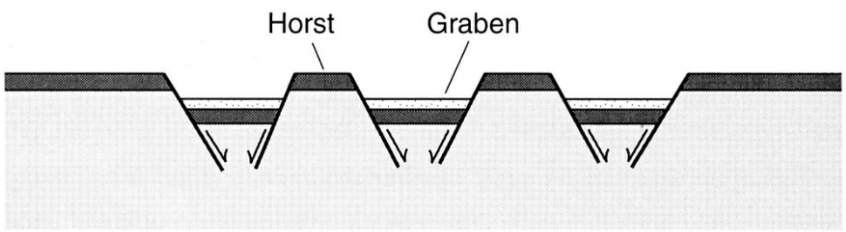

Assemblage of planar faults

Assemblage of listric faults

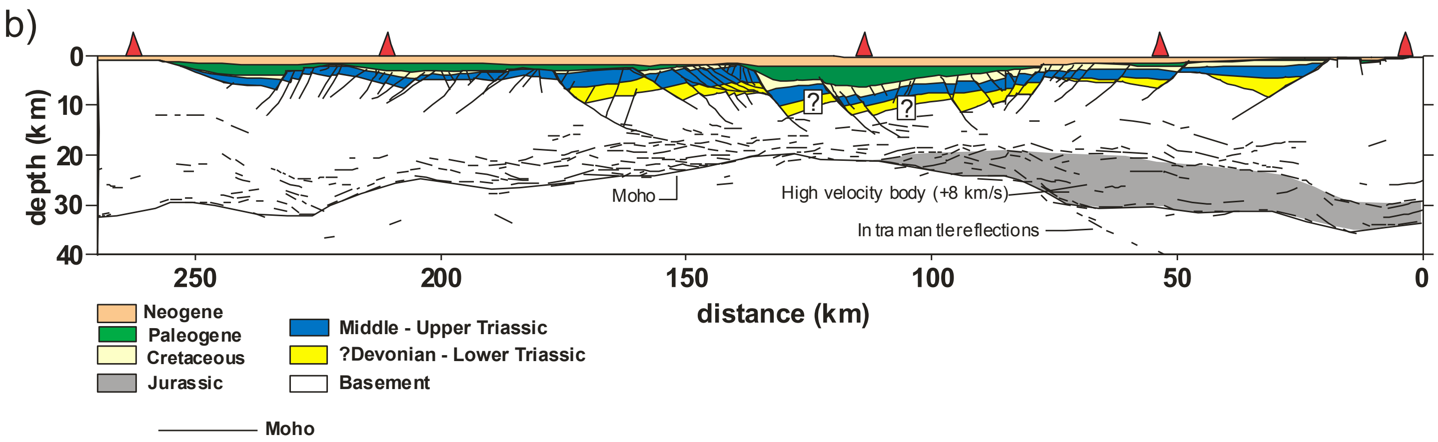

Note: these faults accommodate a pure shear deformation (also called non rotational

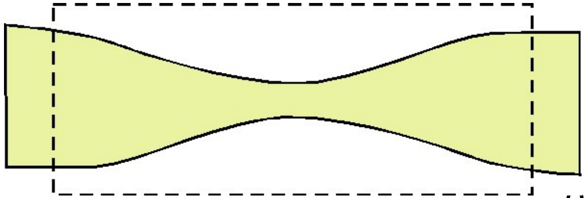

Tectonic Numerical kinematic models predict temperature effects of lithosphere deformation. The 1D McKenzie Model (1978) is a classic for continental lithosphere extension (rifting)

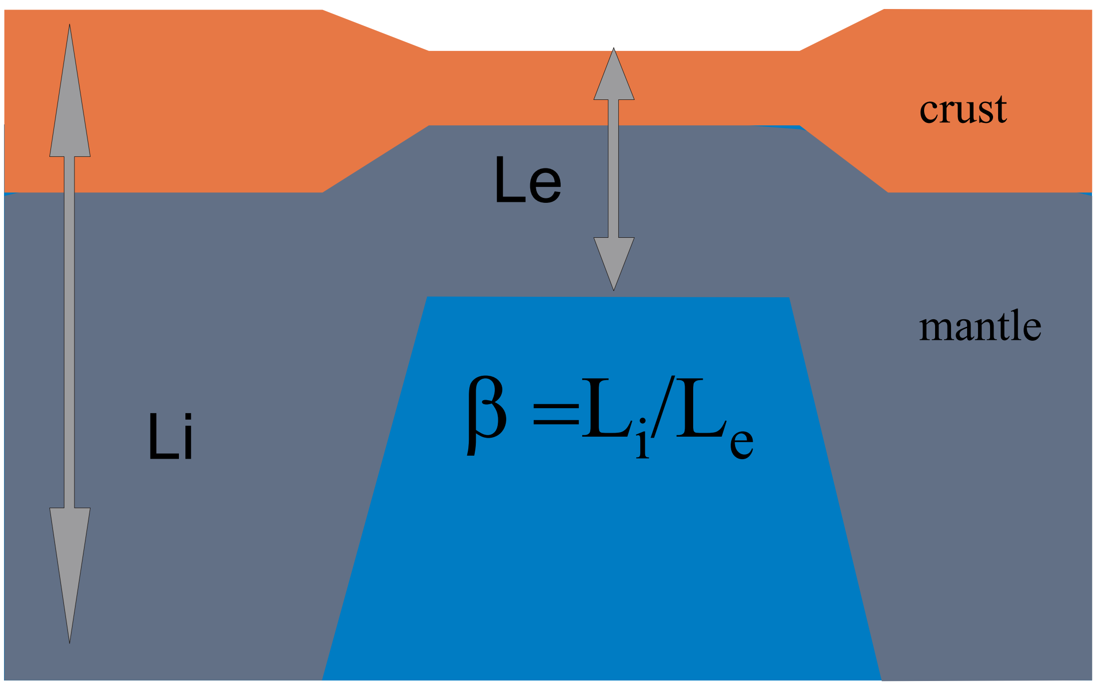

McKenzie model: lithosphere is instantaneously thinned by factor β

Numerical Temperature Model. t=time after rifting Temperature at surface and bottom are fixed (Mckenzie, 1978)

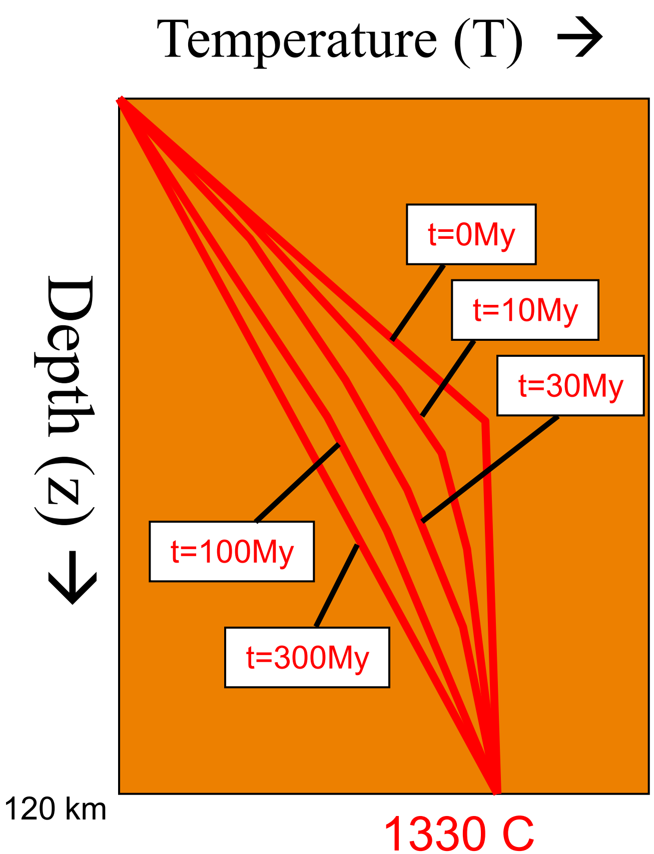

For the McKenzie model a very simple analytical solution for the heat flow exist

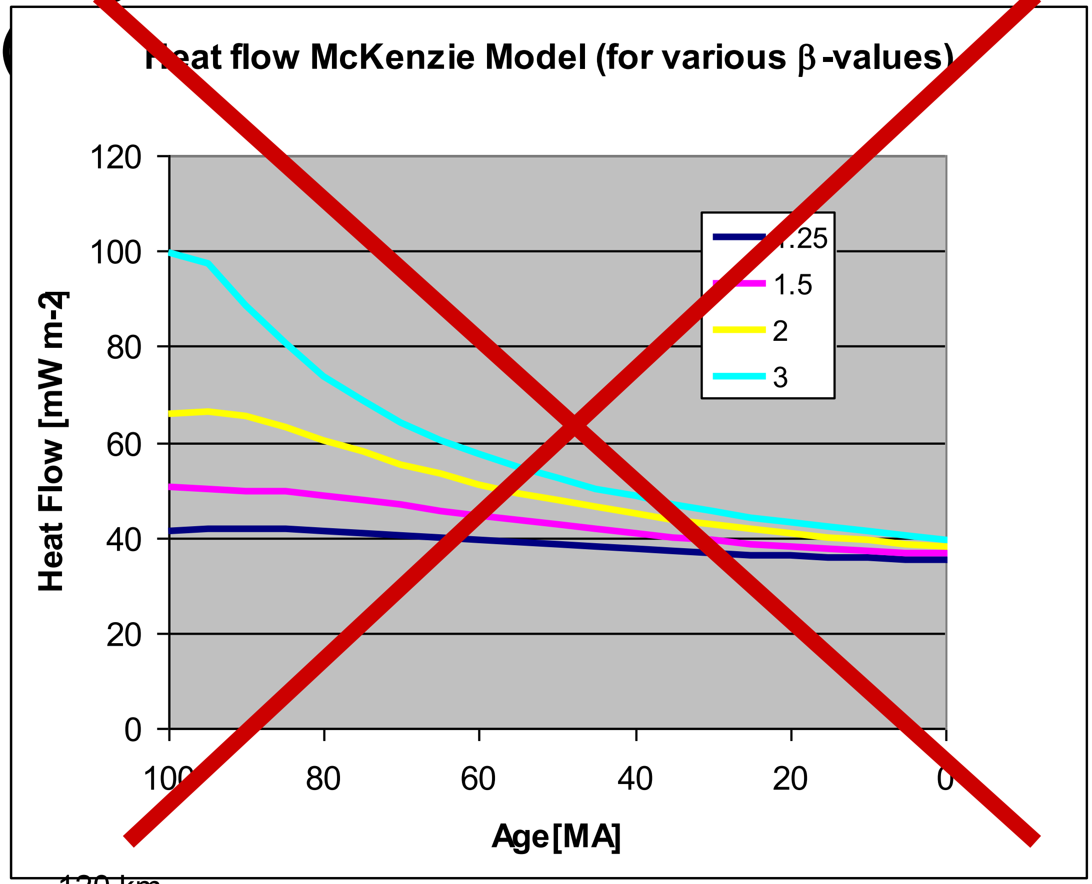

120 km

McKenzie heat flow
No Good:

- No crustal heat production
- No sediment infill

- **Some More on Modelling: heat flow should include sediments→heat flow is lower because of cooling effect of sediment infill.**

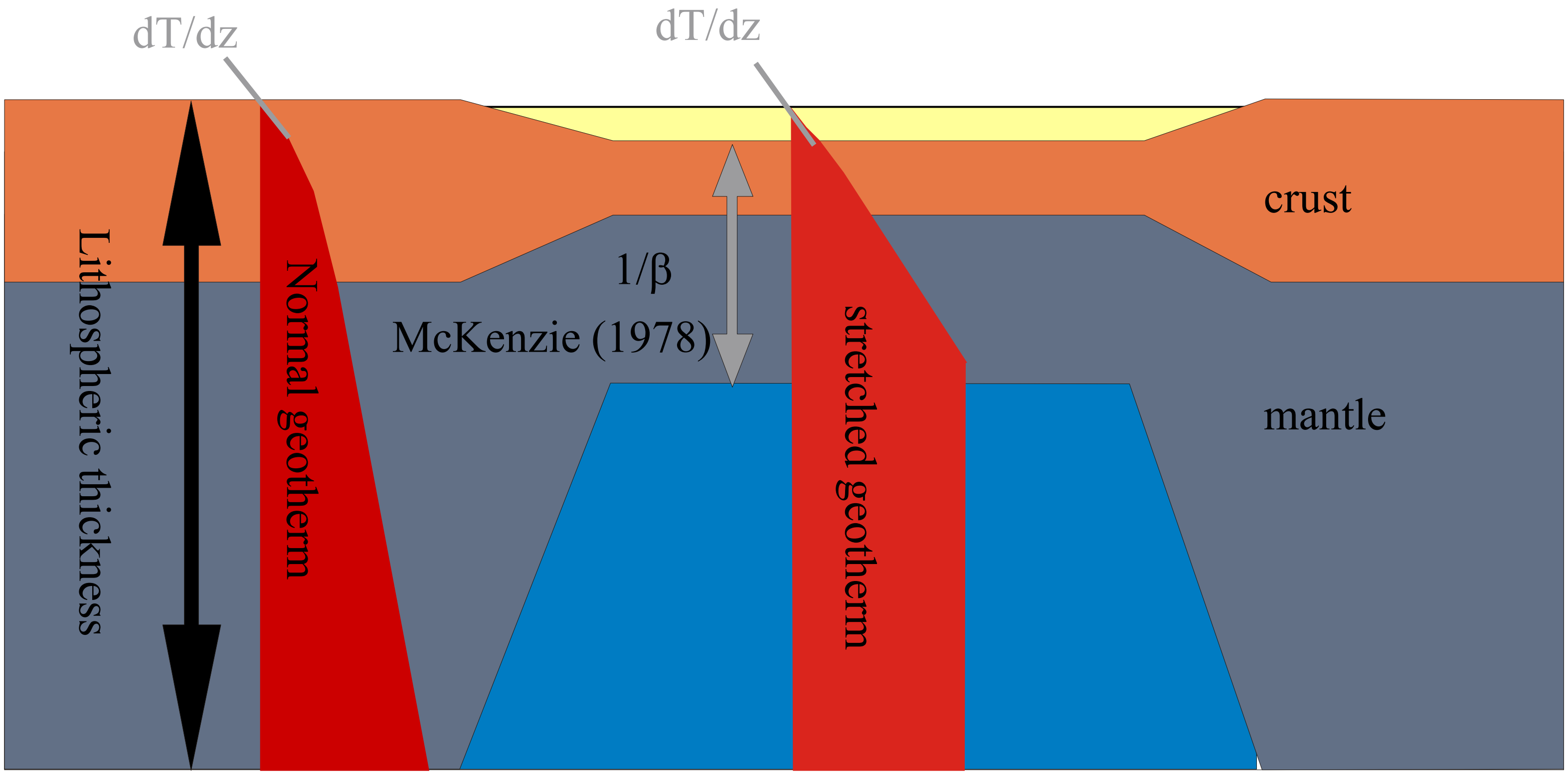

Effects of crustal heat production

- Classis models such as Mckenzie, neglect effects of crustal heat production. Crustal heat production accounts to ca 50% of the surface heat flow, however it diminishes as a result of crustal thinning during extension and is not fully compensated by heat production of sediment replacing crust. The net effect is a reduction of heat flow after extension

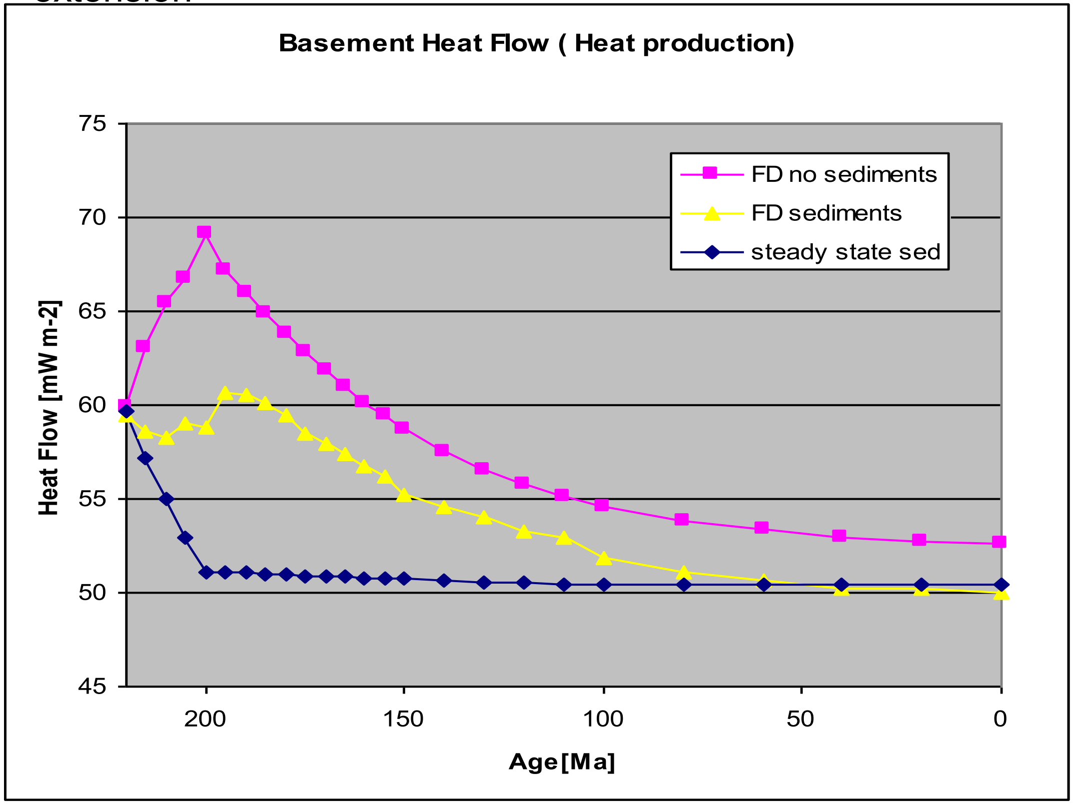

Example for rifting β=1.44 (220-200Ma), with heat production in crust

Sedimentation during rifting is ca 100 m /My, resulting in 15% reduction of basement heat flow.

(from Van Wees et al., 2007)

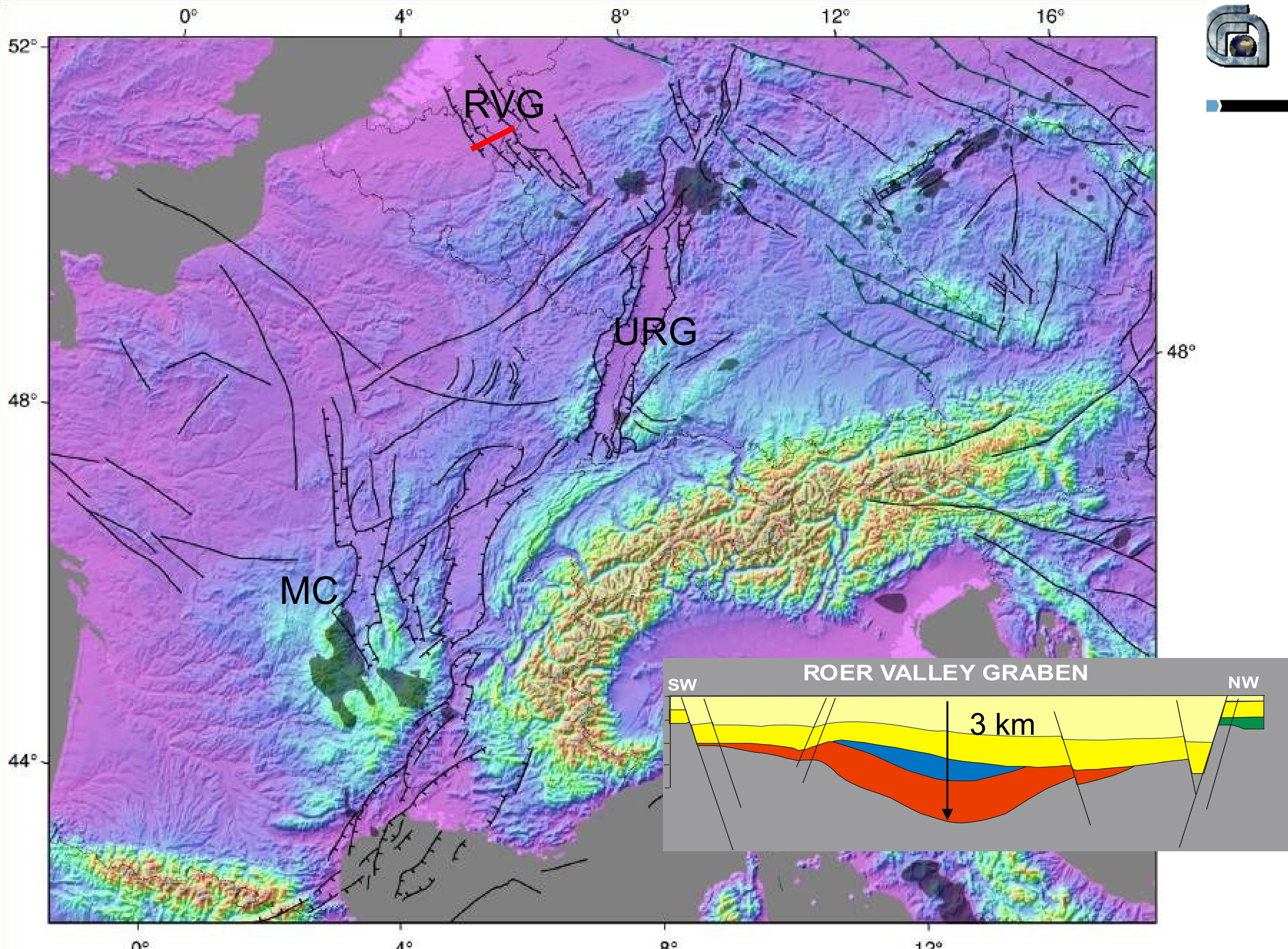

Ziegler and Dezes, 2008

Heat Flow map of Europe

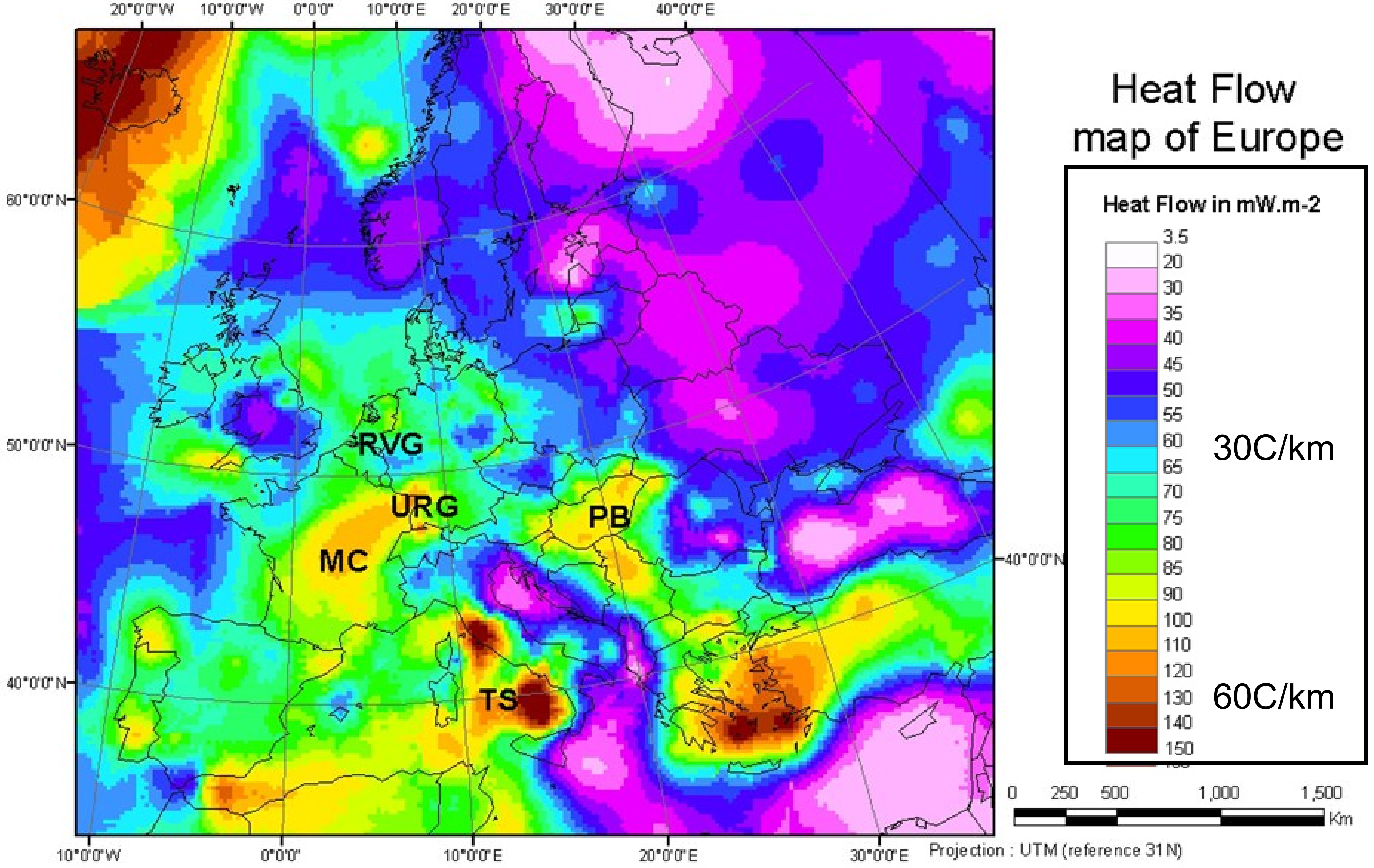

Supported by INTELLIGENT ENERGY

BRGM

TNO innovation for life

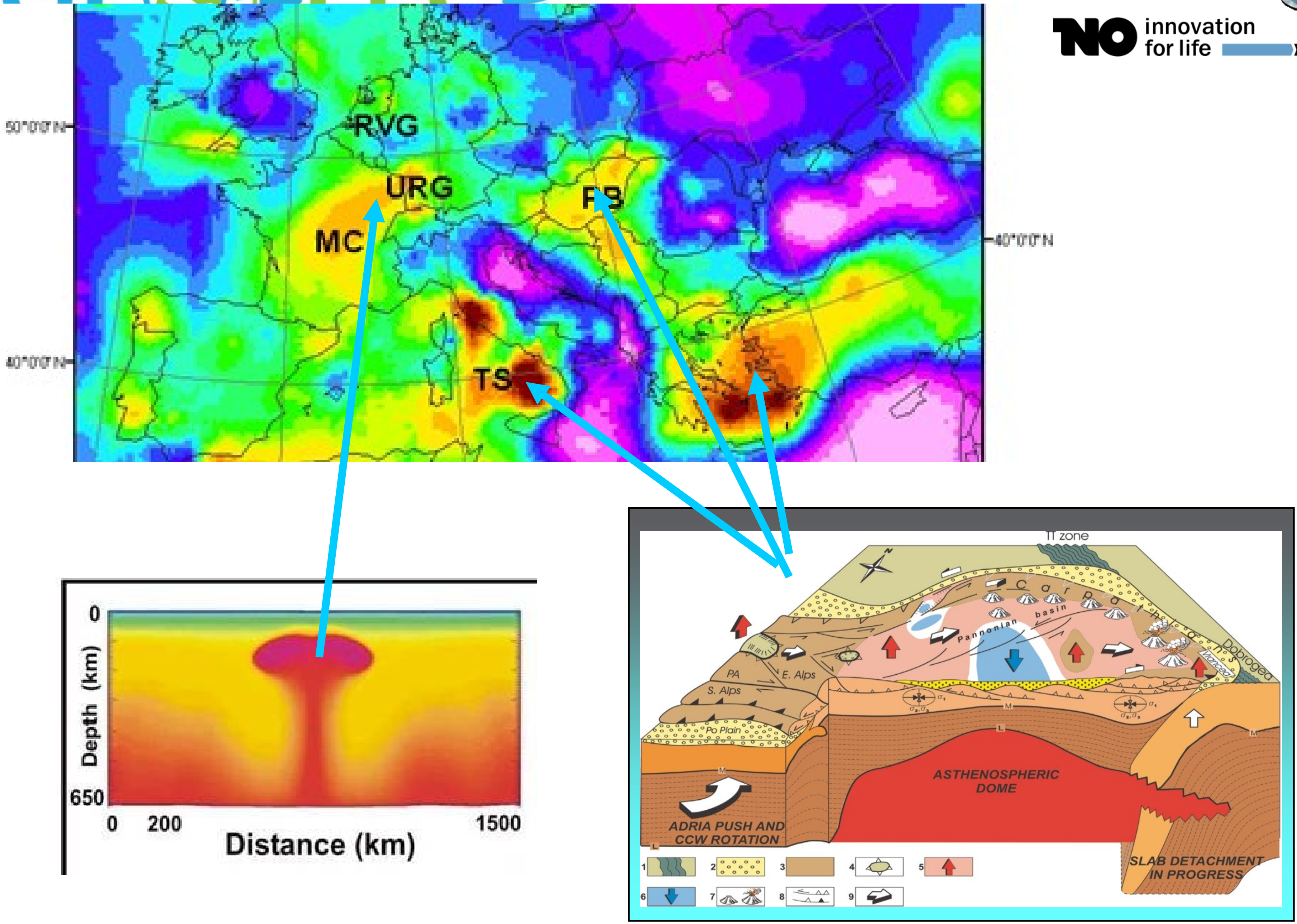

Cloetingh et al., 2006

Supported by INTELLIGENT ENERGY EUROPE

BRGM

Panonian Basin

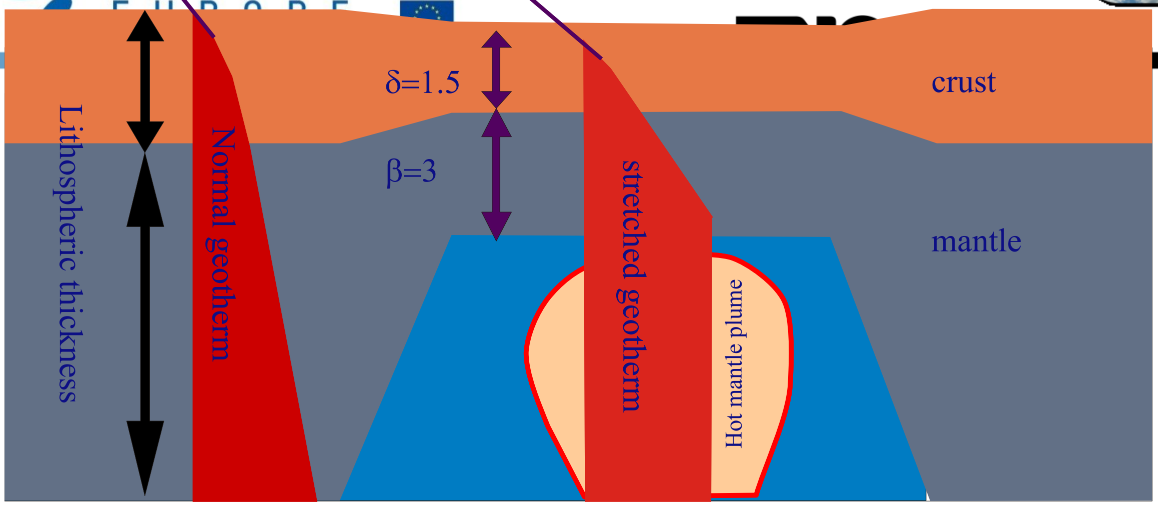

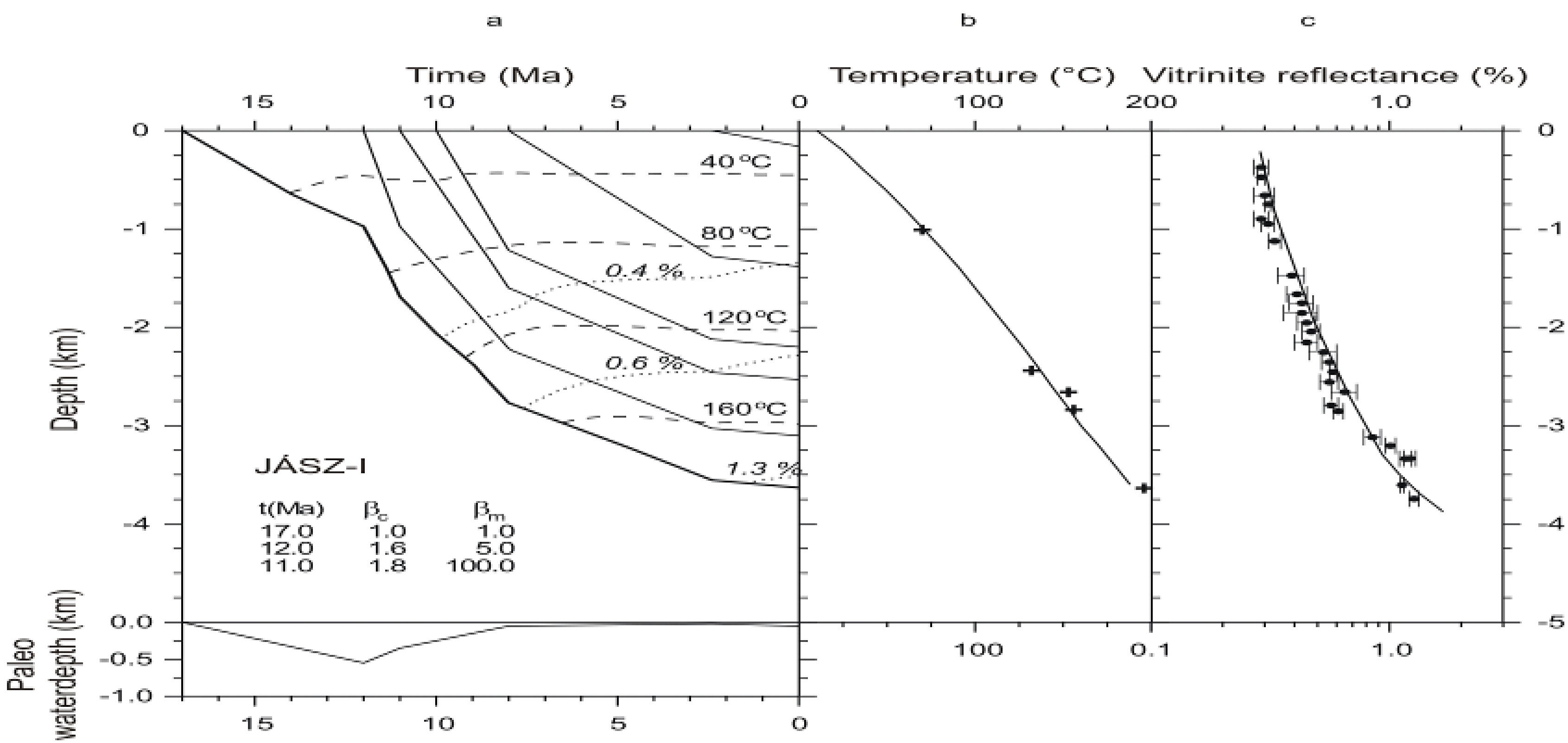

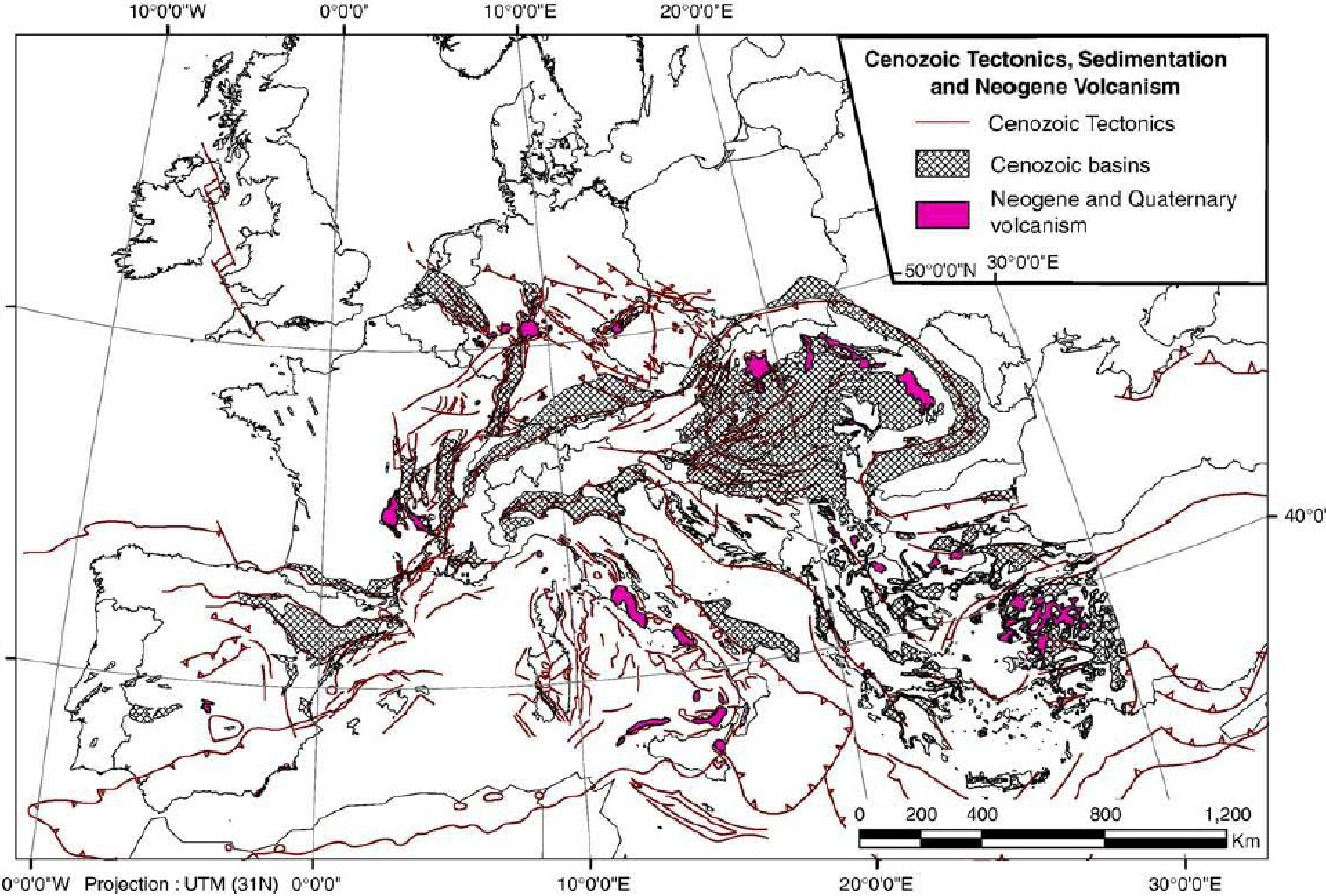

10°0'0"W
0°0'0"
10°0'0"E
20°0'0"E
Cenozoic Tectonics, Sedimentation and Neogene Volcanism
Cenozoic Tectonics
Cenozoic basins
Neogene and Quaternary volcanism
50°0'0"N
30°0'0"E
40°0'
0
200
400
800
1,200
Km
0°0'0"W
Projection : UTM (31N)
0°0'0"
10°0'0"E
20°0'0"E
30°0'0"E

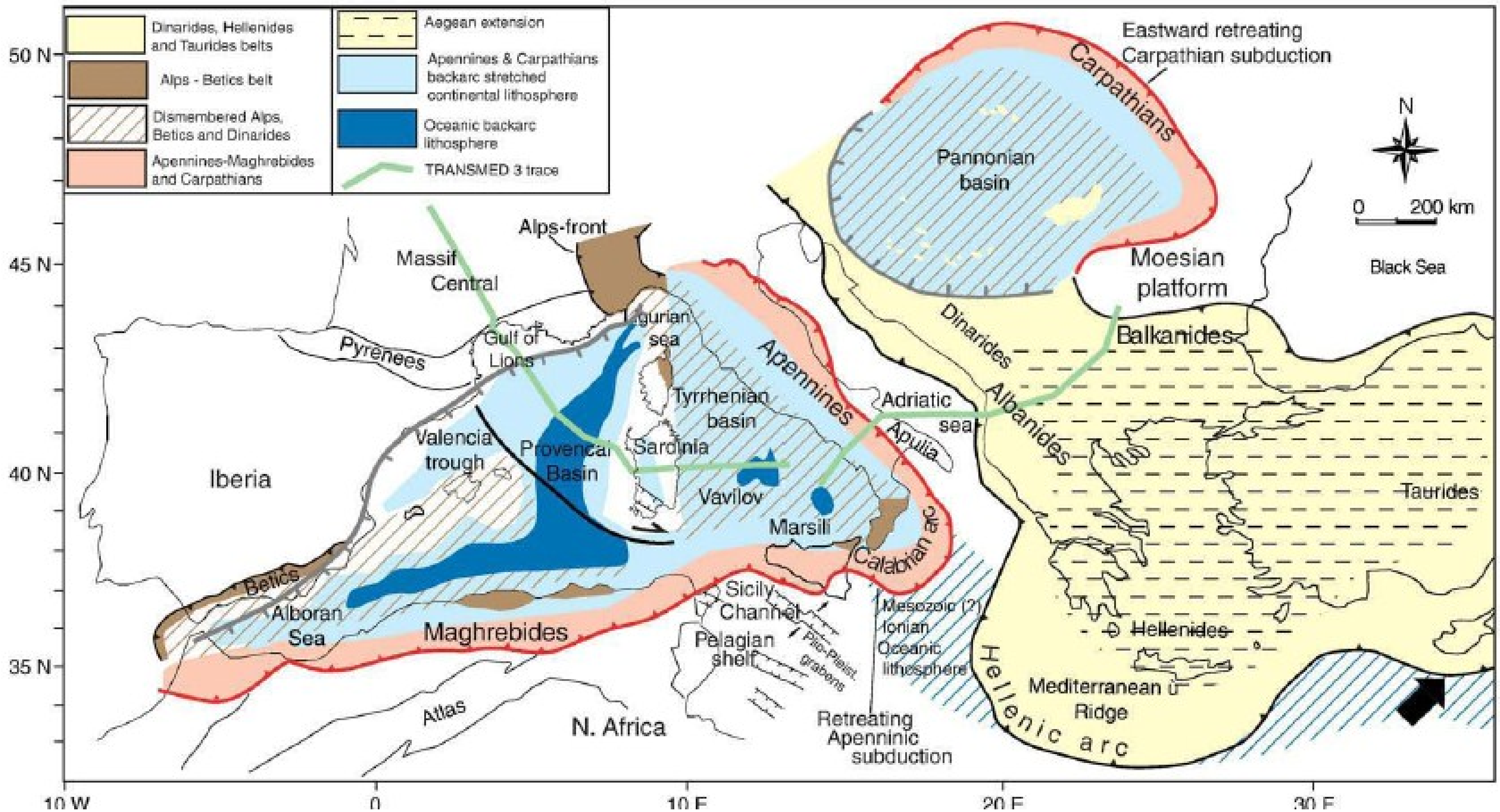
Dinarides, Hellenides and Taurides belts
Alps - Betics belt
Dismembered Alps, Betics and Dinarides
Apennines-Maghrebides and Carpathians
Aegean extension
Apennines & Carpathians backarc stretched continental lithosphere
Oceanic backarc lithosphere
TRANSMED 3 trace
Eastward retreating Carpathian subduction
Carpathians
Pannonian basin
N
0 200 km
Moesian platform
Black Sea
Alps-front
Massif Central
Pyrenees
Gulf of Lions
Ligurian sea
Tyrrhenian basin
Apennines
Adriatic sea
Apulia
Dinarides
Albanides
Balkanides
Taurides
Valencia trough
Provencal Basin
Sardinia
Vavilov
Marsili
Calabrian arc
Iberia
Betics
Alboran Sea
Maghrebides
Sicily Channel
Pelagian shelf
Plio-Pleist. grabens
Mesozoic (?) Ionian Oceanic lithosphere
Hellenides
Mediterranean Ridge
Hellenic arc
Atlas
N. Africa
Retreating Apenninic subduction
50 N
45 N
40 N
35 N
10 W
0
10 E
20 E
30 E

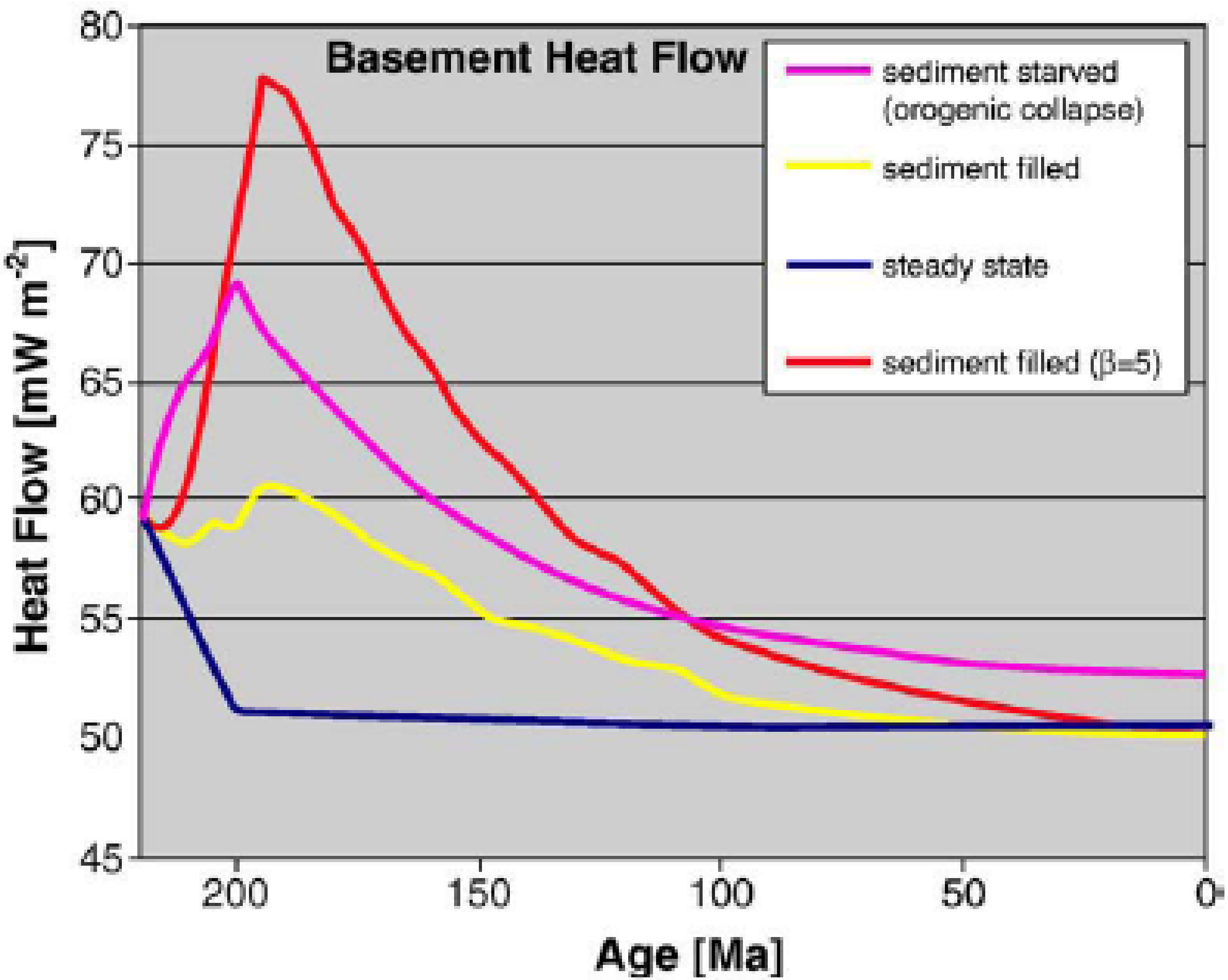
Basement Heat Flow
sediment starved (orogenic collapse)
sediment filled
steady state
sediment filled (β=5)
Heat Flow [mW m-2]
Age [Ma]
80
75
70
65
60
55
50
45
200
150
100
50
0

Interpolation using all datapoints

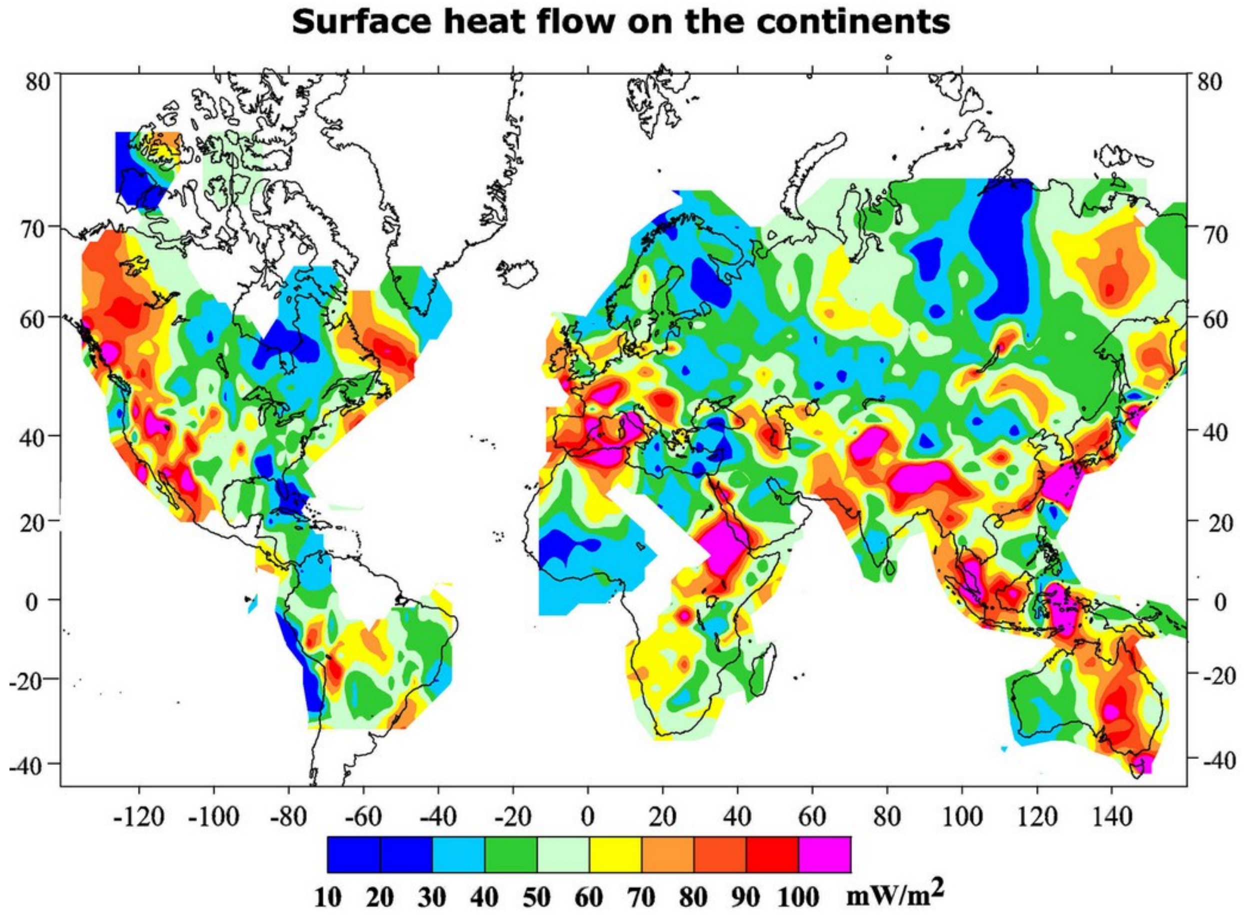

Artimieva et al,2001 and 2006

Adding volcanoe

- Treat each historic active as 150mW (Nagao and Uyeda,1995)
- Treat holocene as 80mW

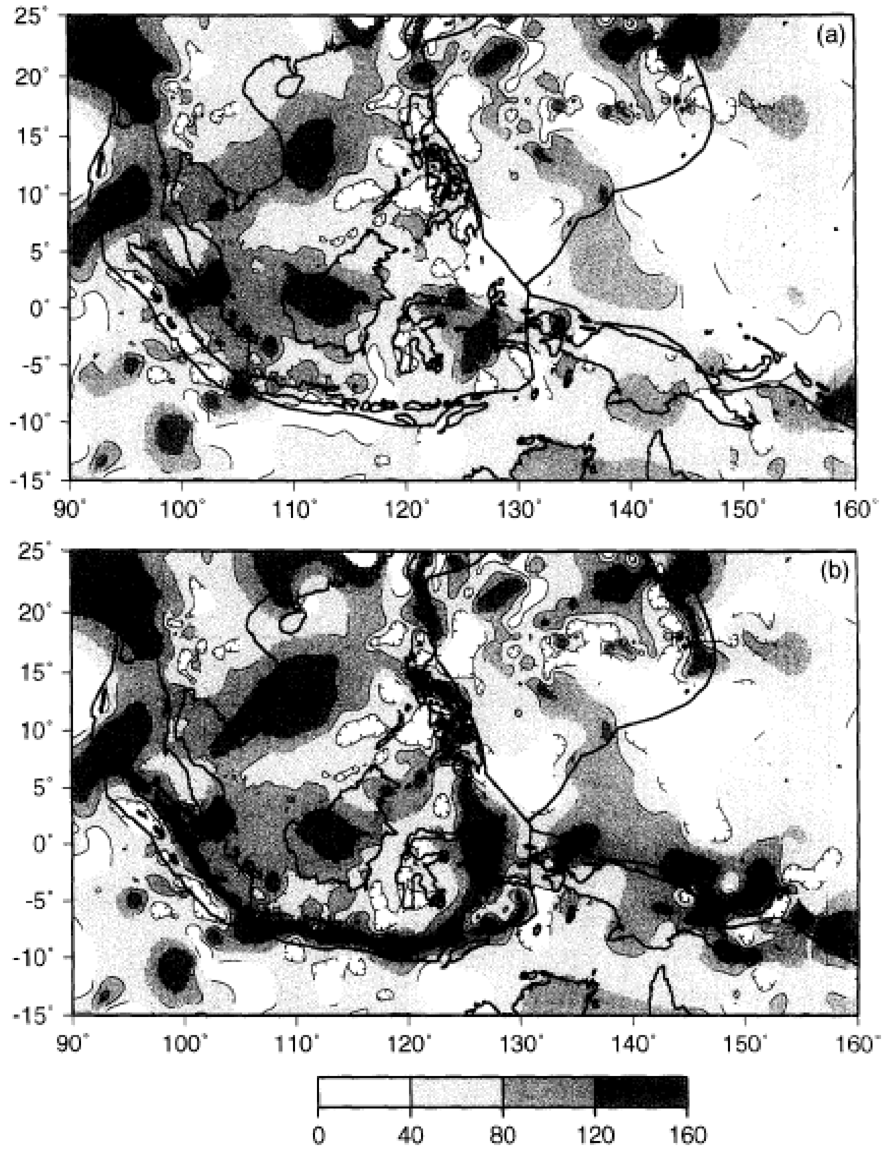

Supported by INTELLIGENT ENERGY EUROPE

BRGM

TNO innovation for life

Heat flow – more detail Adding Volcanoes (www.thermogis.nl/worlaquifer)

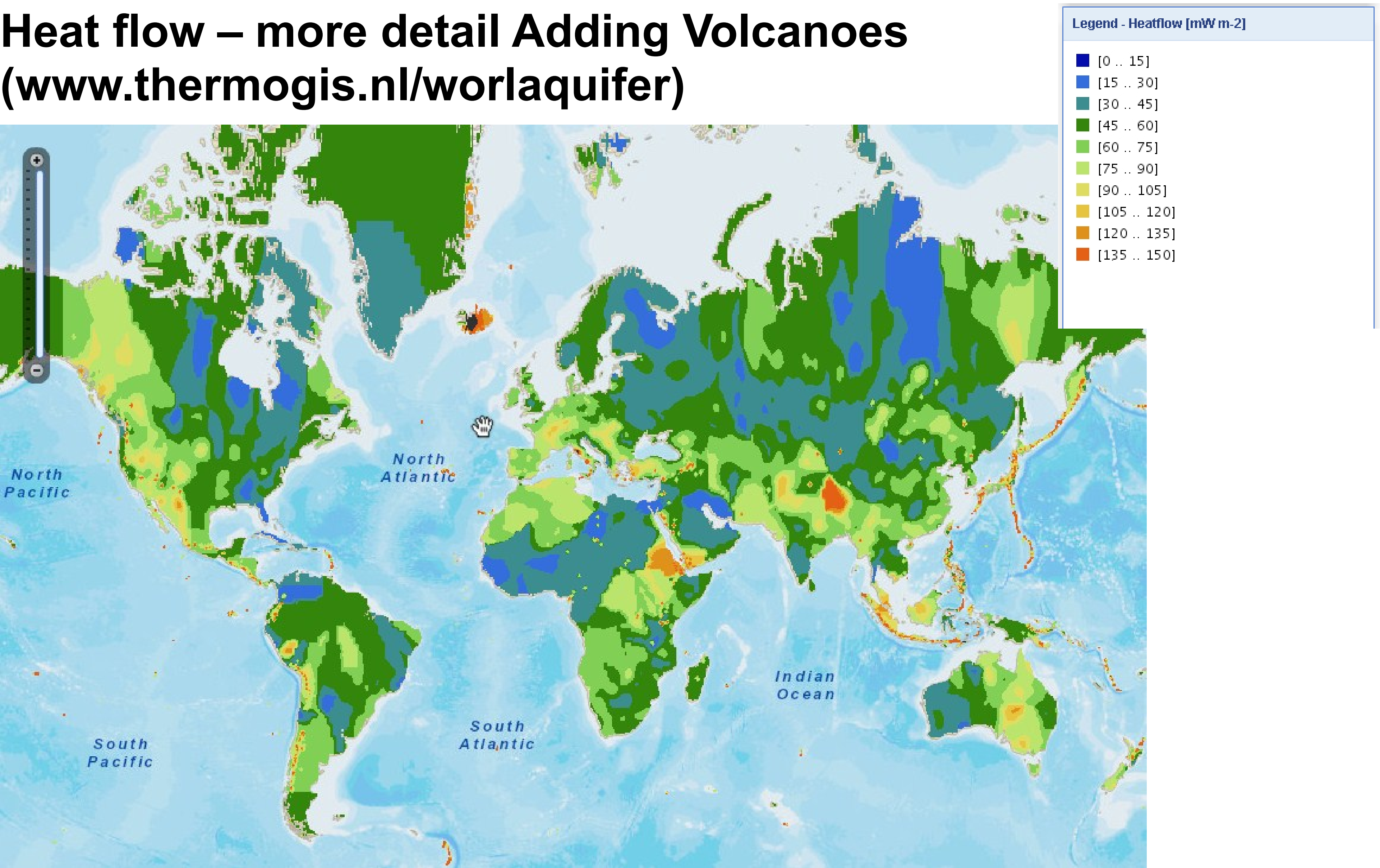

A closer look at europe – active volcanoes – holocene and younger

Magmatism

- Plate tectonics related
  - Mid oceanic ridge (e.g. iceland) and rift (east africa)
  - Subducting plate (e.g. indonesia)
- Mantle plume (core-mantle boundary, e.g. geysers, hawaii, canary islands)
- Orogenic collapse

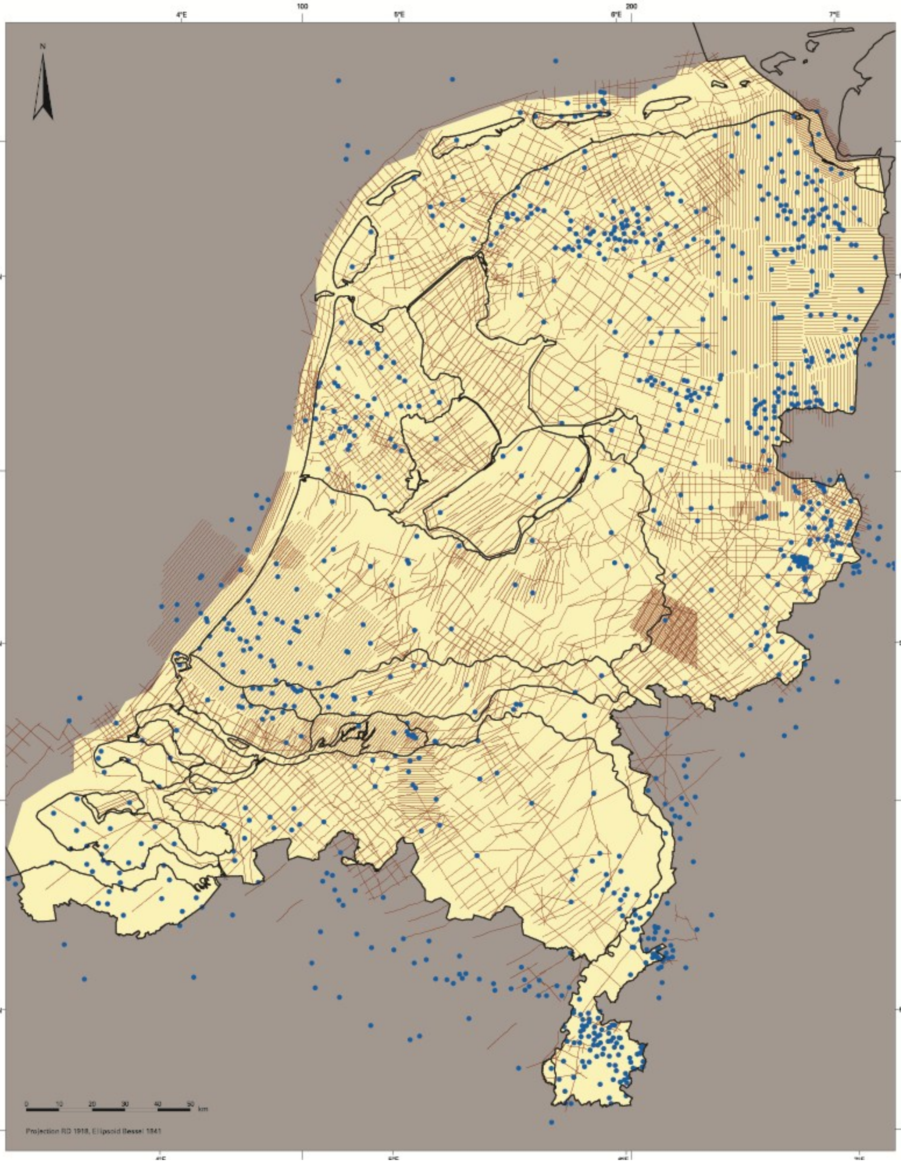

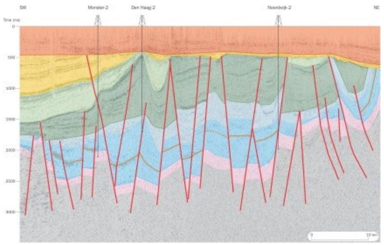

Well & Seismic Data

Wells: 5876 (onshore/offshore)

Seismic: 72.000 km (2D+3D lines)

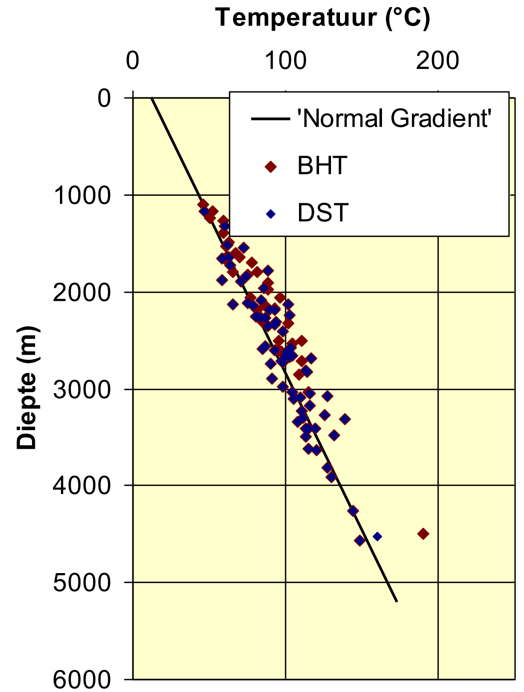

Over 1000 BHT and DST data

Deeper/lateral Requires better models

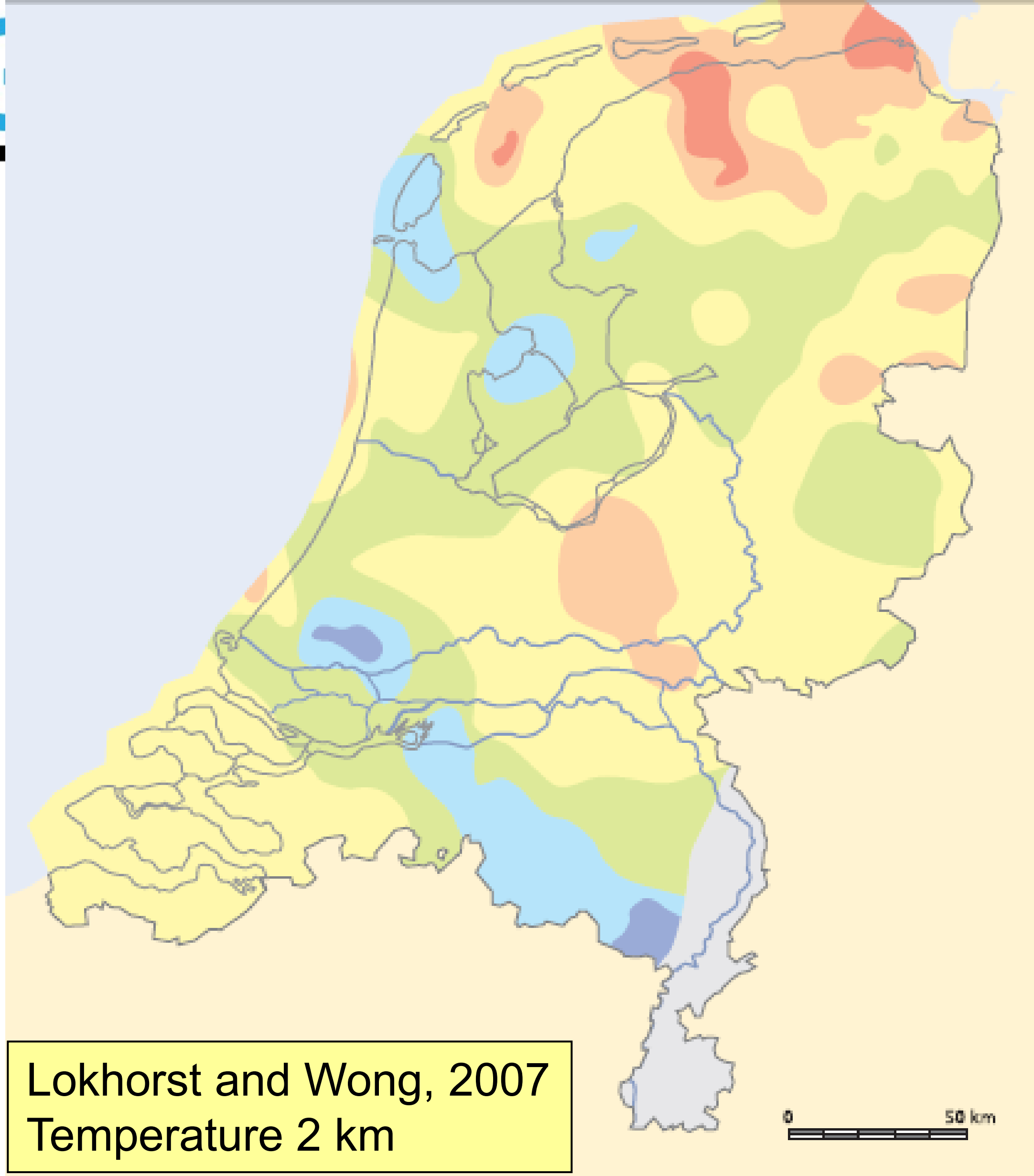

Lokhorst and Wong, 2007
Temperature 2 km

Temperature (°C)

- > 90
- 85 - 90
- 75 - 80
- 70 - 75
- no data available

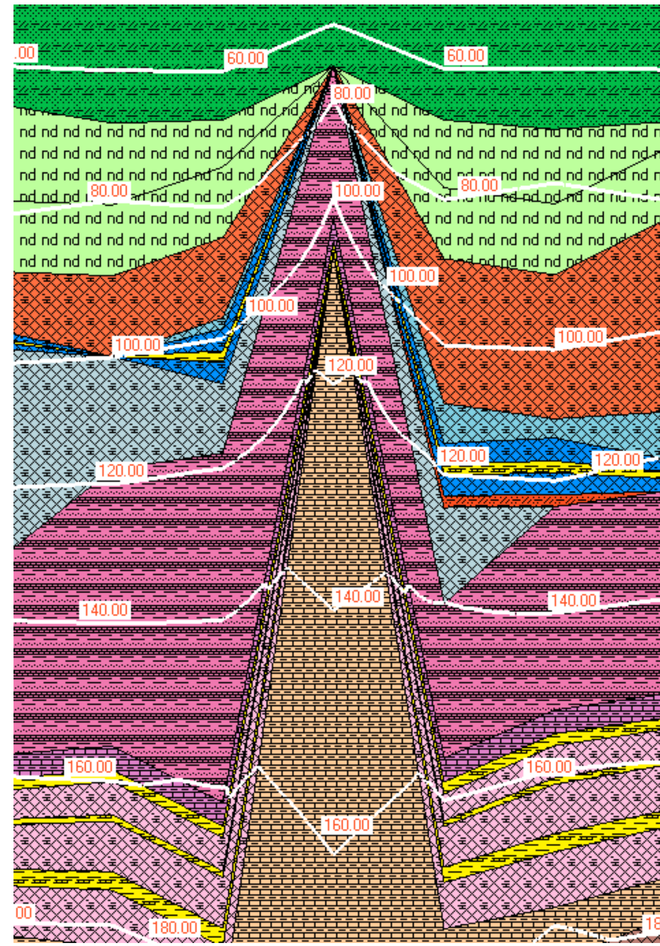

average ca 30C/km

GEOELEC

Supported by INTELLIGENT ENERGY EUROPE

Knowledge of subsurface
Ongoing mapping (public)

- Upper North Sea Group
- Lower and Middle North Sea Groups
- Chalk Group
- Rijnland Group
- Schieland and Niedersachsen Groups
- Altena Group
- Lower and Upper Germanic Trias Groups
- Zechstein Group
- Lower and Upper Rotliegend Groups
- Limburg Group
- Carboniferous Limestone Group
- Devonian
- Silurian
- Ordovician

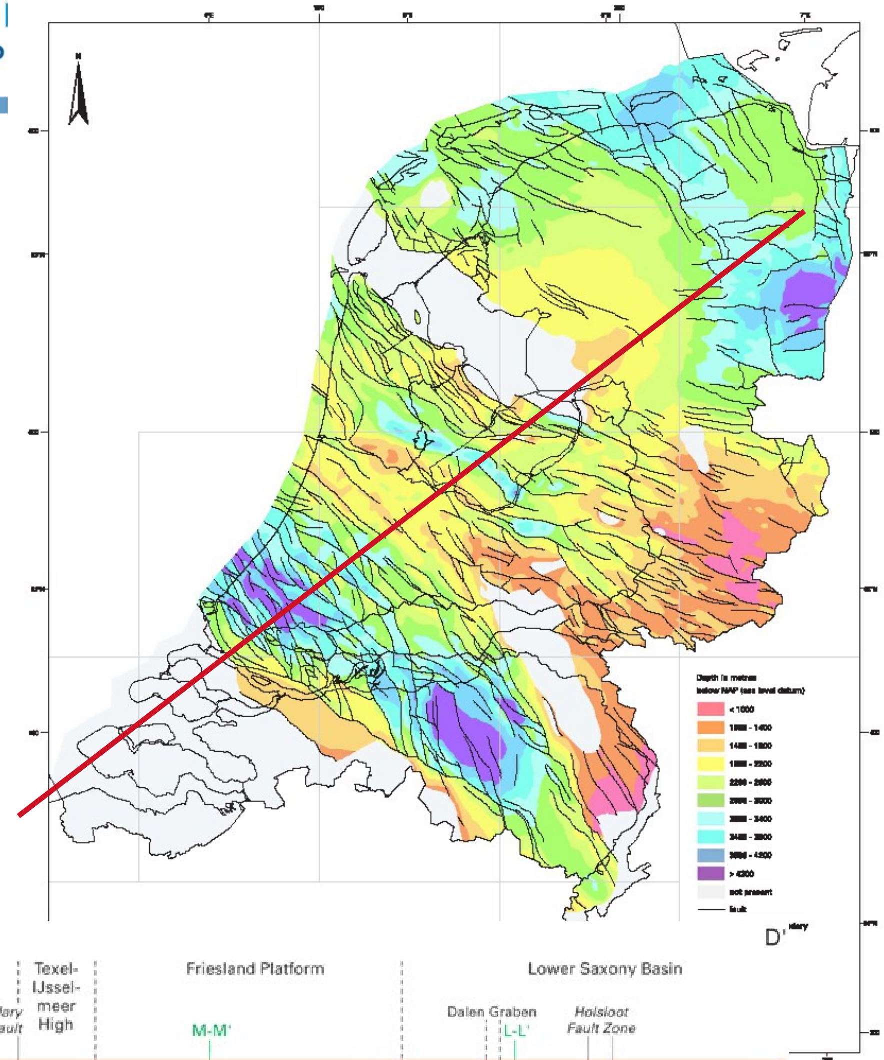

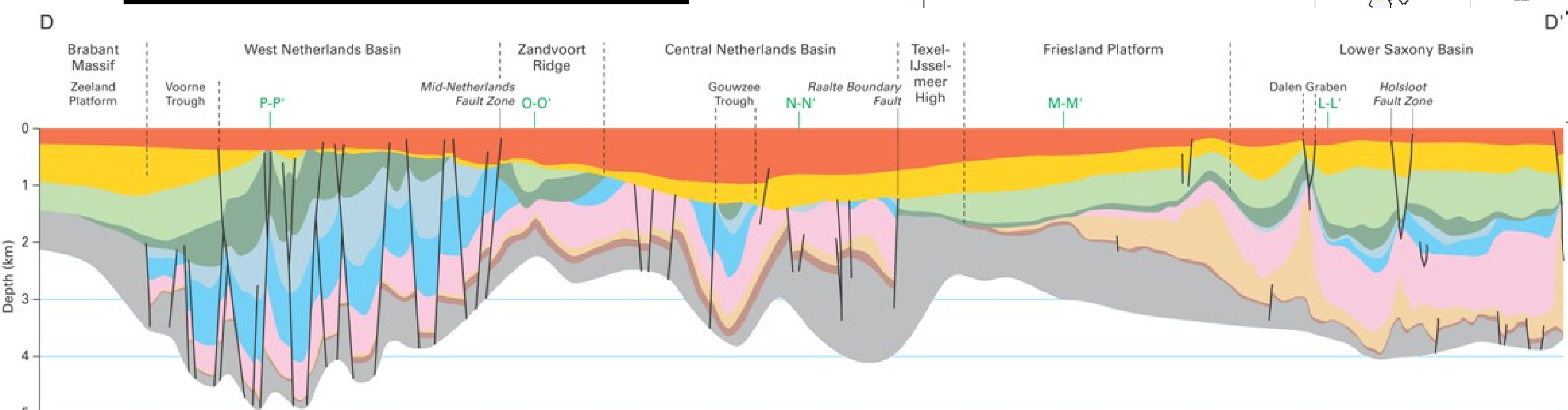

BHT data (n=1241)

BHT wells and E&P licenses

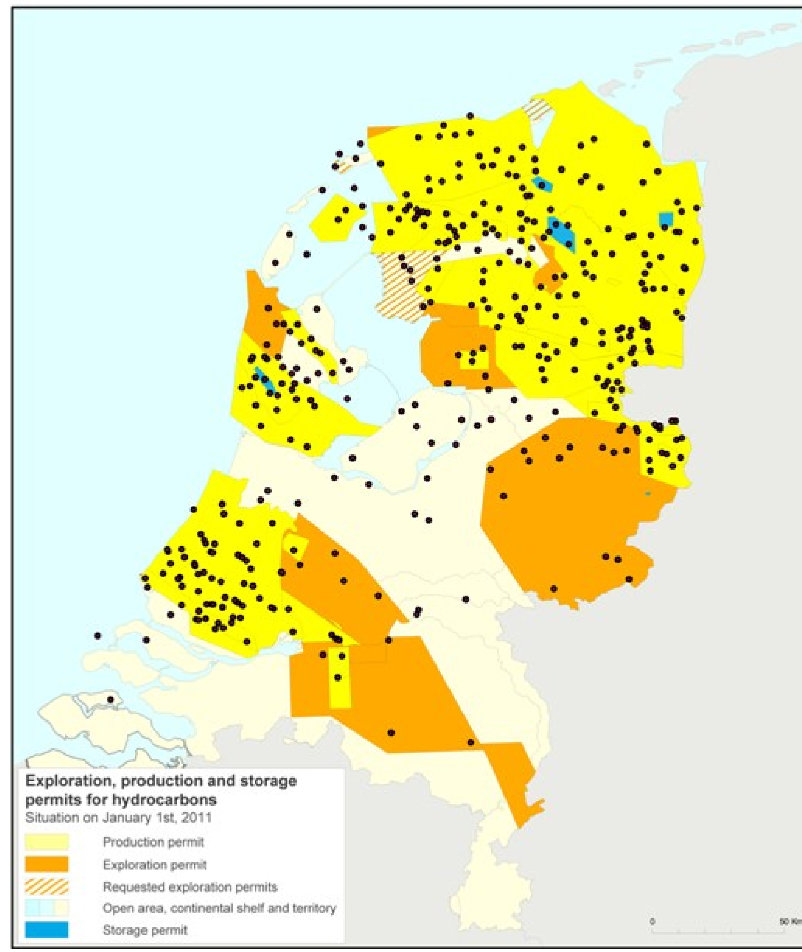

- ICS (n=412)
  - Initial Cylindrical source
  - Used to correct simpler AAPG methods
- AAPG + AAPGcorrected (n=829)

For comparison

DST much less (n=52)

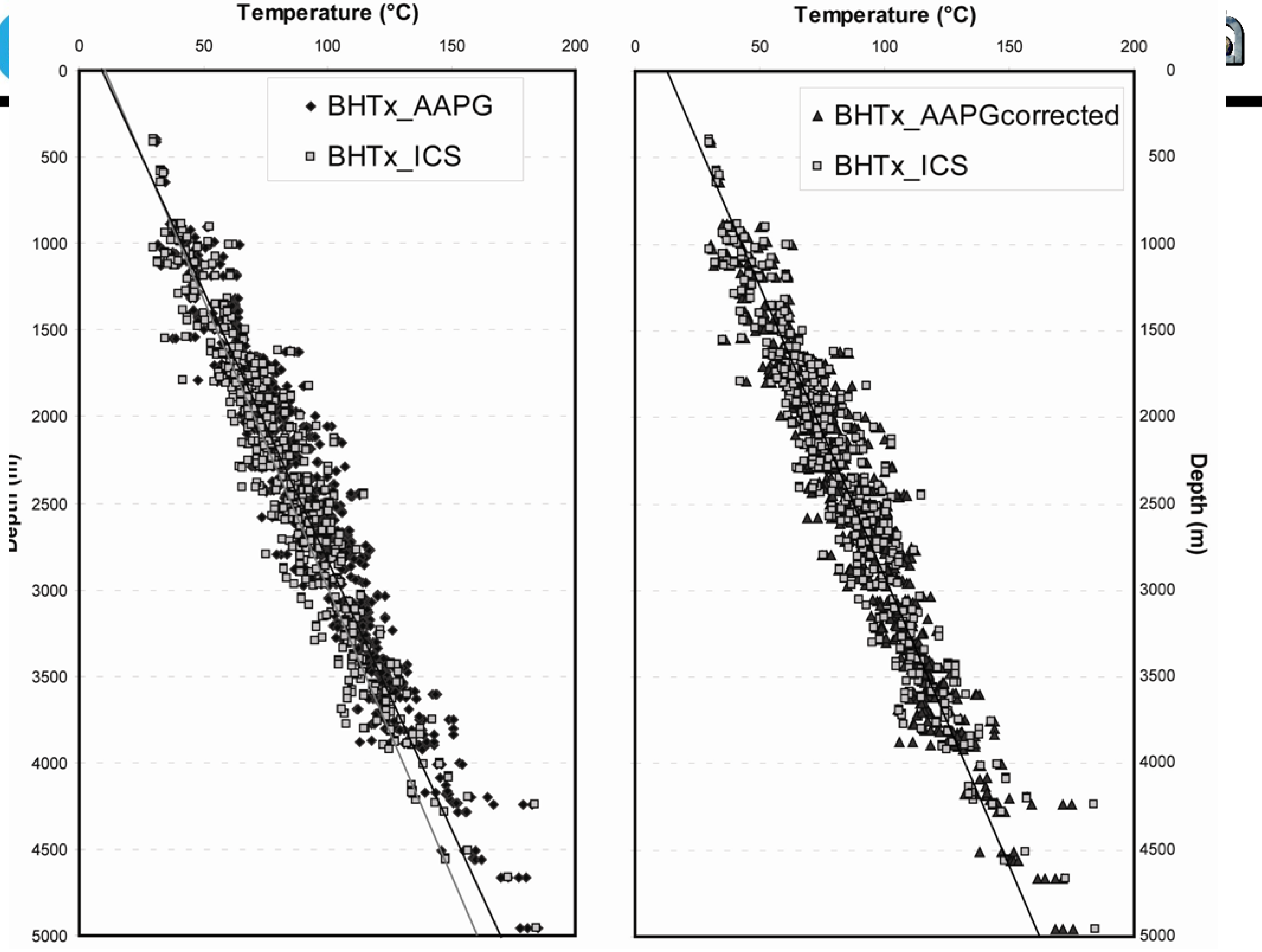
Temperature (°C)
0
50
100
150
200
Depth (m)
0
500
1000
1500
2000
2500
3000
3500
4000
4500
5000
BHTx_AAPG
BHTx_ICS
BHTx_AAPGcorrected
BHTx_ICS

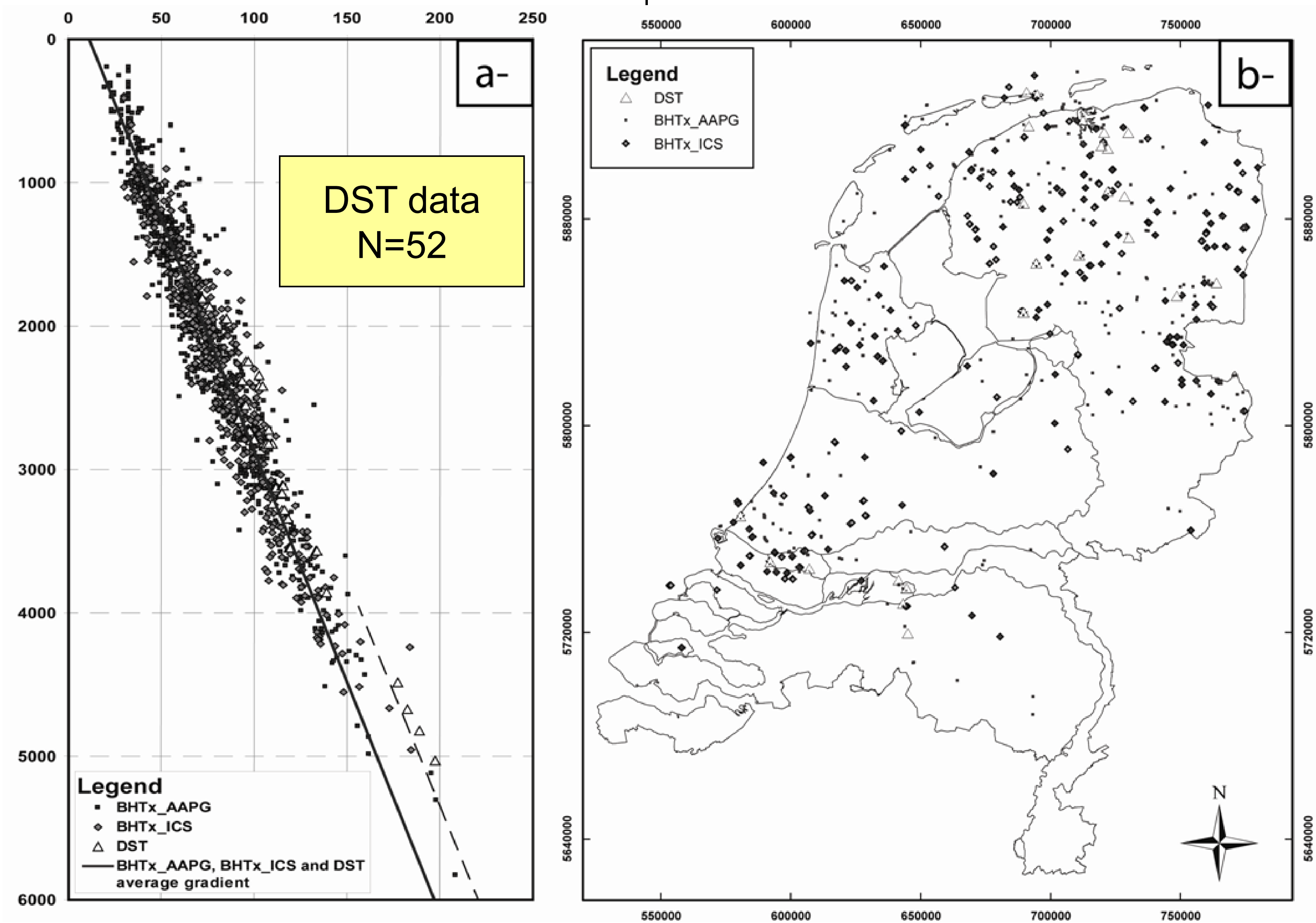
a-
DST data
N=52
0 50 100 150 200 250
0 1000 2000 3000 4000 5000 6000
Legend
BHTx_AAPG
BHTx_ICS
DST
BHTx_AAPG, BHTx_ICS and DST average gradient
b-
Legend
DST
BHTx_AAPG
BHTx_ICS
550000 600000 650000 700000 750000
5880000 5800000 5720000 5640000
N

conductivity

- Strong spatial variation

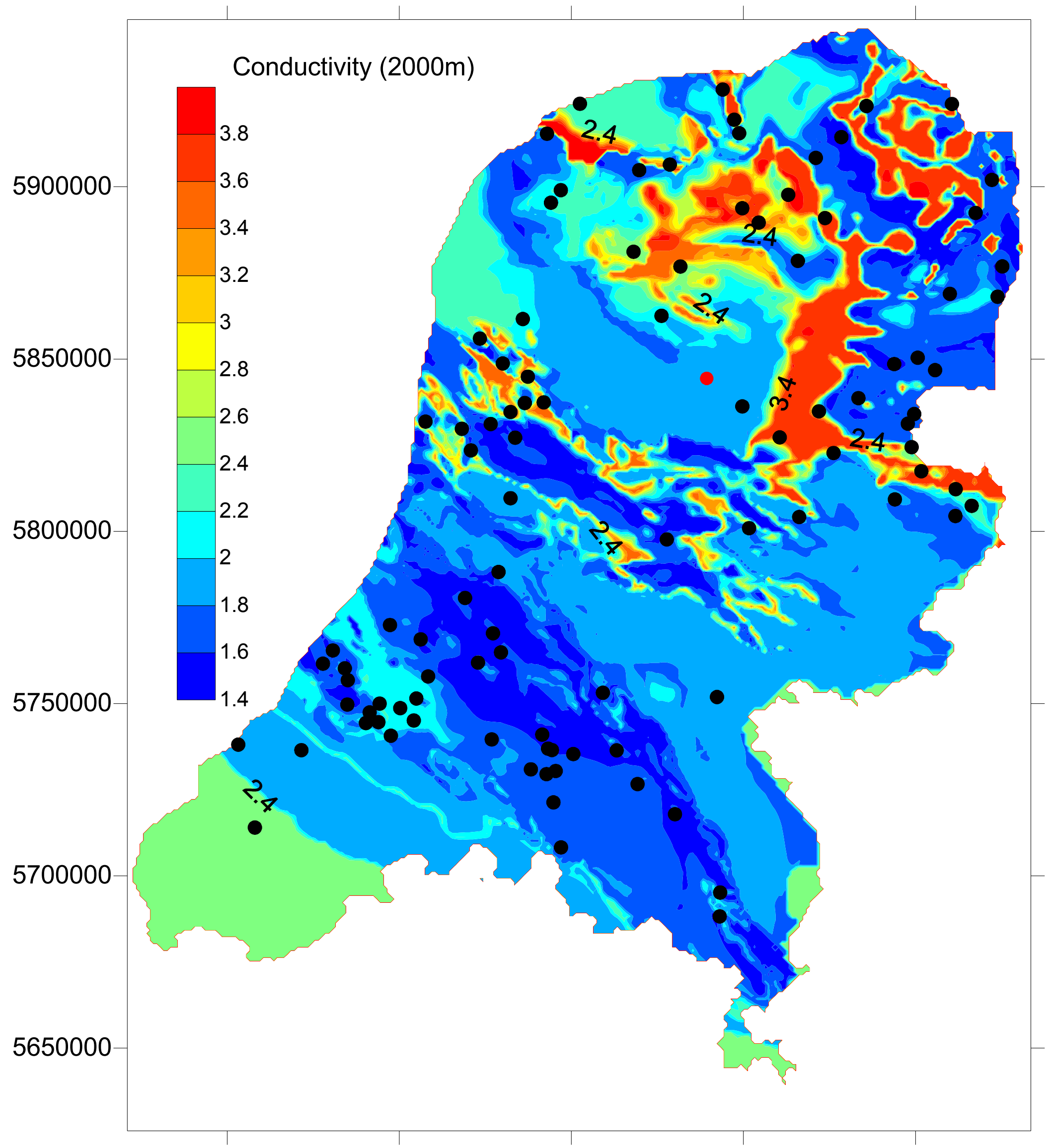

Carboniferous

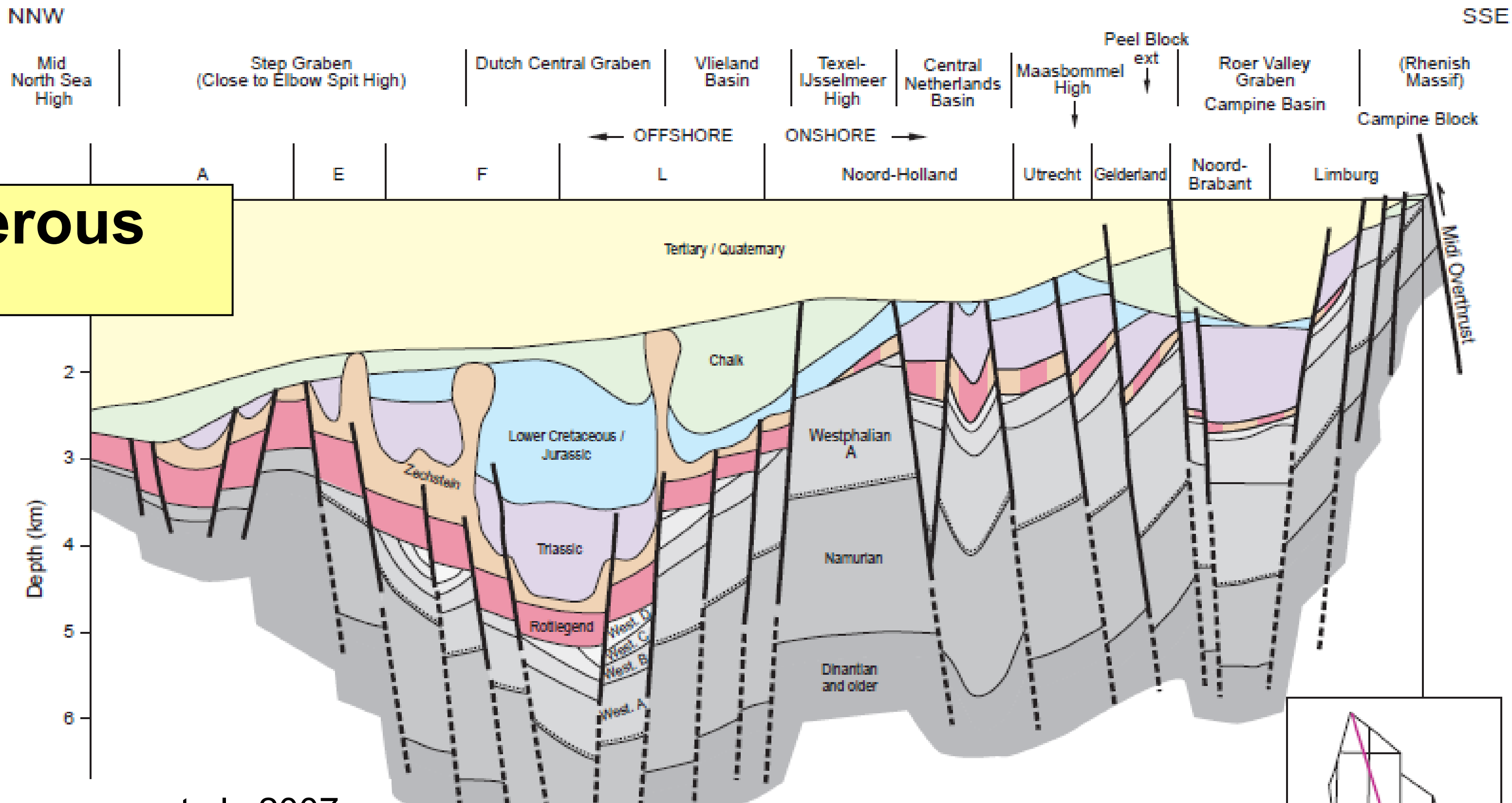

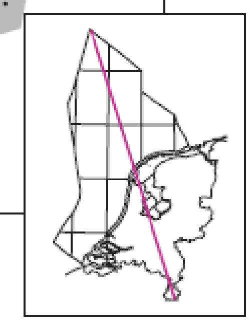

Buggenum et al., 2007

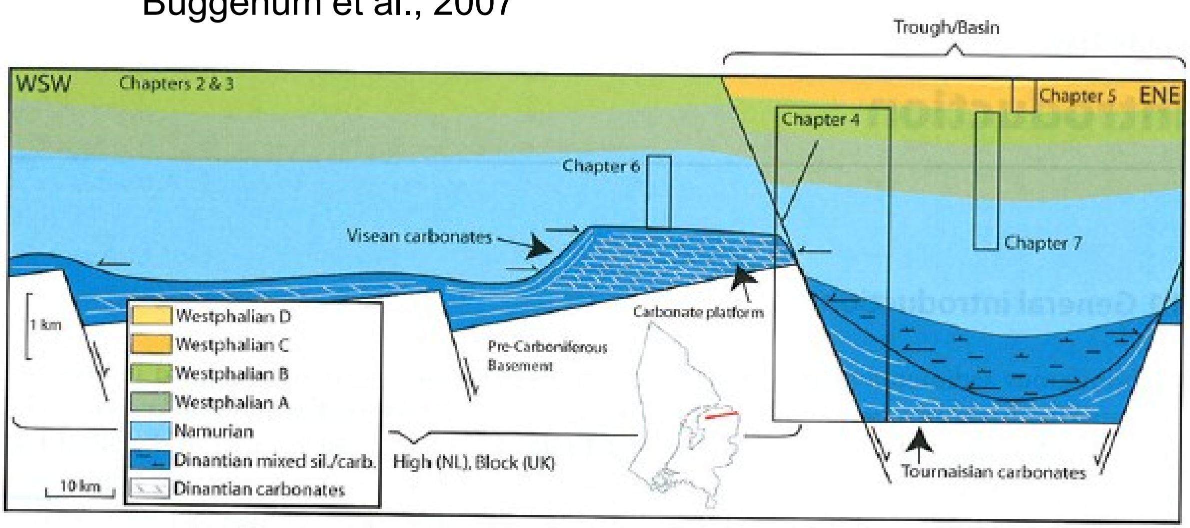

Kombrink, 2008

Surface Temperature

- Cooling last 3my, Heating last 10kY → Effect is non steady state steepening of temperature gradient in top 2-3 km (→ transient correction 2-3 degrees)

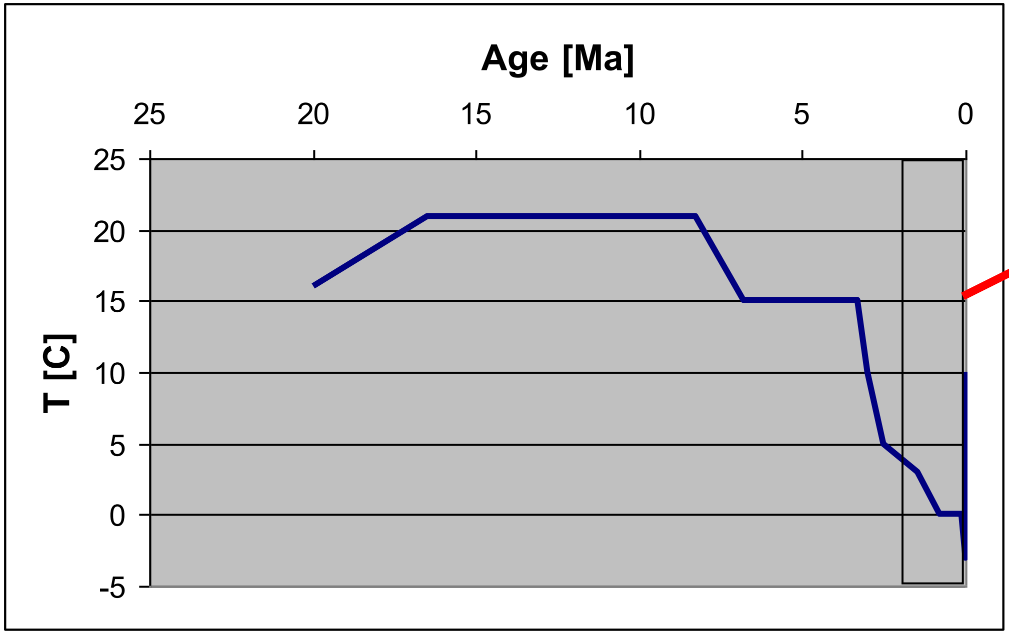

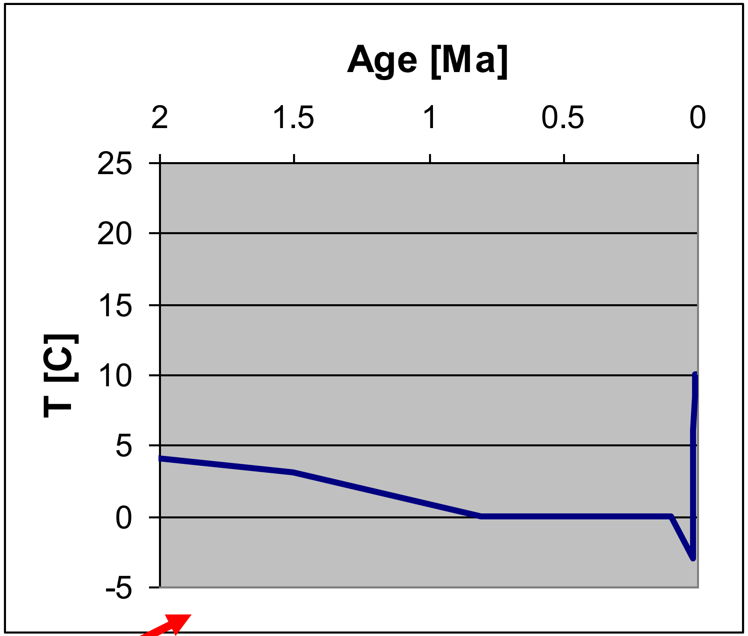

Results - temperature (1)

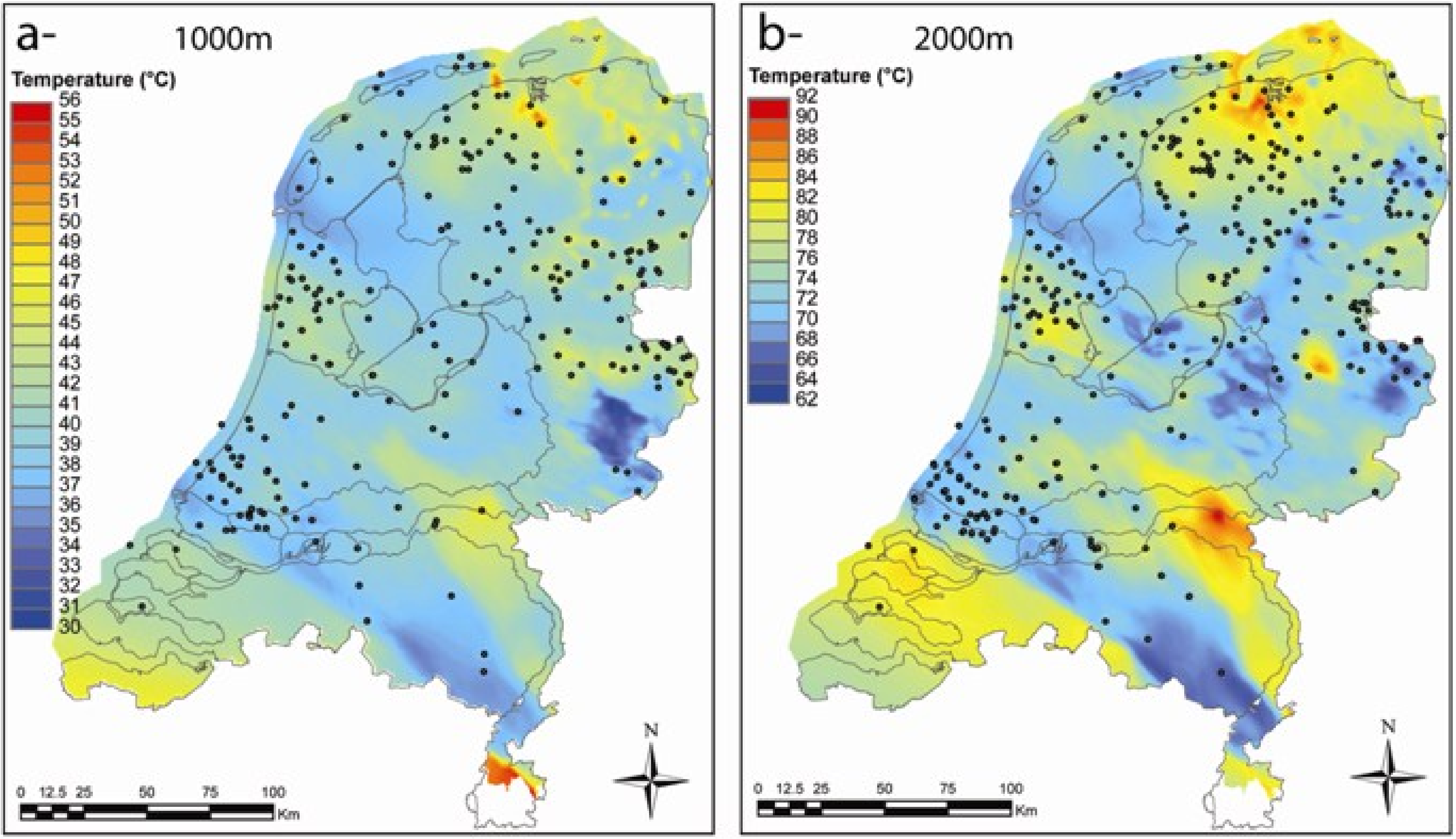

GEOELEC Supported by INTELLIGENT ENERGY EUROPE BRGM TNO innovation for life

Results - temperature (3)

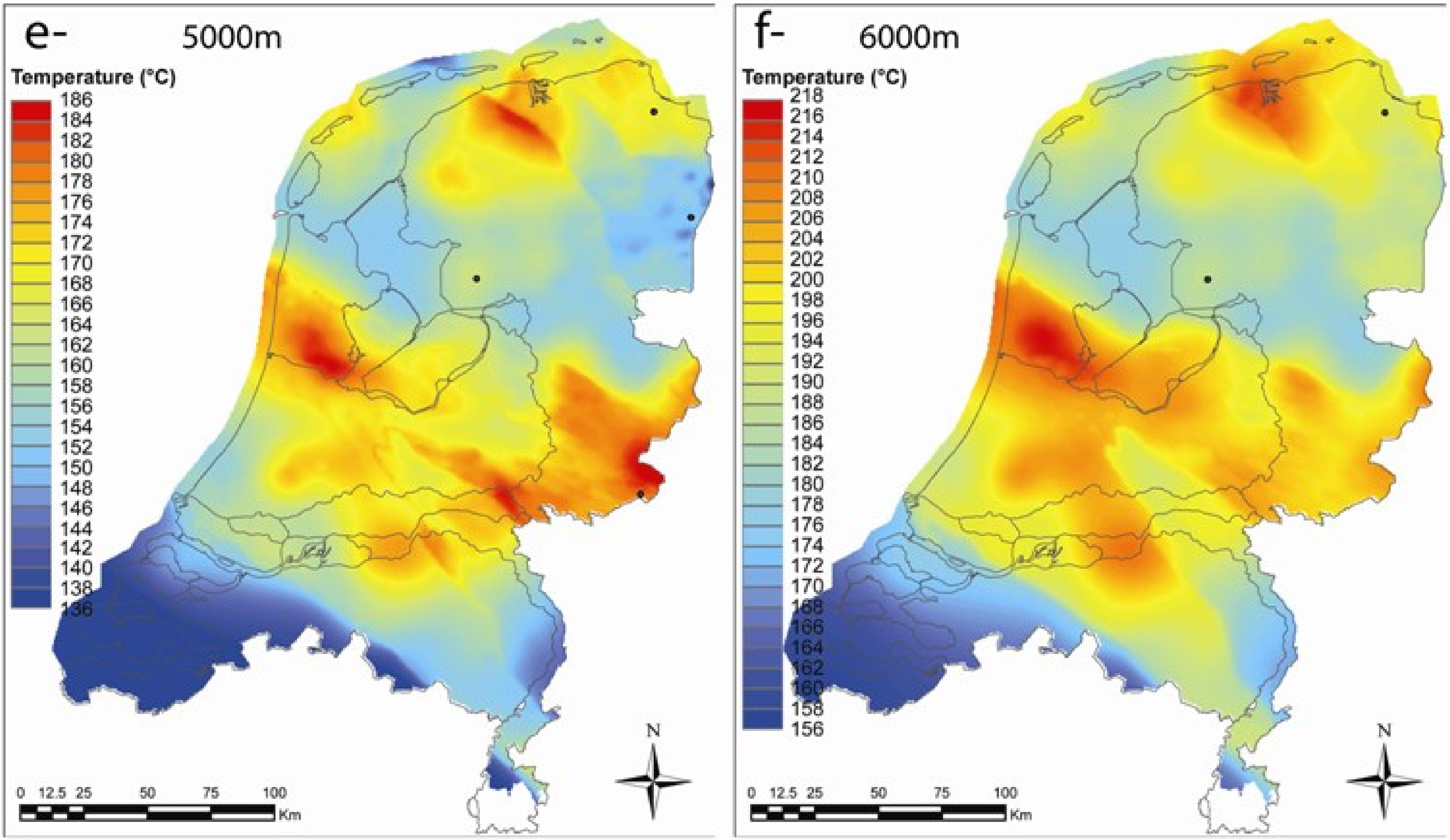

Temperature fit to well data

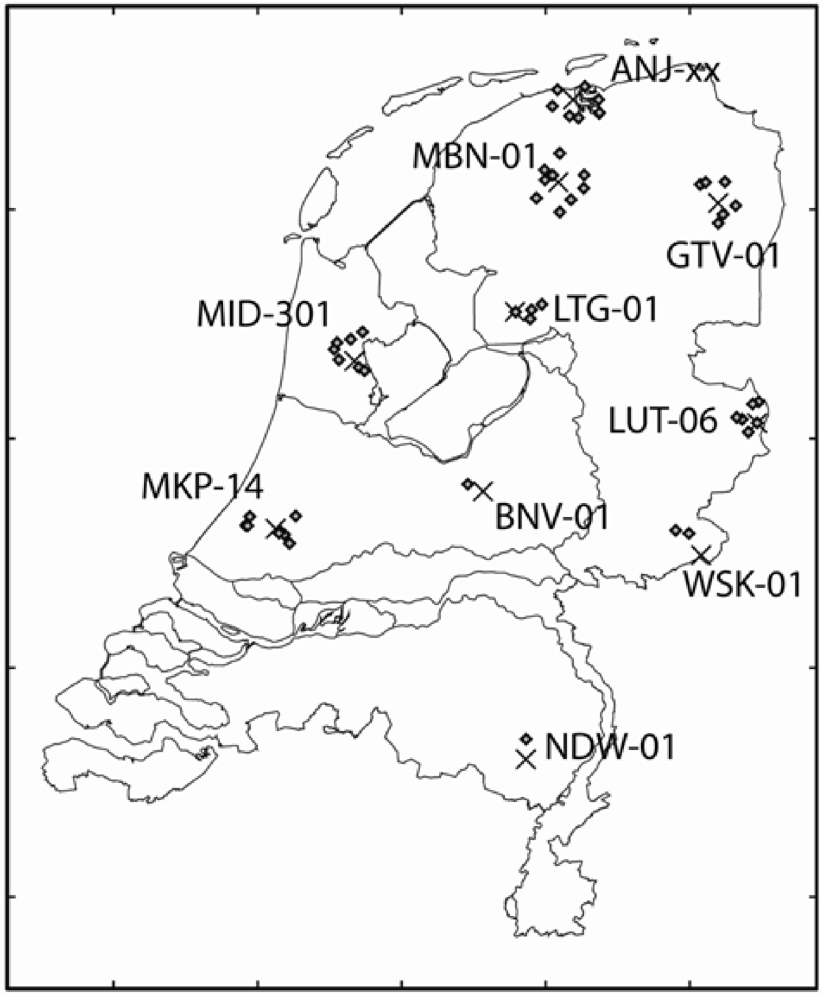

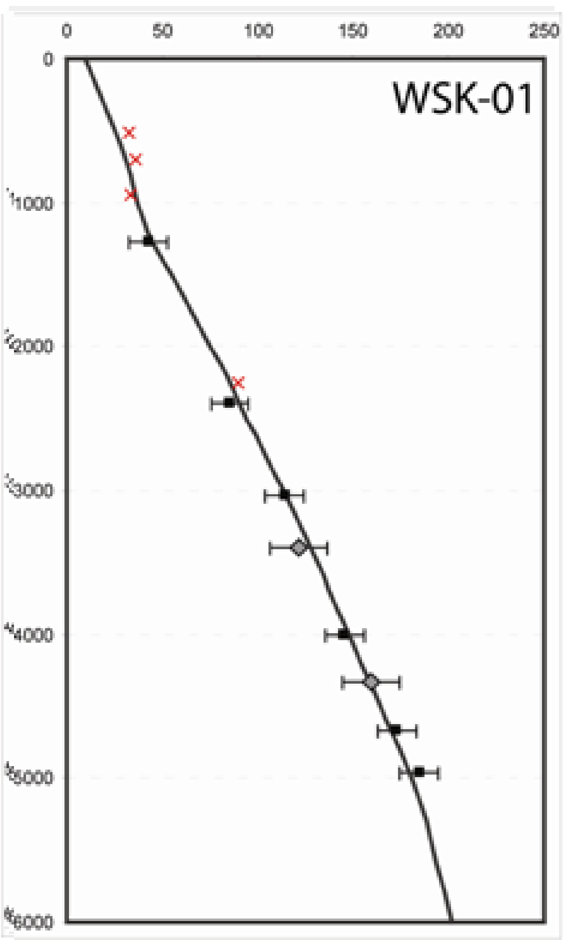

Temperature fit to well data

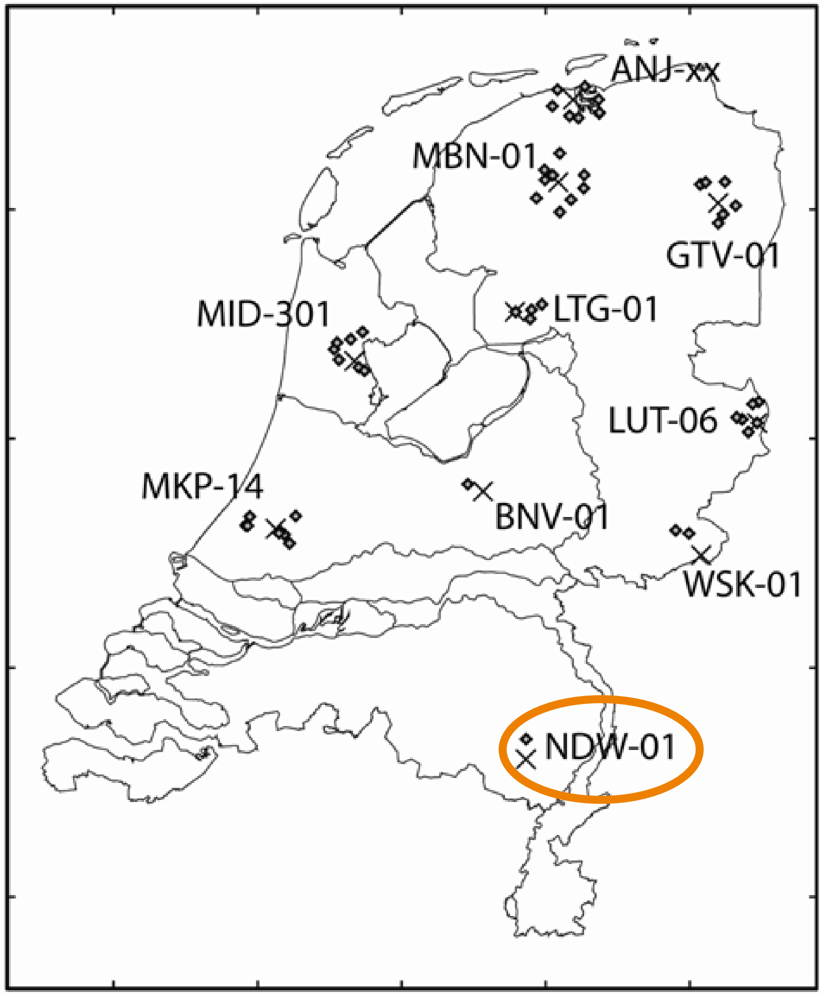

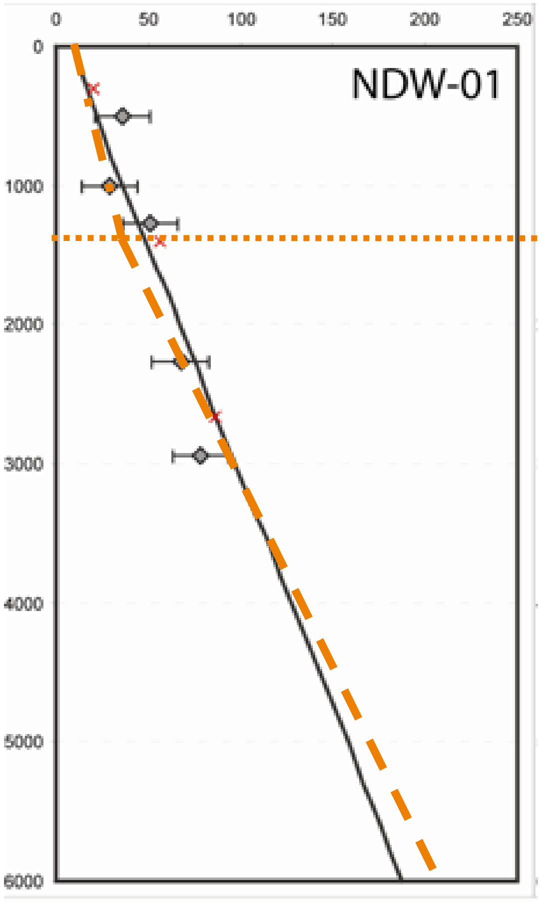

Meteoric water convection

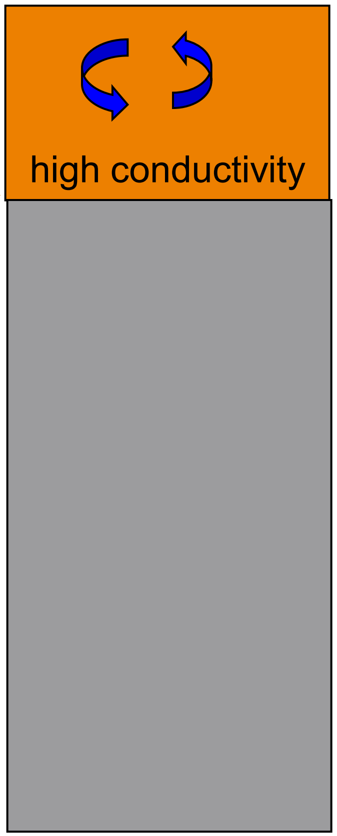

Luijendijk, 2010

Temperature fit to well data

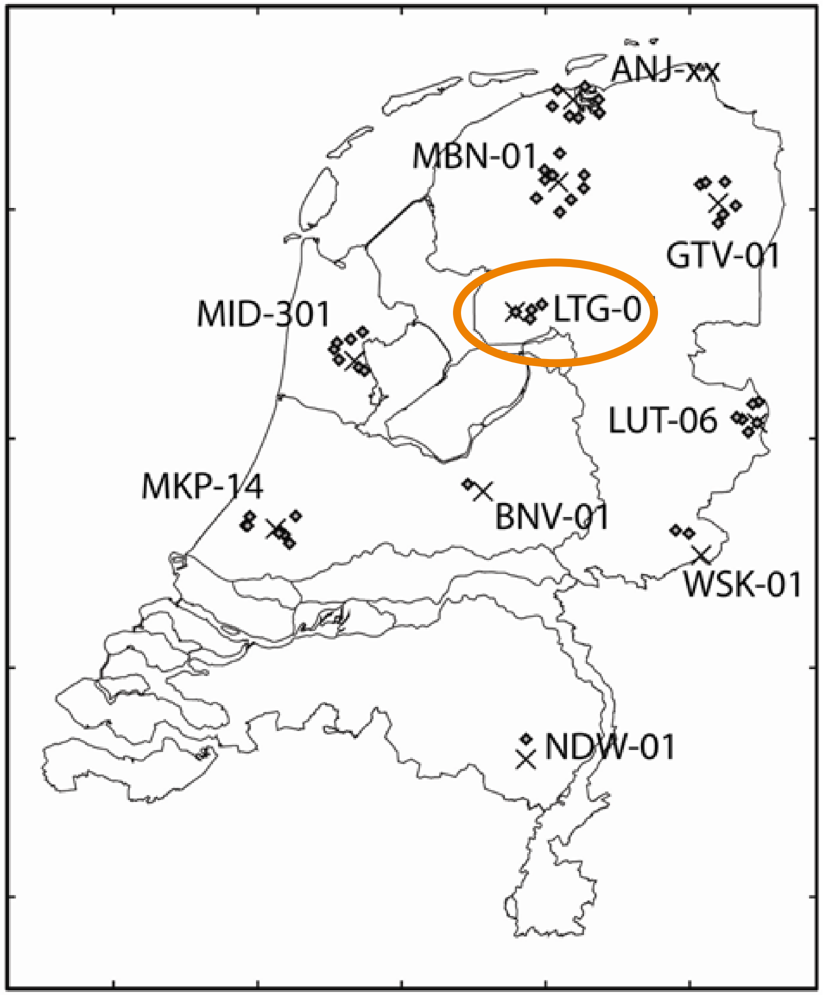

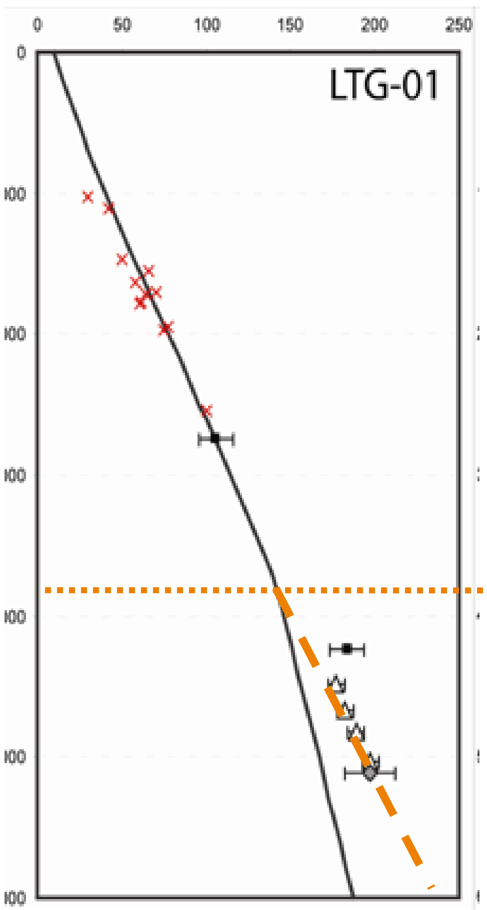

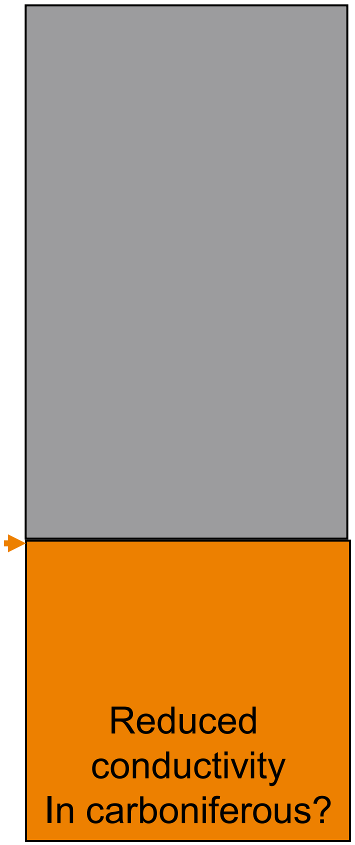

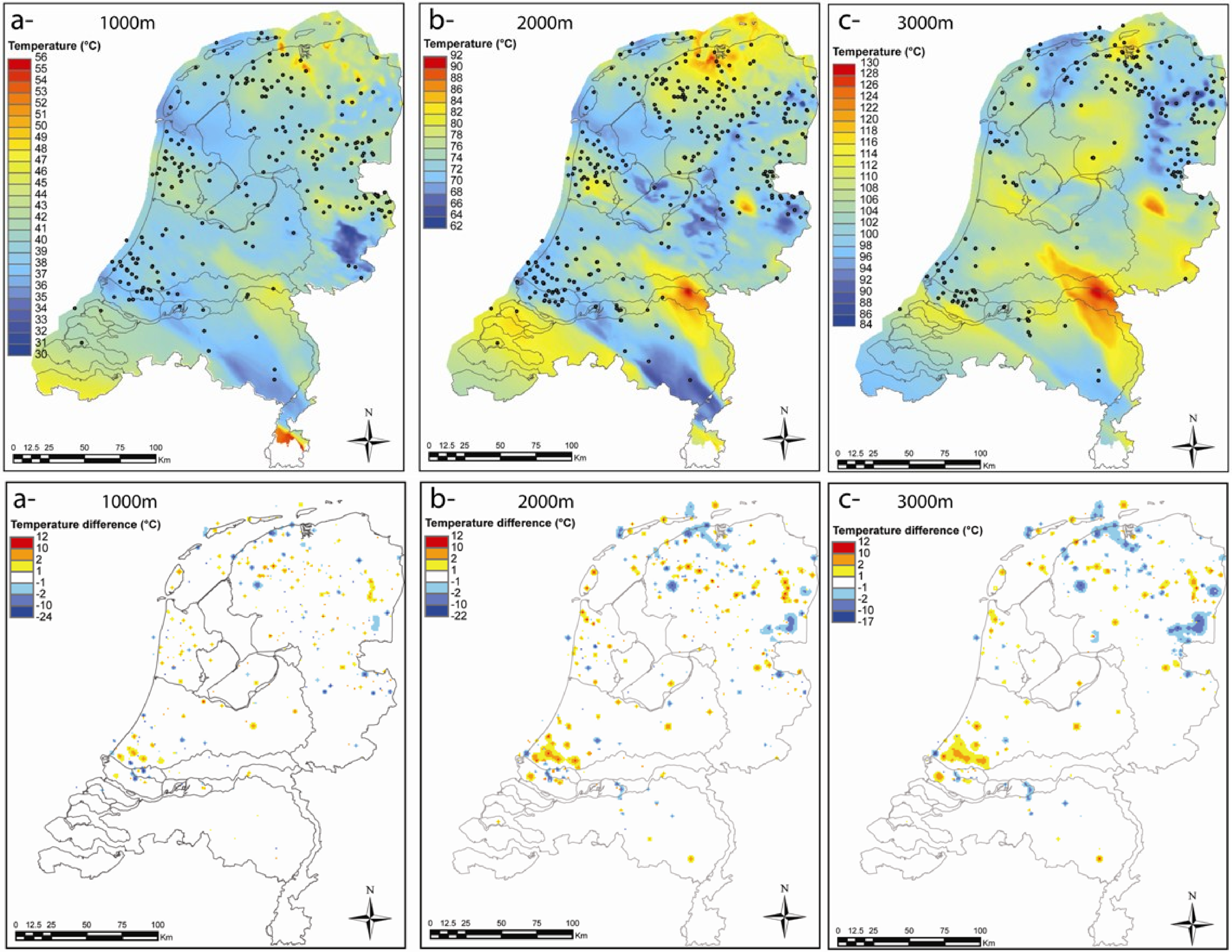
a- 1000m
Temperature (°C)
56 55 54 53 52 51 50 49 48 47 46 45 44 43 42 41 40 39 38 37 36 35 34 33 32 31 30
b- 2000m
Temperature (°C)
92 90 88 86 84 82 80 78 76 74 72 70 68 66 64 62
c- 3000m
Temperature (°C)
130 128 126 124 122 120 118 116 114 112 110 108 106 104 102 100 98 96 94 92 90 88 86 84
a- 1000m
Temperature difference (°C)
12 10 2 1 -1 -2 -10 -24
b- 2000m
Temperature difference (°C)
12 10 2 1 -1 -2 -10 -22
c- 3000m
Temperature difference (°C)
12 10 2 1 -1 -2 -10 -17
N
0 12.5 25 50 75 100
Km

Implications for EGS

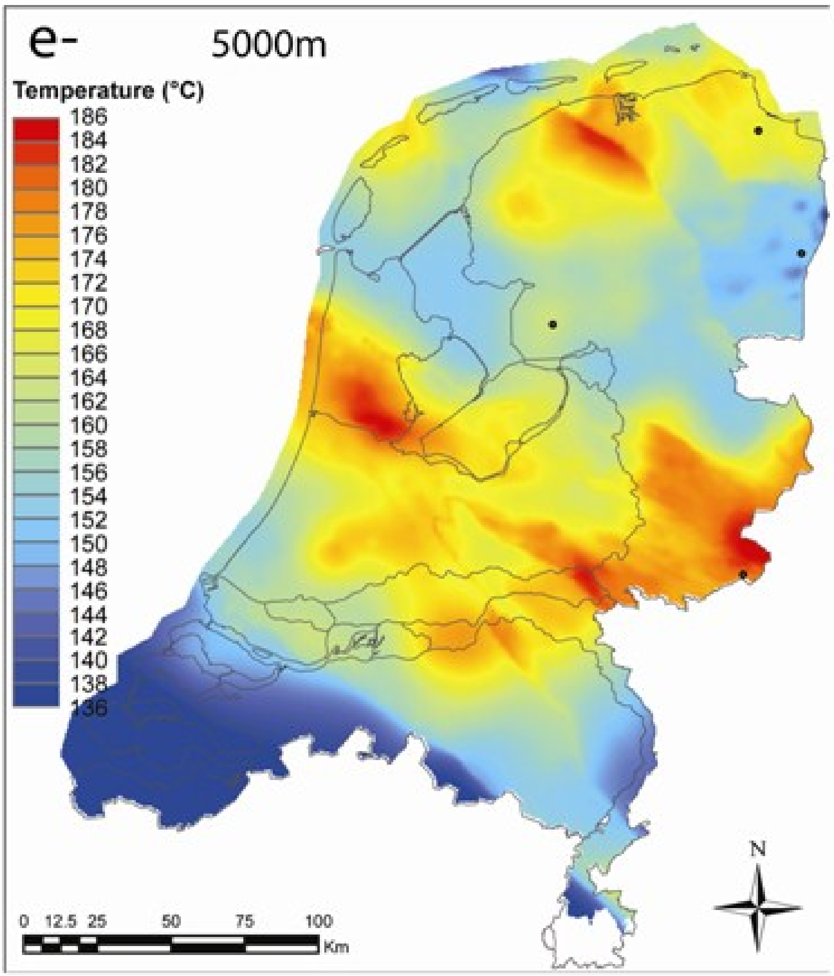

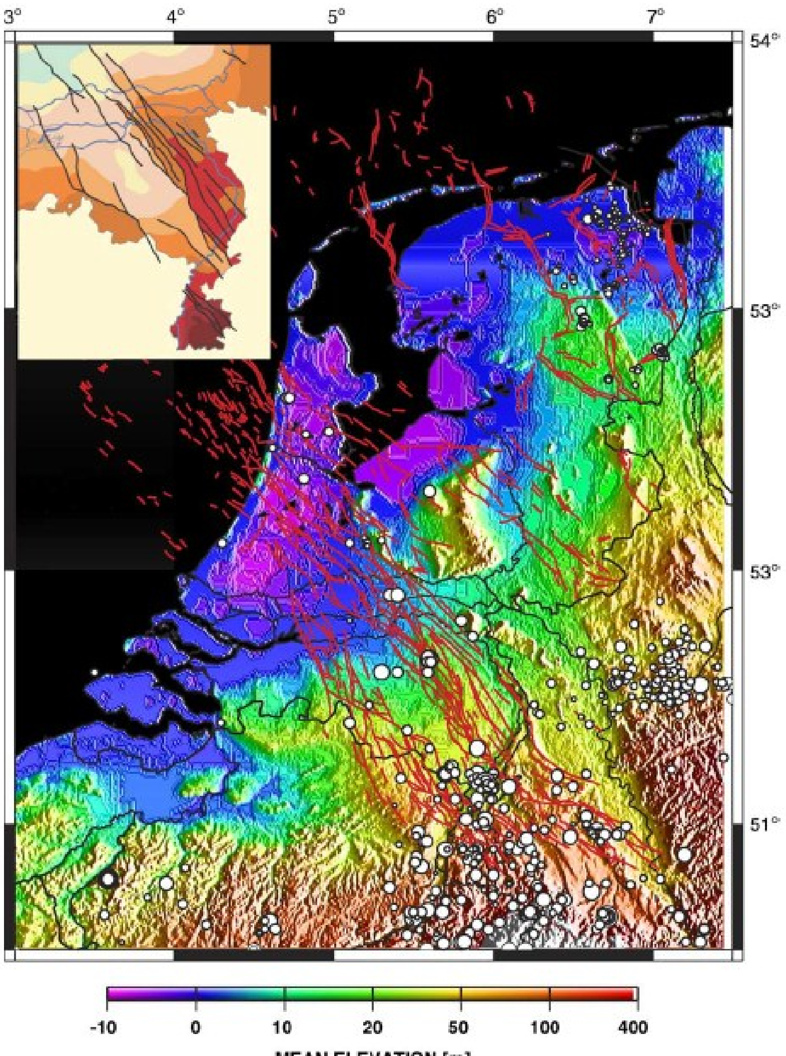

GEOELEC

Supported by INTELLIGENT ENERGY EUROPE

BRGM

TNO innovation for life

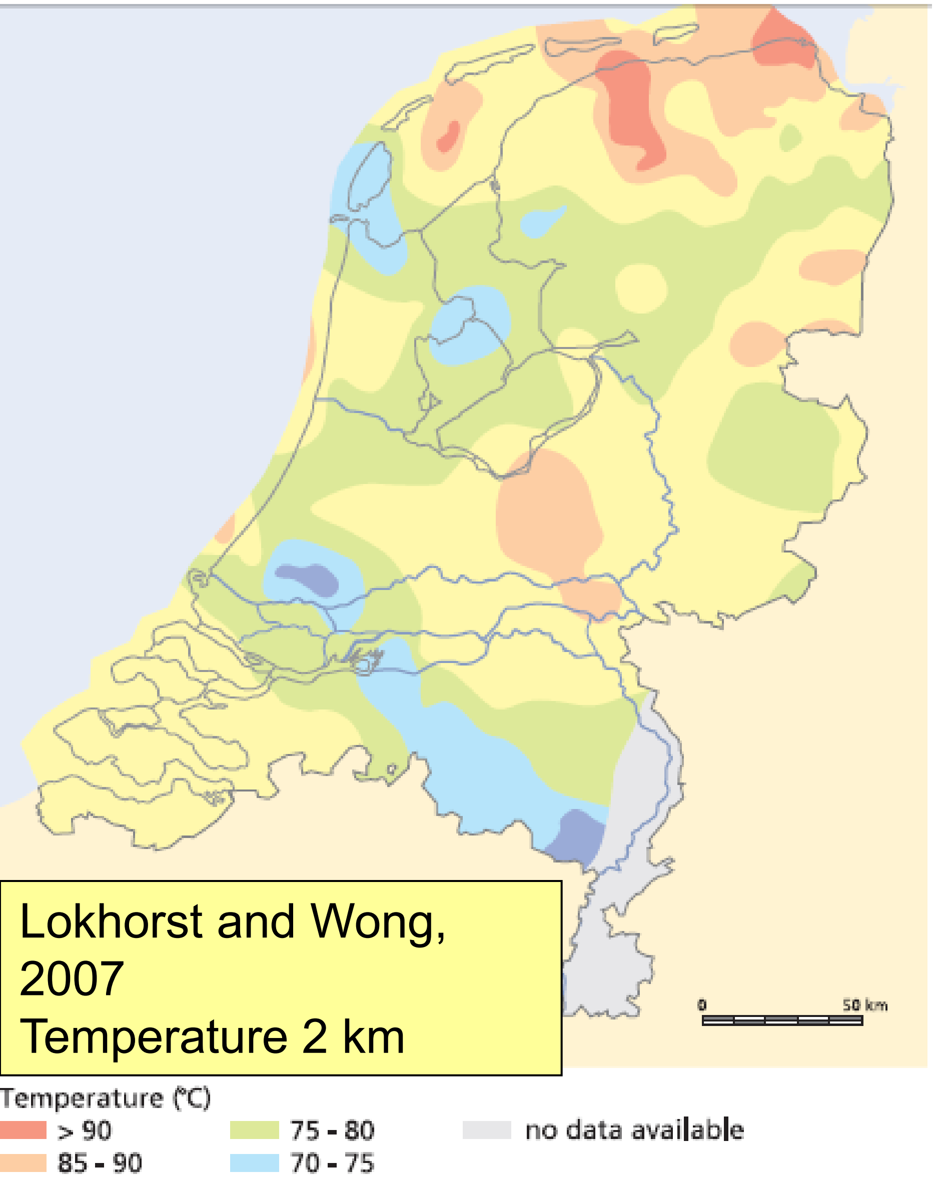

Lokhorst and Wong, 2007
Temperature 2 km

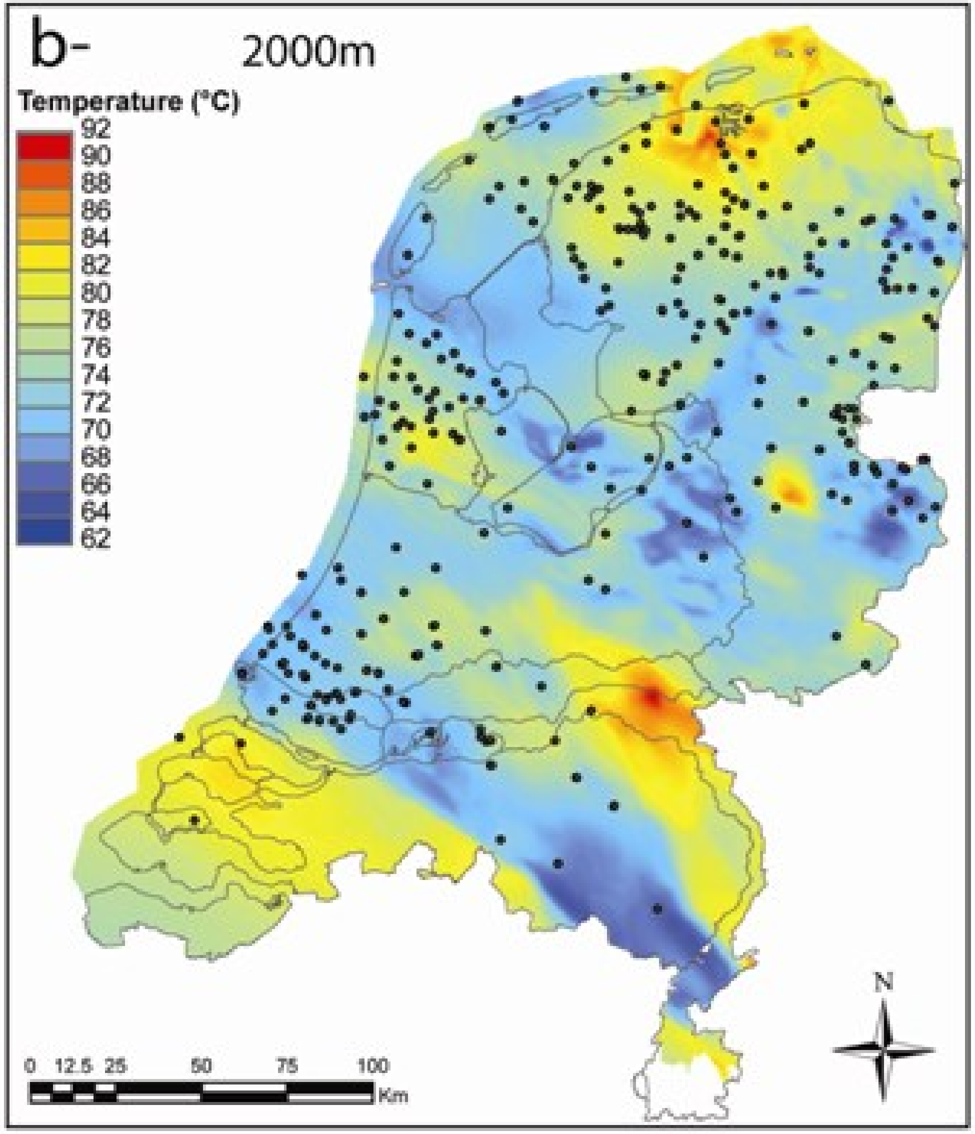

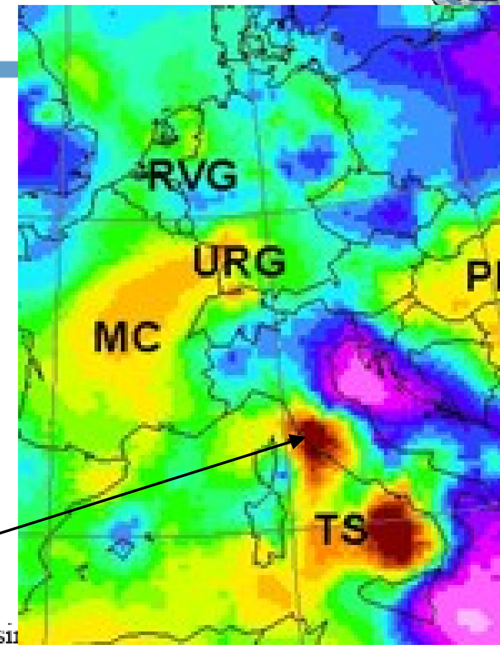

Geothermal fields Larderello **(Italy)**
→ ca 800 MWe

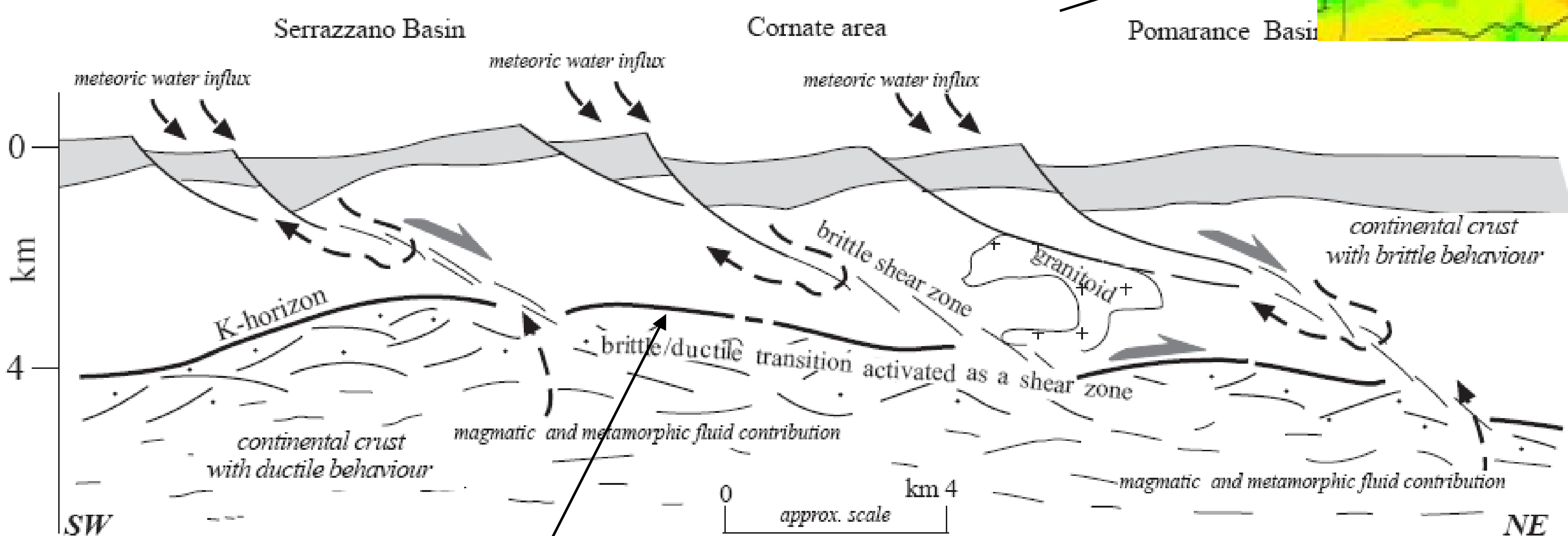

400 C

Ranalli and Rybach, 2005

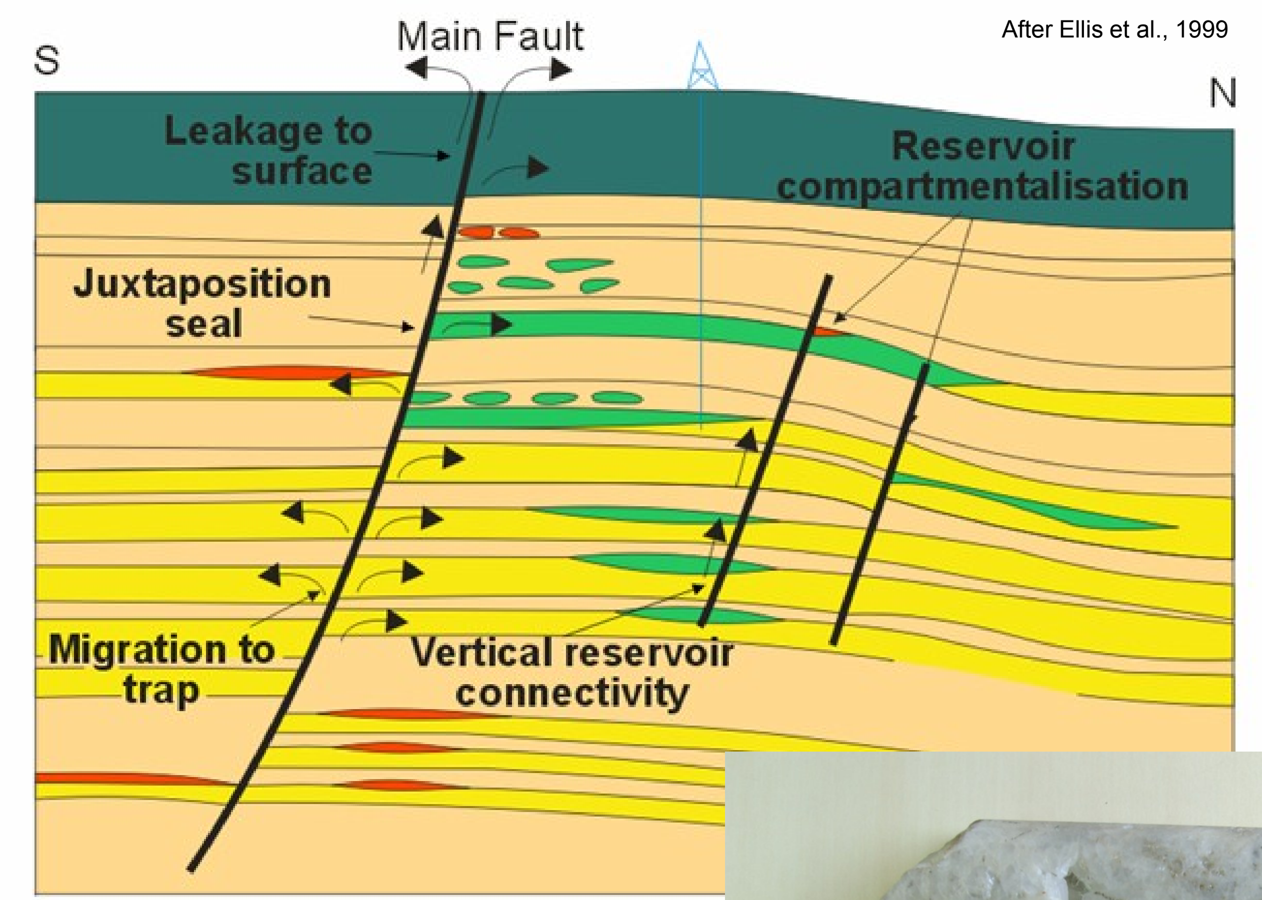

Soultz, core of fault zone
4 km depth (HAFZ)

Active faults allow hydro-thermal conduit zones

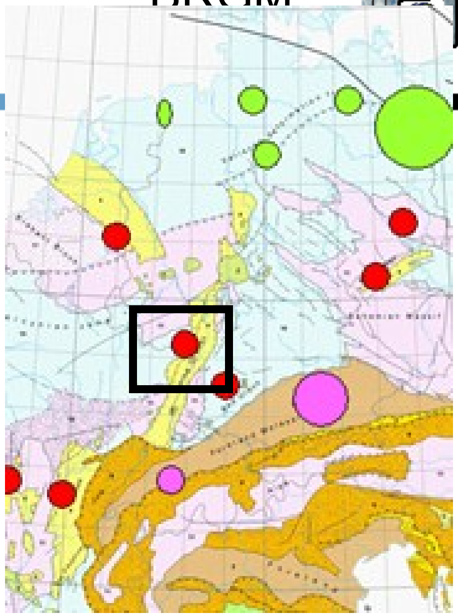

Soultz - Fluid circulation appears to play an important role in enhancing shallow heat flows at the expense of diminishing heat flow at deeper levels

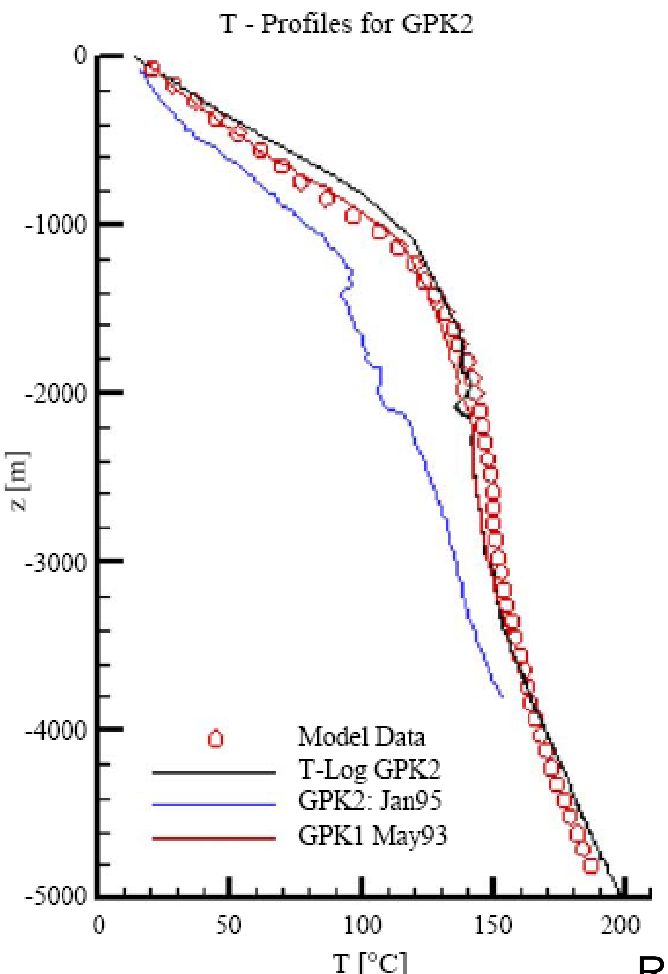

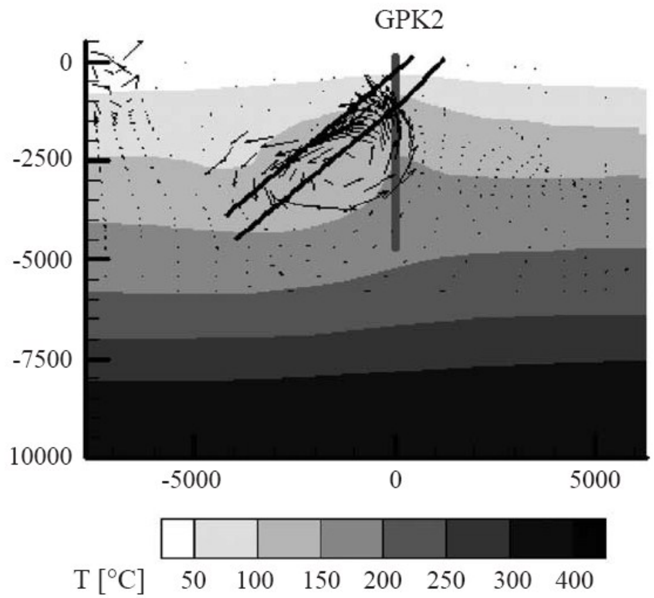

Ranalli and Rybach, 2005

IBERIA: intrap

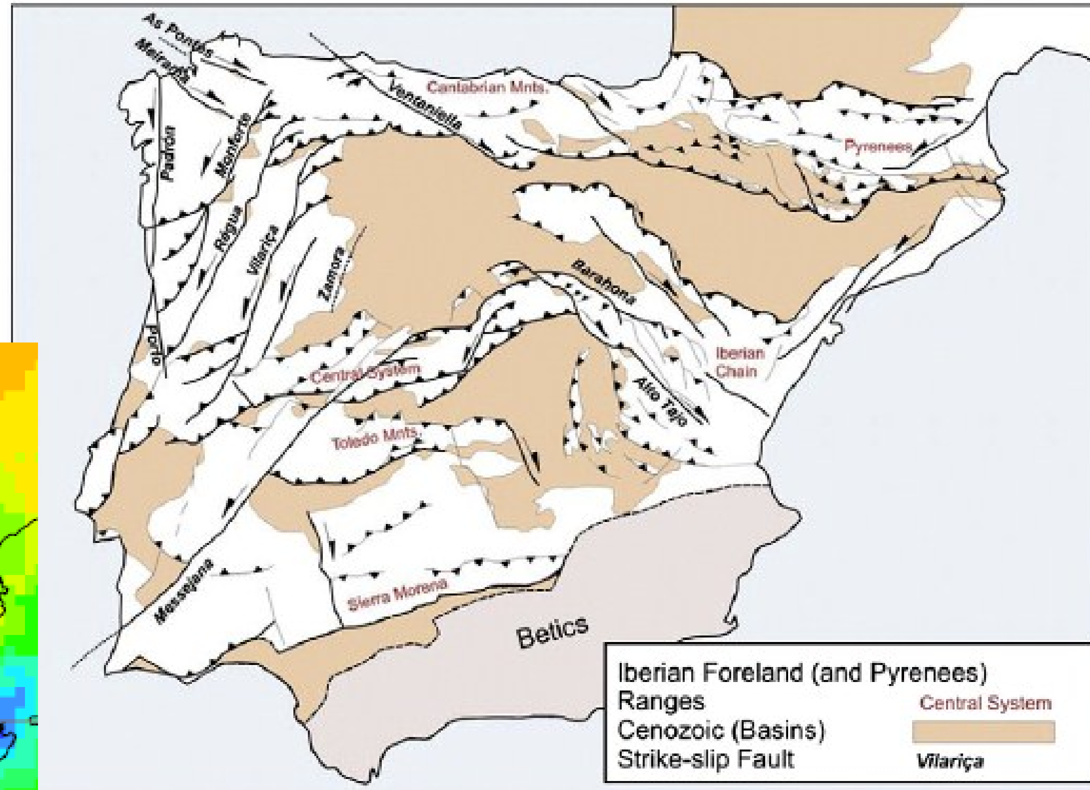

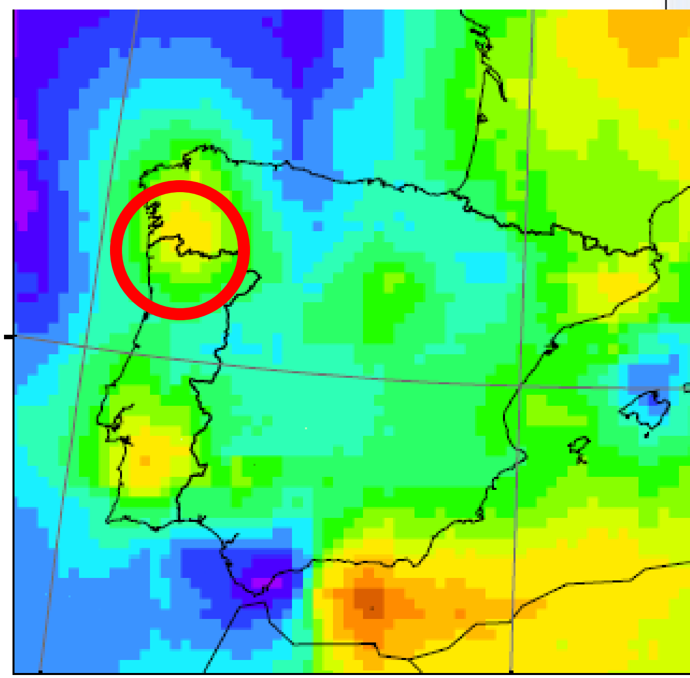

deVicente et al. 2011 (Tectonophysics)

:ive faults, fault g

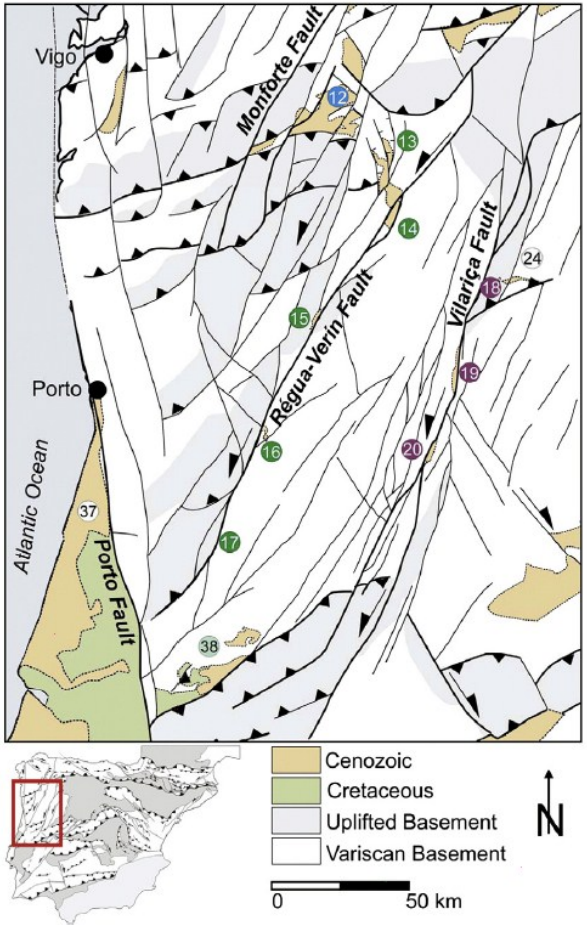

deVicente et al. 2011 (Tectonophysics)

fluid-path ways

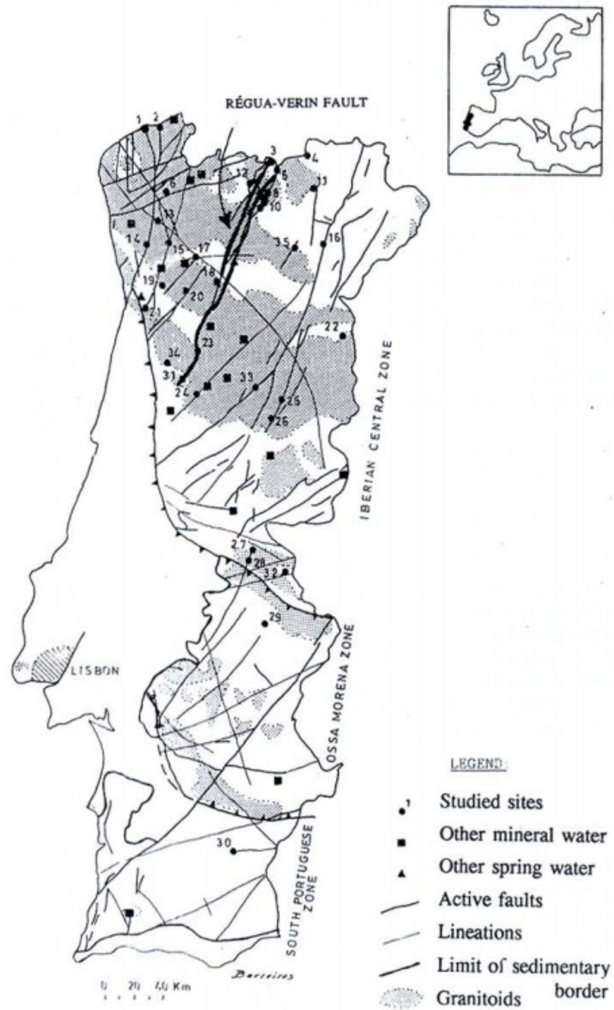

Carvalho 1993

Geophysical and geochemical methods to find high temperatures (advective dominated)

- **How to find high temperatures** (not just from surface heat flow)
  - Magmatic areas and tectonics (geochemistry-covered by Pierre)
  - Volcanoes,Surface phenomena (fumeroles – covered by Pierre)
  - Geothermometers (covered by Pierre

- Micro-seismicity (IDDP)

EM, TEM, MT

- TEM
  - T→Telluric (natural electricity)
  - E→Electric (human electricity)
  - M→Magnetic (natural or induced)

MAGNETIC SURVEYS

Several minerals containing iron and nickel display the property of ferromagnetism. Rocks or soils containing these minerals can have strong magnetization and as a result can produce significant local magnetic fields. Rock magnetism is acquired when the rock forms, and it reflects the orientation of the magnetic field at the time of formation. But rock magnetism can also change with time, **if the rock is subjected to temperatures above a certain point, called the Curie temperature, above which it loses its magnetic properties**, and it is remagnetised once it cools down again, now induced by the magnetic field present at that time.

Magnetic surveying…

Investigation on the basis of anomalies in the Earth´s magnetic field resulting from the magnetic properties of the underlying rocks (magnetic susceptibility and remanence)

MAGNETIC SURVEYS

Measurements are performed using magnetometers either at the surface or airborne, if the objective is regional mapping.

Silicate minerals, rock salt (halite) and limestones (calcite) have a very low magnetic susceptibility and are therefore not useful for magnetic measurements.

Consequently, sedimentary rocks usually have much lower magnetic susceptibilities than igneous or metamorphic rocks. Thus the magnetic method has traditionally been used for identifying and locating masses of igneous rocks that have relatively high concentrations of magnetite, which is the most common of the magnetic minerals.

Strongly magnetic rocks include basalt and gabbro, while rocks such as granite, granodiorite and rhyolite have only moderately high magnetic susceptibilities.

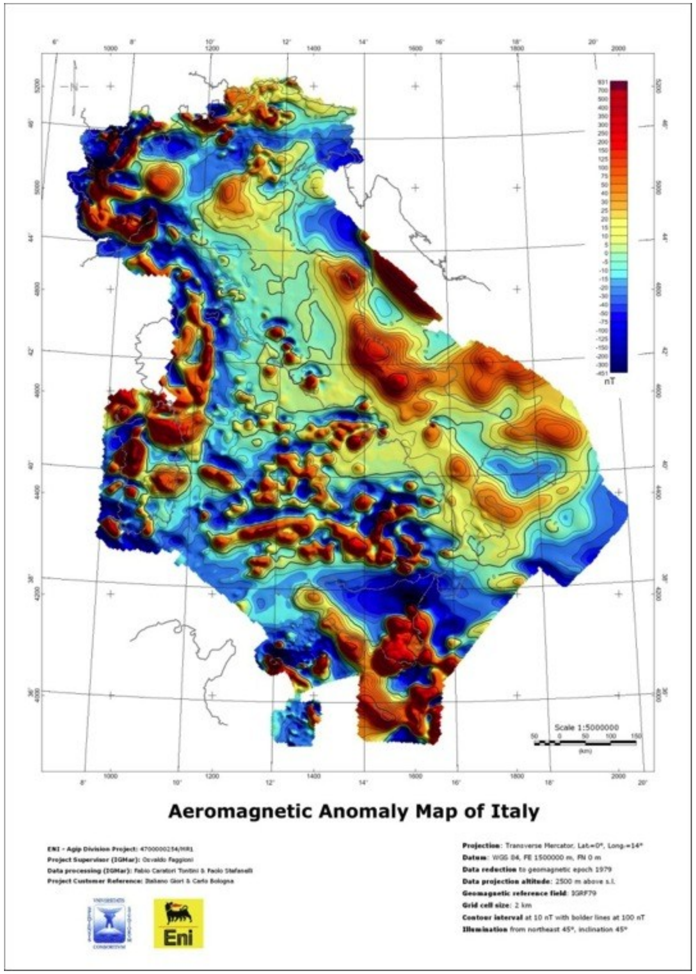

MAGNETIC SURVEYS

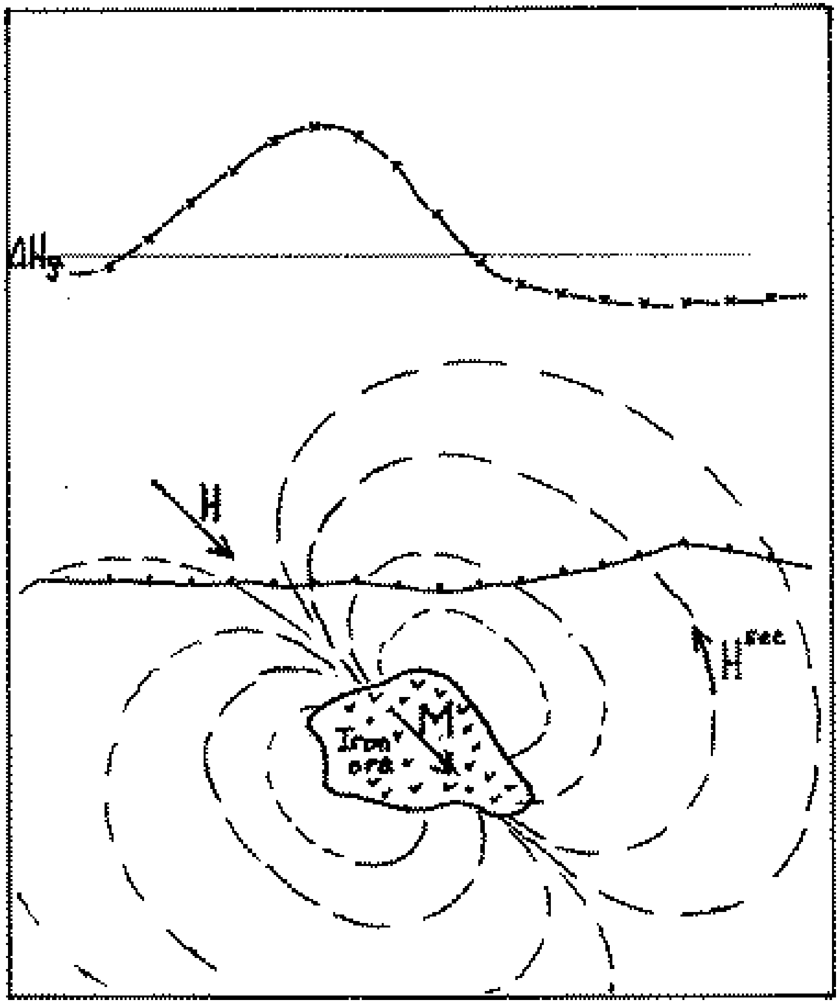

An object in this case, an iron ore deposit, has been magnetized with a magnetization **M** in the direction of the earth's field **H**. The magnetized body has its own magnetic field **H**^{sec}, which for this body has the roughly dipolar form shown by the dashed lines in the figure. These secondary fields add vectorally to the inducing (Earth's) field. Accurate measurements of the magnetic field along a profile over the body will reveal a characteristic pattern or anomaly caused by the body.

MAGNETIC SURVEYS

The shape and magnitude of a magnetic anomaly depends primarily on two factors:

•The shape and orientation/position of the magnetic body and

•The latitude of the location.

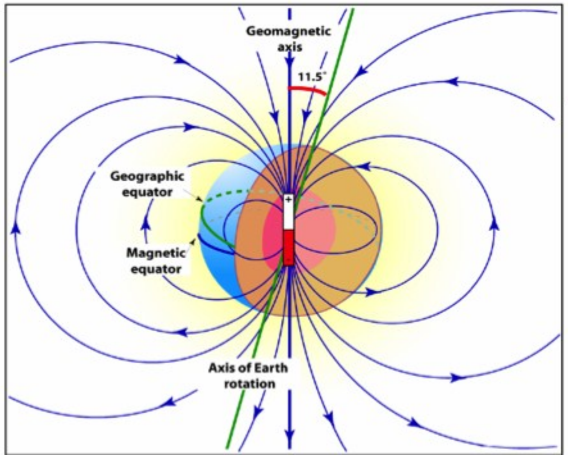

This factor is important because of the dipolarity of Earth's magnetic field. The inducing magnetic field has a dip angle that varies from place to place over the surface of the earth: At the magnetic North pole, it is vertical, and the pattern of magnetic anomalies is symmetrical, while the patterns of anomalies that are recorded become more complex away from the pole.

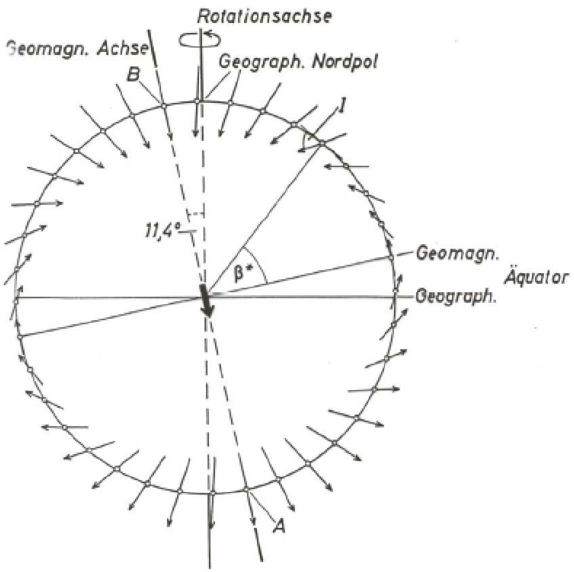

Diurnal variations

- Variations of external origin. Results from the magnetic field induced by the flow of charged particles within the ionized ionosphere towards the poles
- Movements in ionosphere:

  Difference in temperature in atmosphere

  Sun-Moon attraction
- Varies with latitude and seasons (max. in summer, max in polar regions)
- Smooth variations. Amplitude 20-80 nT

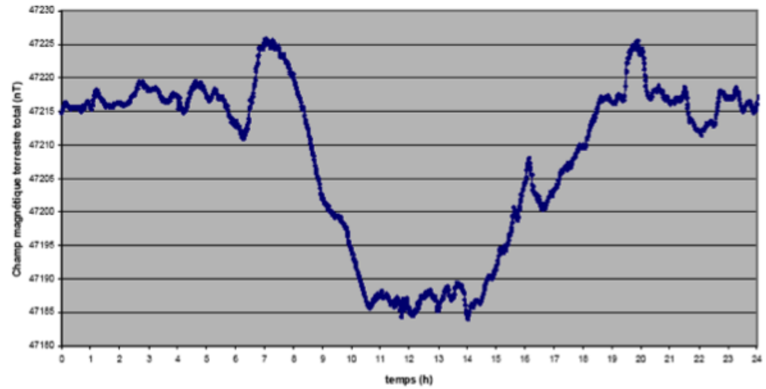

MAGNETIC SURVEYS

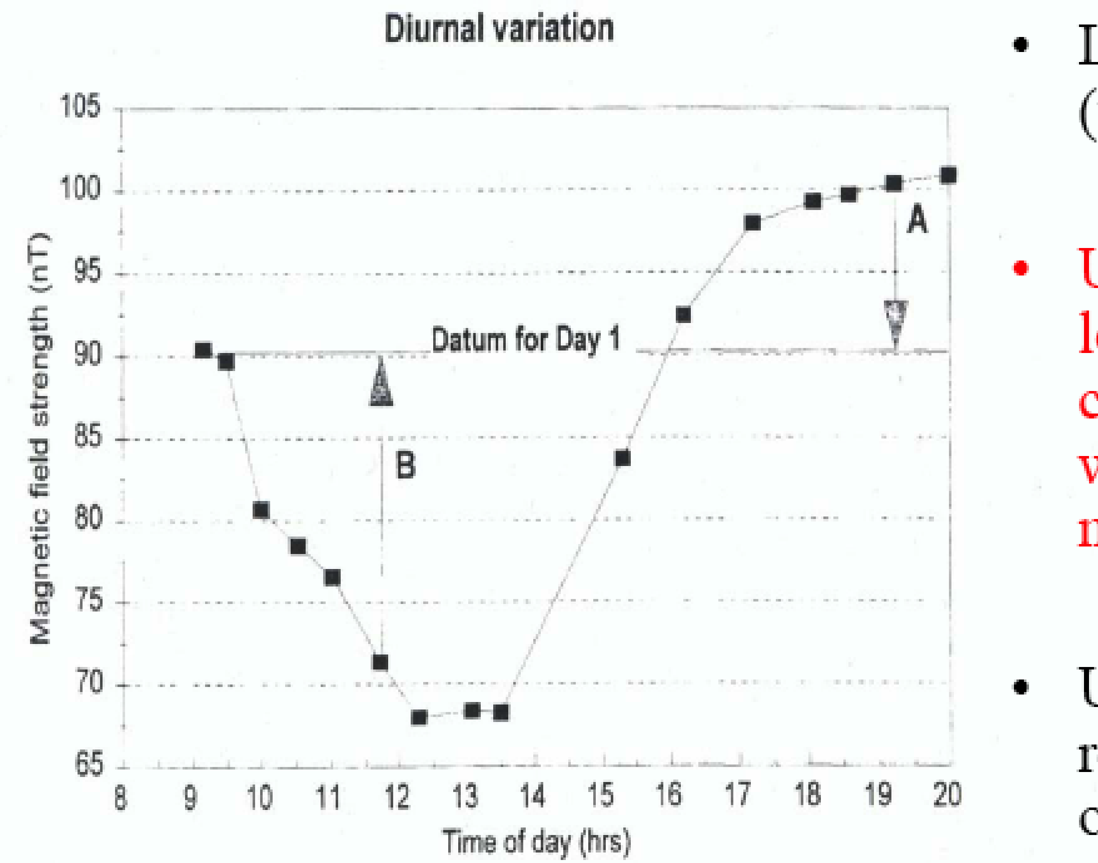

- Loop to a reference basis (tedious…)
- Use a fixed magnetometer located at the basis to correct the data collected with a second magnetometer
- Use the record of a regional magnetic observatory

MAGNETIC SURVEYS

Magnetic storms

- Associated with intense solar activity, results from the arrival in ionosphere of charged solar particles
- Less regular than diurnal variations. Amplitude up to 1000 nT!
- No magnetic surveys during storms (impossibility of correcting the data)

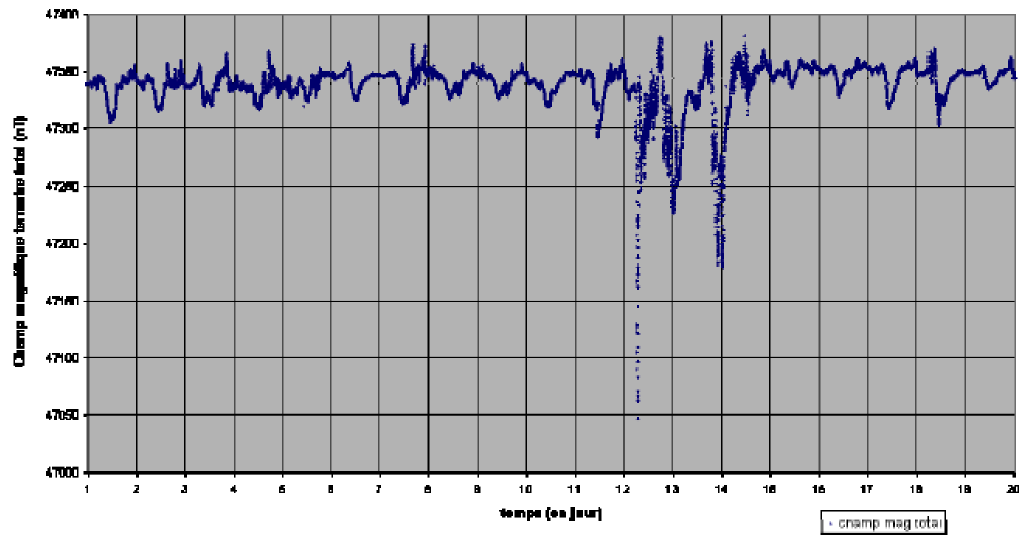

Two types of magnetometers are frequently used in magnetic surveying:

- Proton magnetometer
- Optically pumped magnetometer
- Other device: fluxgate magnetometer

MAGNETIC SURVEYS

MAGNETIC SURVEYS

Curie temperature is in the range of a few hundred to 570°C for titano-magnetite, the most common magnetic mineral in igneous rocks

Magnetisation at the top of the magnetic part of the crust

$\Downarrow$

relatively short spatial wavelengths

Magnetic field from the demagnetisation at the Curie point in depth

$\Downarrow$

longer wavelength and lower amplitude magnetic anomalies

This difference in frequency characteristics between the magnetic effects from the top and bottom of the magnetised layer in the crust can be used to separate magnetic effects at the two depths and to determine the Curie point depth.

ELECTRICAL AND EM METHODS

Why Resistivity? – Porosity

Per la maggior parte delle rocce è valida una relazione empirica, stabilita da *Archie (1942)*, tra il rapporto della resistività della matrice di roccia ρ_b e la resistività del fluido nei pori ρ_f, detto fattore di formazione F, e la porosità, φ. Questa relazione, nota come legge di Archie, è:

$$\frac{\rho_b}{\rho_f} = F = a\phi^{-m}$$

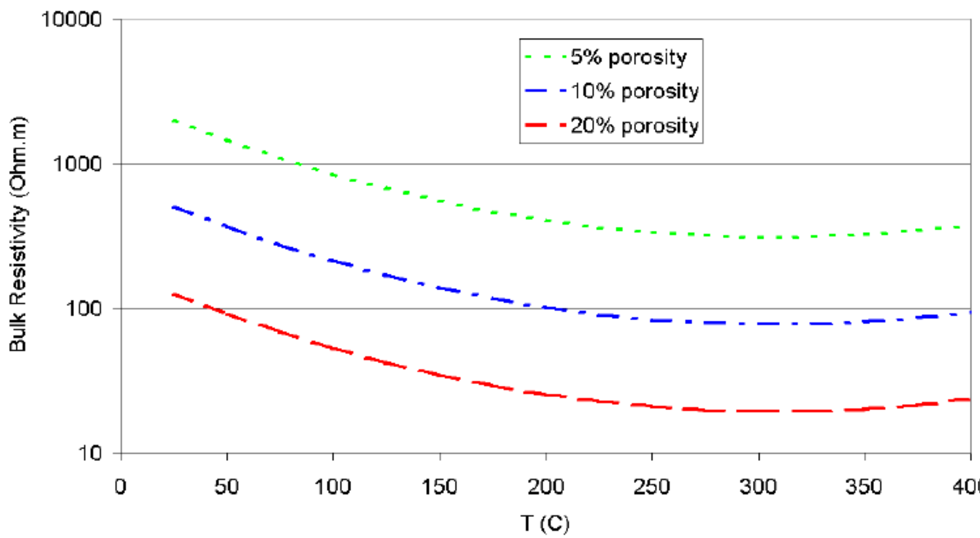

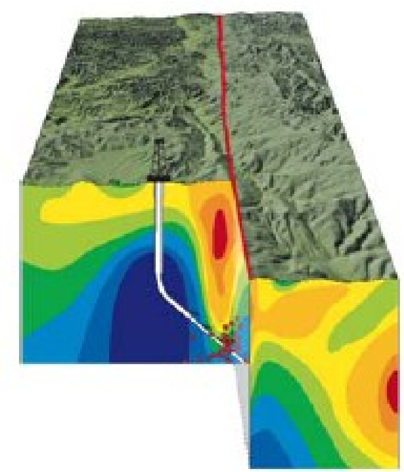

Resistività di rocce saturate con soluzioni di 1000 ppm di NaCl utilizzando la legge di Archie. Tratto da Ussher et al., WGC2000.

Why Resistivity? – Fluid flow

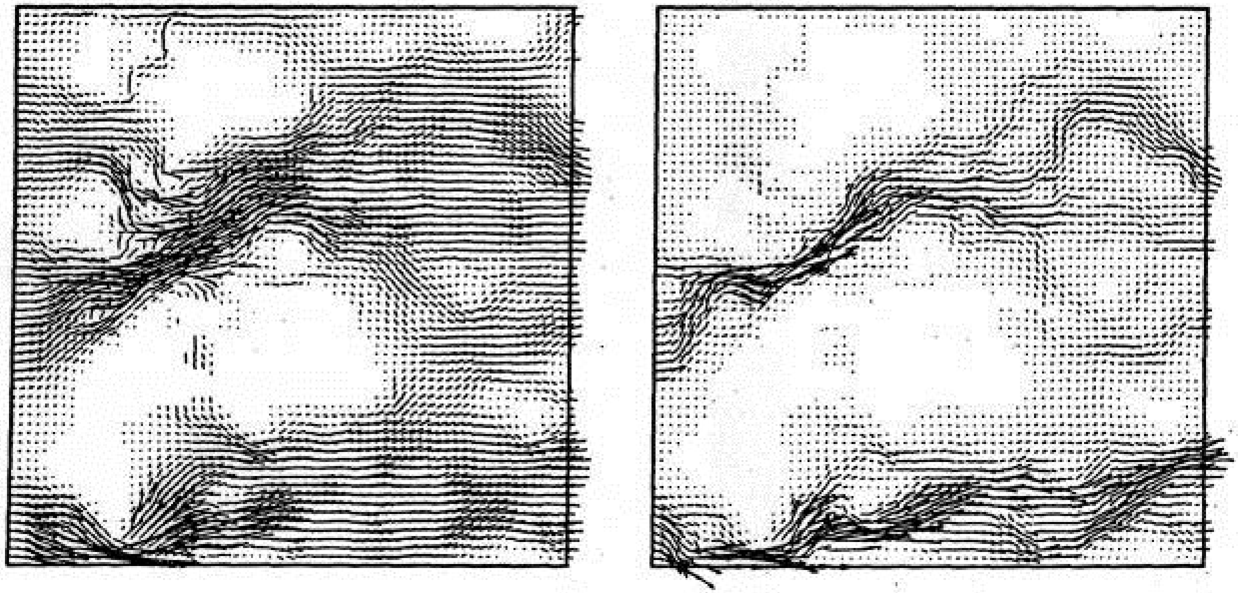

Fig. 5. Electric current and volume flow rate fields for the same fracture as Figure 4. The surface separation is $d_m = 1\sigma$. The magnitude and direction of the local electric current and volume flow rate are represented by small vectors. For comparison, the longest volume flow rate and electric current vectors were scaled to have the same length. Contact areas are shown as blank patches.

Lab measurements have shown that hydraulic and electric flow follow the same paths, but currents are more diffusive

ELECTRICAL (DC) METHODS

The best tested of the techniques is the **Schlumberger** sounding method. With the Schlumberger array, electrodes are placed along a common line and separated by a distance, which is used to control the depth of penetration.

The outer two electrodes drive current into the ground, while the inner two, located at the midpoint between the outer two, are used to detect the electric field caused by that current.

The outer two electrodes are separated by progressively greater distances as a sounding survey is carried out, so that information from progressively greater depths is obtained.

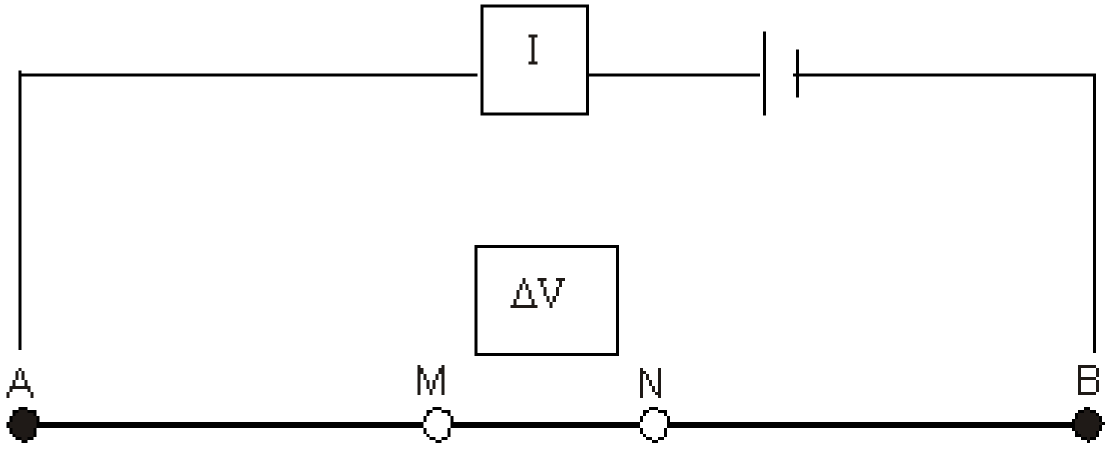

Electromagnetic (EM) sounding methods used in geothermal exploration:

natural-source induction methods
(magnetotellurics, audiomagnetotellurics and self-potential)

controlled-source induction methods
(Tdm, Vlf)

direct current methods
(SeV, electric tomography)

Their objective is the mapping of electrical structures at depths that are meaningful in terms of geothermal exploration.

These depths must be several kilometres at least when looking for the anomaly in conductivity associated with reservoir rocks, and several tens of kilometres when seeking the thermally excited conductive zone associated with the source of a geothermal system.

The **total** EM field measured at the surface (receiver Rx) is the sum of the primary and the secondary field.

E = electric
H = magnetic

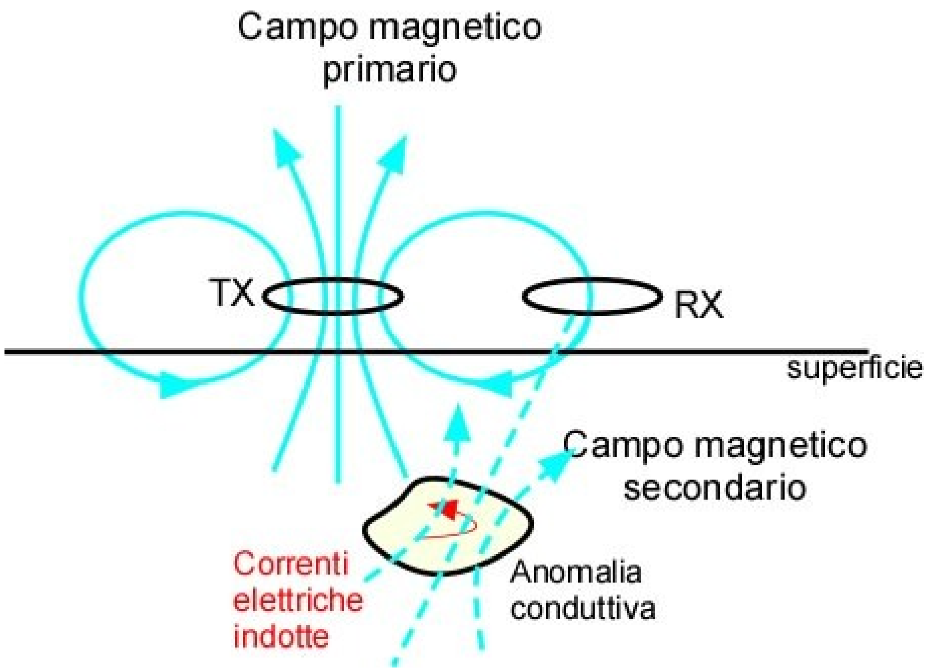

Any EM inductive method follows this scheme.
Depending on the method, the fields can be measured as a function of time or of frequency

ELECTRICAL AND EM METHODS

Magnetotellurics (MT for short) is a technique which utilizes the earth's naturally occurring electromagnetic field to image the subsurface's electrical resistivity structure.

Natural electromagnetic waves are generated in the earth's atmosphere by a range of physical mechanism:

High frequency signals originate in lightining activity

Intermediate frequency signals come from ionospheric resonances

Low frequency signals are generated by sun-spots

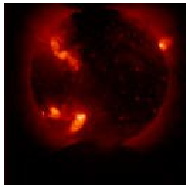

Even if the two types of sources create incident EM fields with different features, the almost plane-wave propagates on the vertical inside the ground, due to the large difference of resistivity between atmosphere and earth.

MAGNETOTELLURIC METHOD

As these waves travel into the Earth's interior they decay at a rate dependent upon their wavelengths.

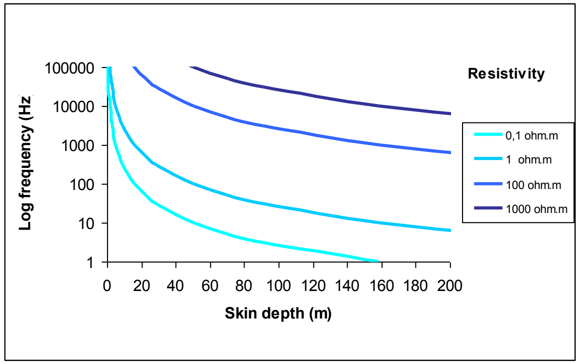

These electromagnetic waves penetrate the earth and return to the surface bearing information on its electrical resistivity structure.

By some tortuous mathematics it is possible to demonstrate that the ratio between electric (E) and magnetic (H) fields at the earth's surface is independent from the source electromagnetic field, but depends only on the electrical resistivity structure of the subsurface.

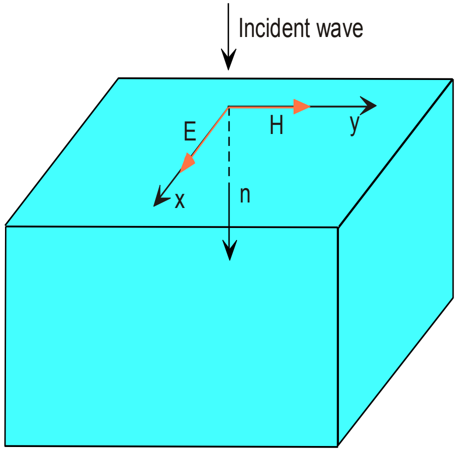

By measuring E and H at the surface we can generate electrical resistivity models of the earth. Electrical resistivity can then be interpreted, guided by other fields observations, such geological and other geophysical constraints.

MAGNETOTELLURIC METHOD

We therefore measure the variation of E and H in time over the sounding spot:

Array geometry

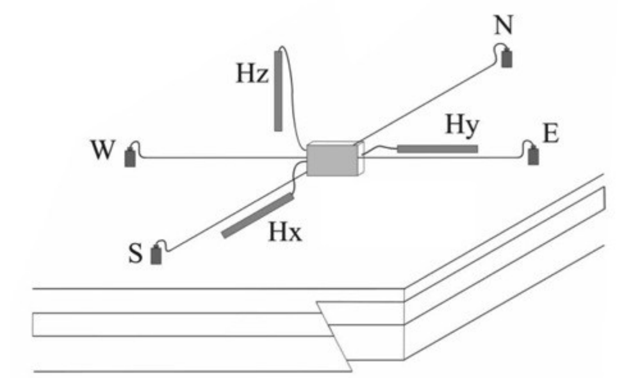

Time-series **FFT**

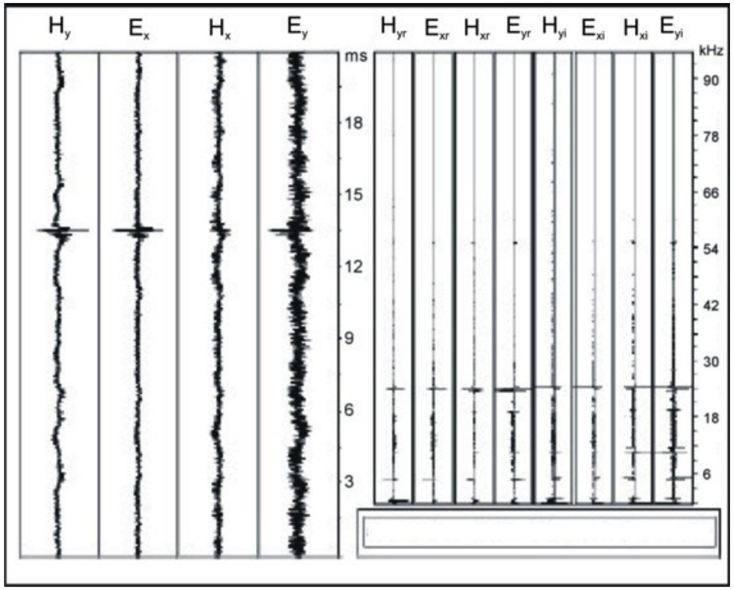

Transfer function Z impedance tensor

$$\begin{pmatrix} E_i(\omega) \\ E_j(\omega) \end{pmatrix} = \begin{pmatrix} Z_{ii}(\omega) & Z_{ij}(\omega) \\ Z_{ji}(\omega) & Z_{jj}(\omega) \end{pmatrix} \begin{pmatrix} H_i(\omega) \\ H_j(\omega) \end{pmatrix}$$

i,j, two perpendicular directions

MT data are acquired in the field, as measurements of electric and magnetic fields with time

$E_x(t)$, $E_y(t)$, $H_x(t)$, $H_y(t)$, $H_z(t)$

Timing is obtained from GPS time signals.

Care must be put on the choice of the site, trying to avoid possible noise sources, such as power lines, electrified railways, pipelines.

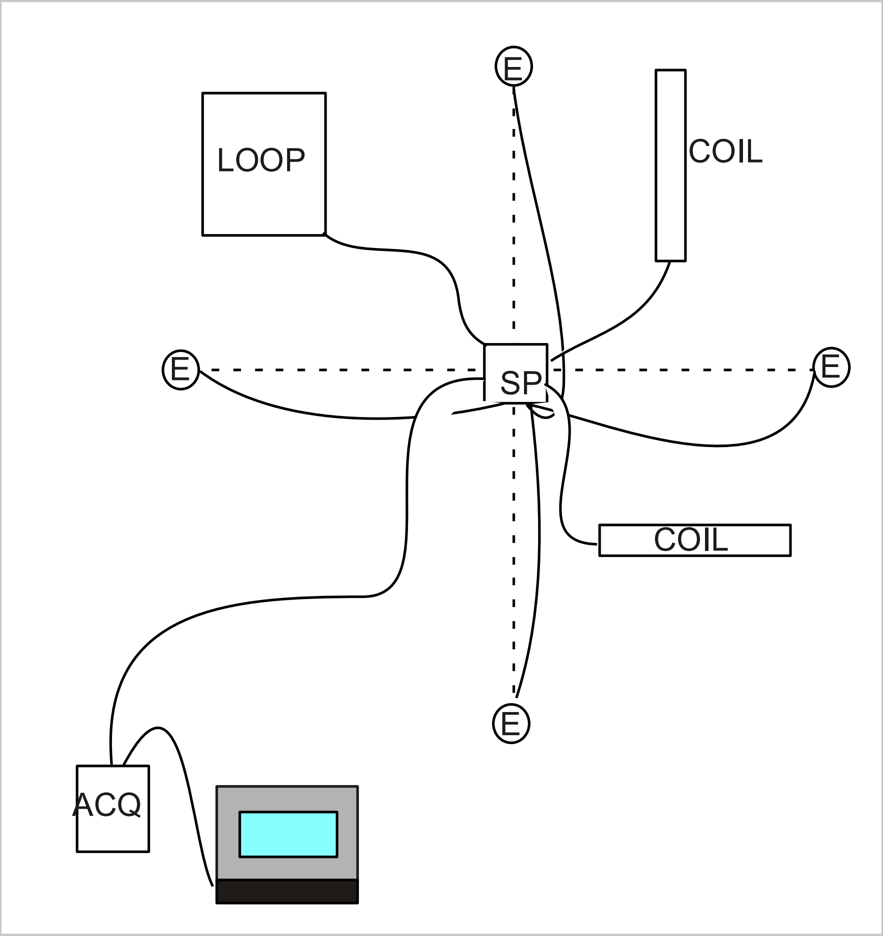

MAGNETOTELLURIC METHOD

As these waves travel into the Earth's interior they decay at a rate dependent upon their wavelengths.
This is the main advantage of MT: large depths can be reached by using a low frequency, without the need of an artificial source

Depth of penetration α sqrt (period x resistivity)

Resistivity of ground $\alpha \left(\frac{E}{H}\right)^2$

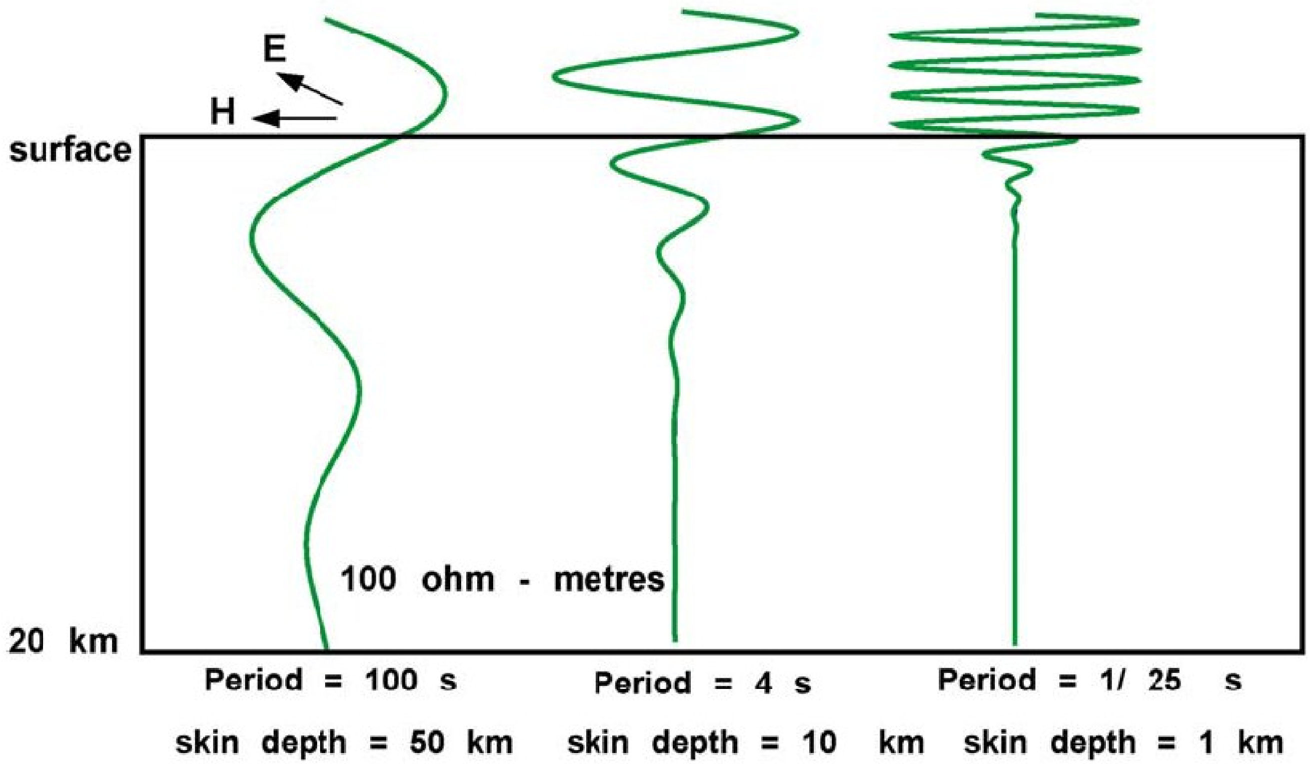

BRGM

It is important to consider which part of the Earth is being sampled in such a measurement. Since the EM fields attenuate in the Earth with a length scale of a skin depth (δ), this measurement samples a **hemisphere around the observation site, radius δ.**

Data derive not only from the geometrical-physical features on the vertical of the recording site, but depends also on the later features: this lateral dimension increases with depth (decreases with frequency)

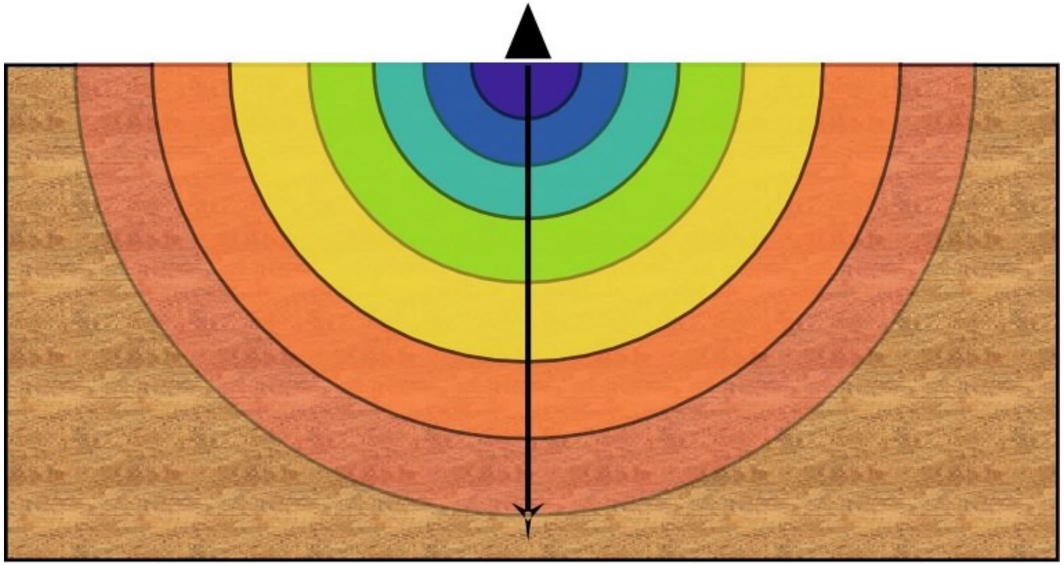

MAGNETOTELLURIC METHOD

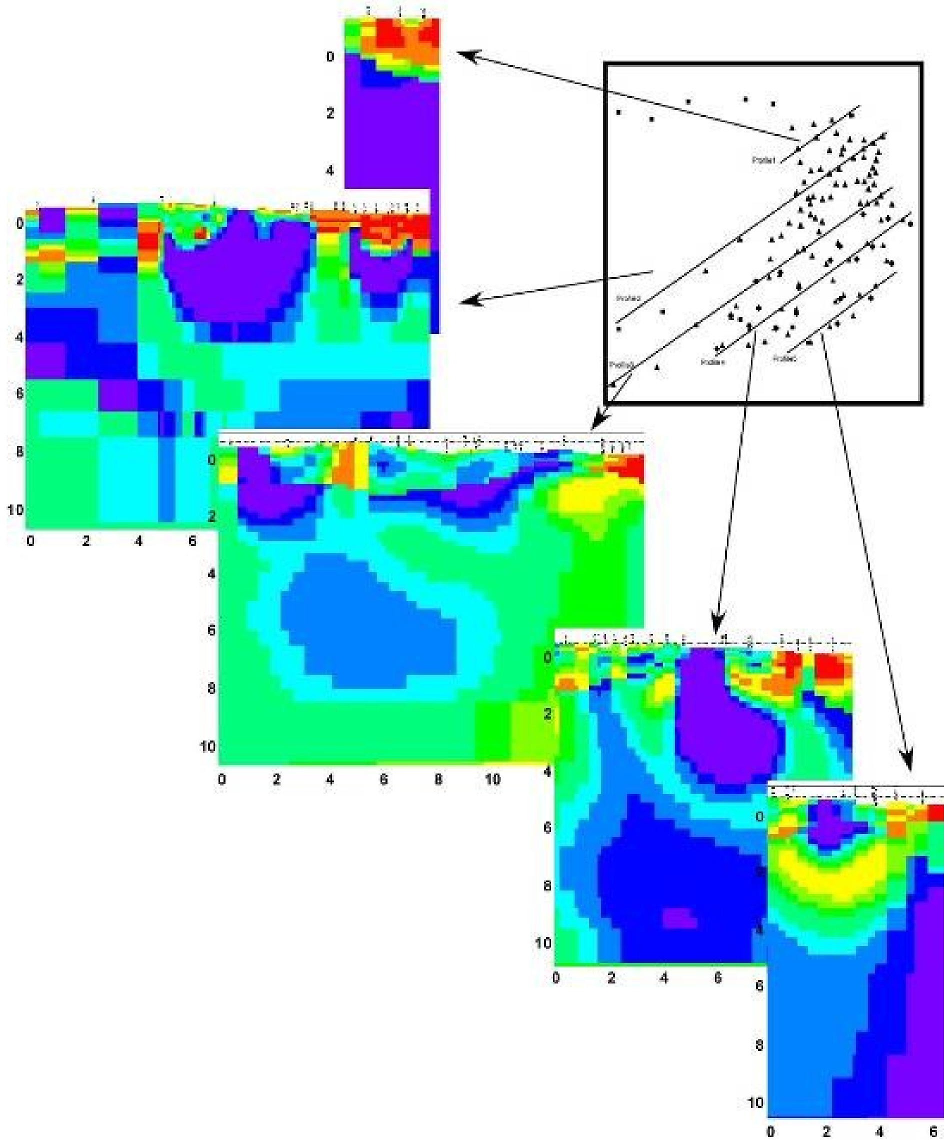

Magnetotelluric data, after processing and modelling, provide the resistivity distribution at depth of various km.

Example: 2D inversion models in Larderello, Italy

ACTIVE EM METHODS - TEM

Active electromagnetic (EM) methods are used mainly for shallow depth resistivity studies and to help with static shift corrections of MT data. Most commonly central loop TEM is used, which is based upon inducing currents in the ground electro-magnetically via a loop laid on the surface. The loop has a square shape, each side measuring several hundred meters. A magnetic spool is placed at the centre of the square, after which DC current is applied to the loop. The current is abruptly switched off and the decaying magnetism induces eddy currents in the formation that try to counteract the magnetic decay. The spool at the loop's centre measures the magnetic decay at the surface with time elapsed since the current was switched off. This permits calculation of the formation resistivity below the loop.

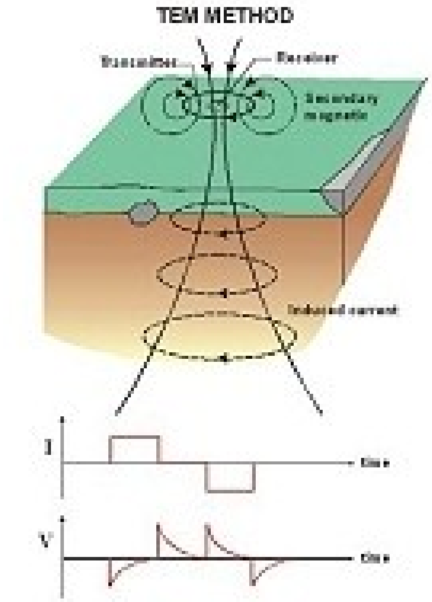

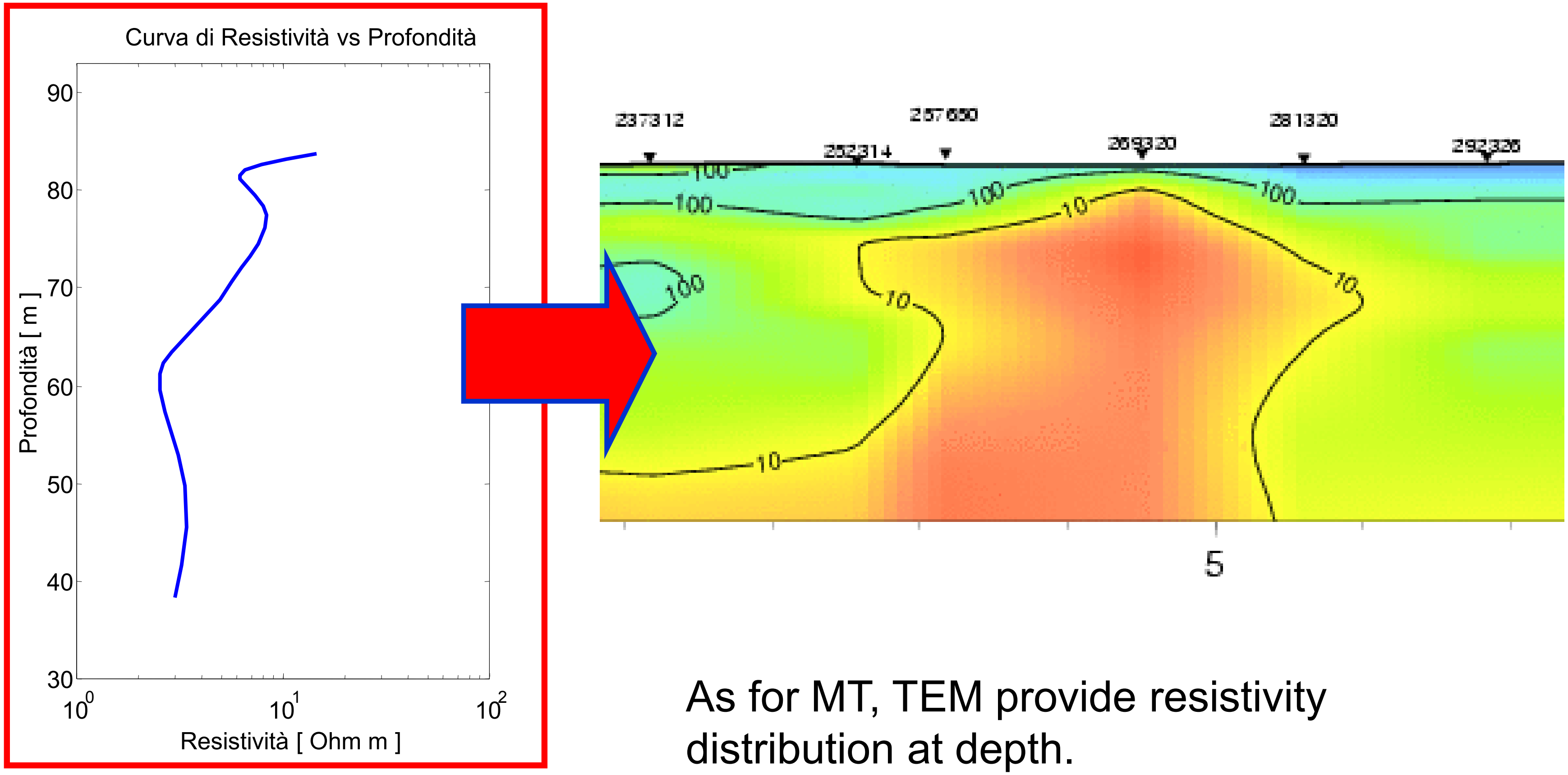

As for MT, TEM provide resistivity distribution at depth.
Byi nterpolation of 1D models along profiles, it is possible to obtain 2D and 3D resistivity distribution at depth.

ACTIVE EM METHODS - TEM

ACTIVE EM METHODS - TEM

Advantages
over DC methods:

- less expensive
- interpretation is less time consuming
- more downward focused
- excellent resolution
- requires significantly less area than other electric methods
- MT Static shift correction
- in DC sounding, the monitored signal is low when subsurface resistivity is low, as in geothermal areas, whereas in TEM soundings the situation is the reverse, the lower the resistivity the stronger the signal

Over MT method:

- cheaper and has a much higher resolution at lower depths.

Disadvantage:
Limited depth of penetration (similar to most electrical methods)
1D models

History of methods in Iceland

- 70s
  - Dipole-dipole resistivity (Schlumberger DC)
  - 1D inversion, penetration up few hundred m depth
- 80s and beyond (first done in Iceland)
  - TEM method: Central-loop transient electromagnetic
  - Much deeper 1D inversion, more cost effective
  - 300x300 m loops at surface
  - Also MT method

B. Oskooi et al. / Physics of the Earth and Planetary Interiors 150 (2005) 183–195

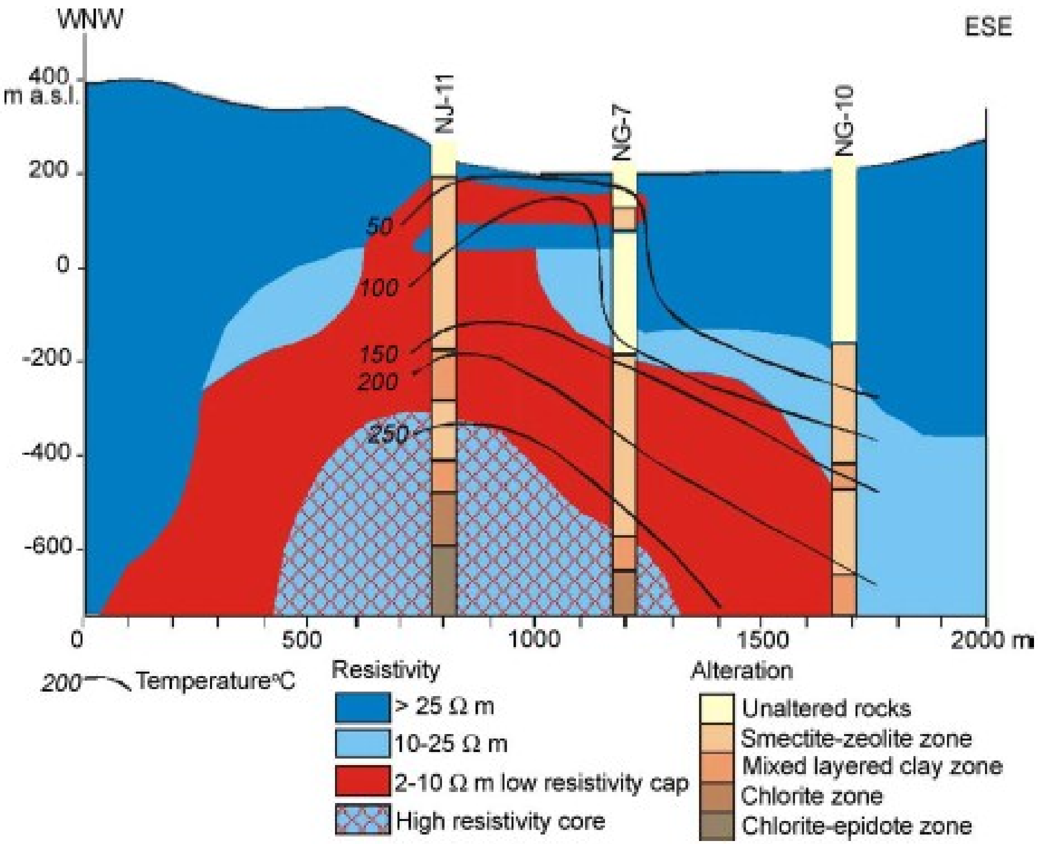

Iceland-non-saline

- Resisitivity
  - top high resistivity (>25)
  - lowering resitivity zone)(<<25)
  - High resisitivity core (>25)

- EM up to 1 km depth
- MT – deeper to 10 k, lower resolution

Surprise: expecting low resistivity
At larger depths

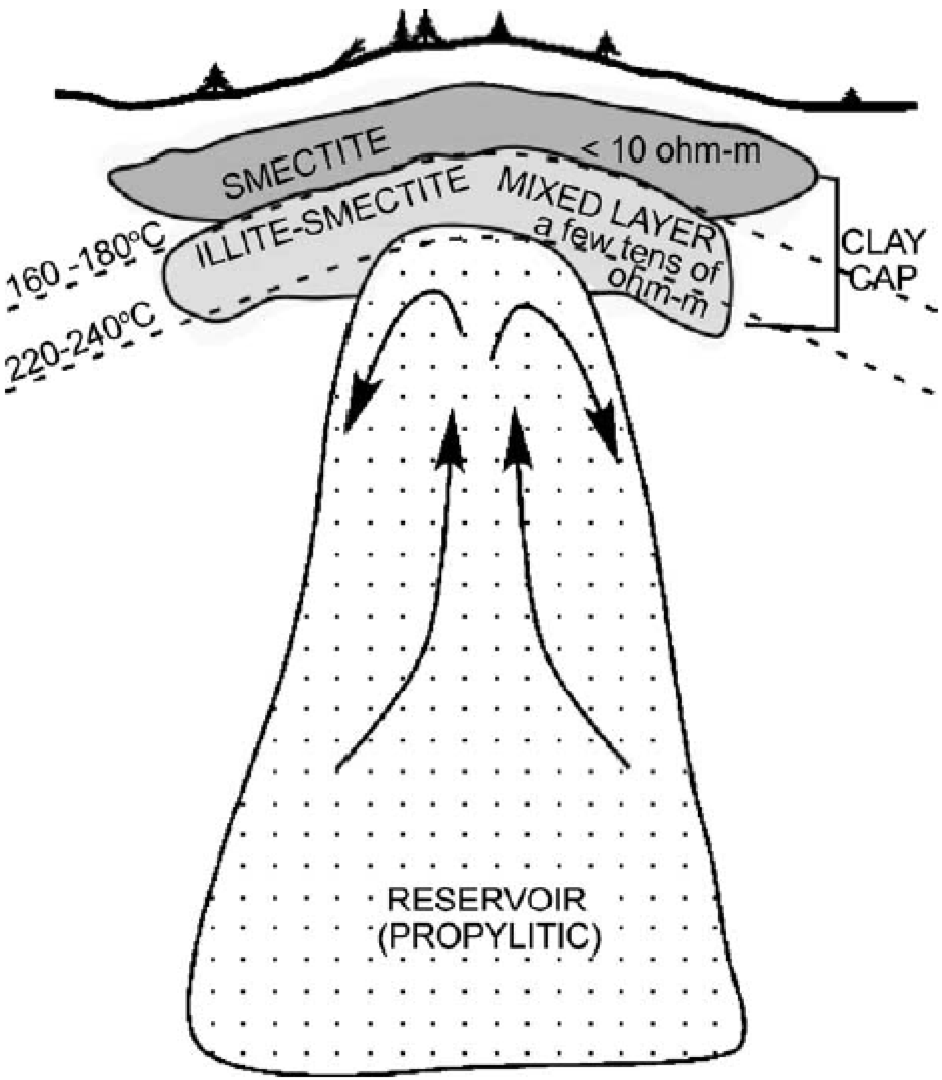

Oskooij et al., 2005

Iceland

- Resisitivity
  - top high resistivity
  - Clay minerals → low resitivity
    - Smectite-zeolite
    - illite-smectite
  - High resisitivity core

- EM (human source) up to 1 km depth
- MT (natural source+human) – deeper to 10 km, lower resolution

B. Oskooi et al. / Physics of the Earth and Planetary Interiors 150 (2005) 183–195

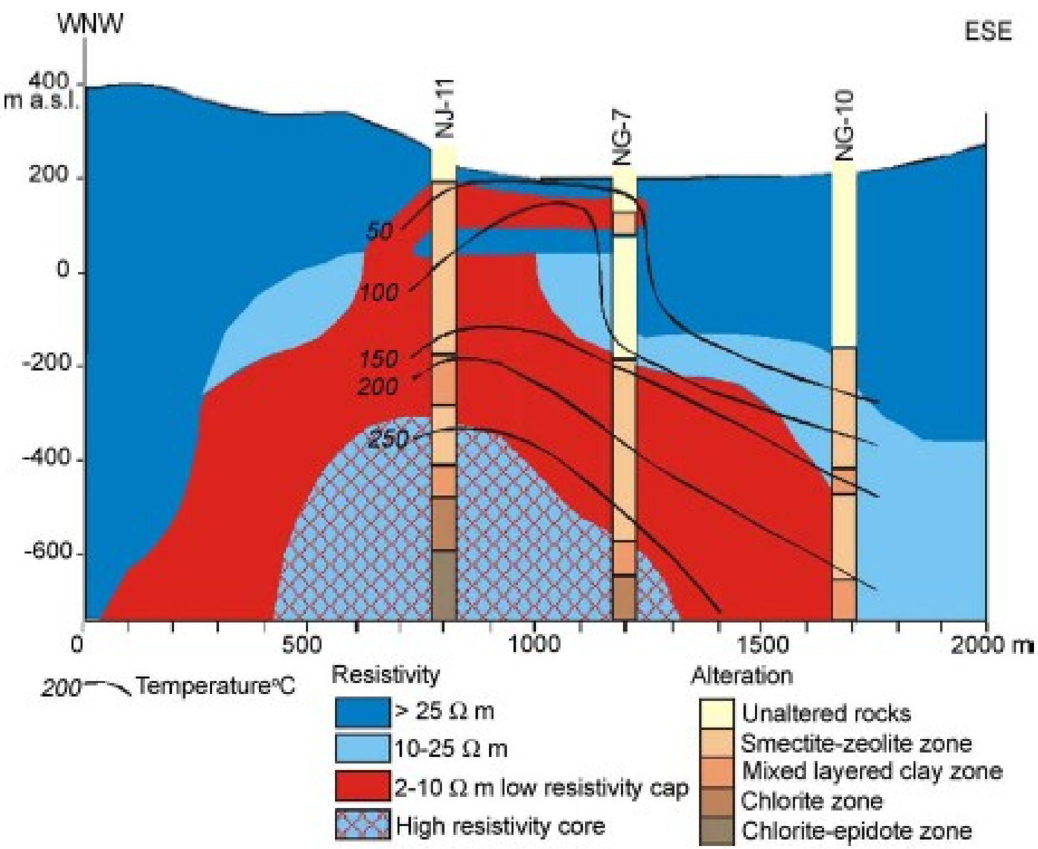

Iceland-non-saline

- Explanation resisitivity - Clay minerals
  - Low resisitivity
    - Smectite-illite-zeolite
  - High resisitivity
    - Chlorite-epidote

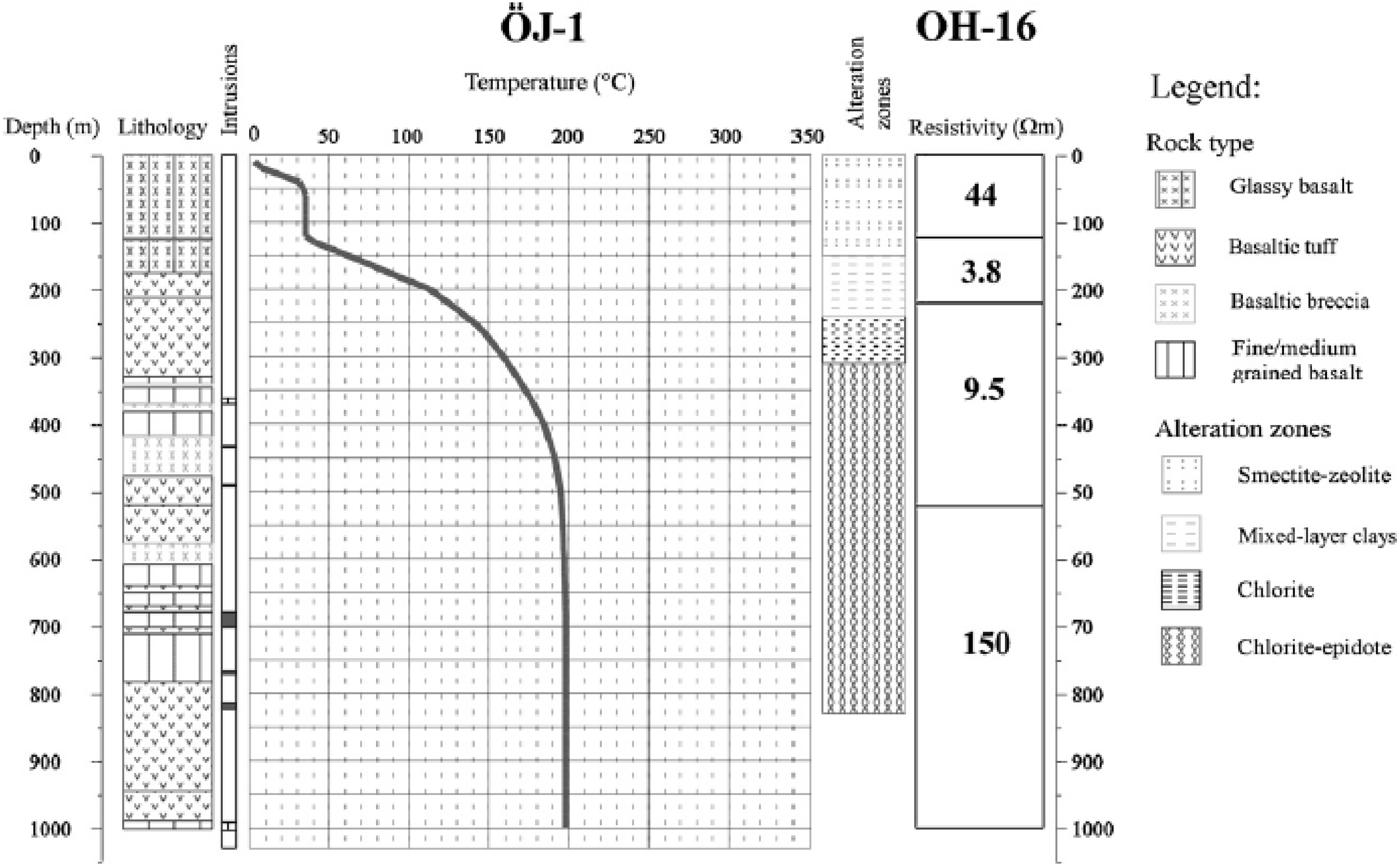

Arnason et al., 2010

Iceland - Hengill

MT – inversion

(Arnason, 2010)

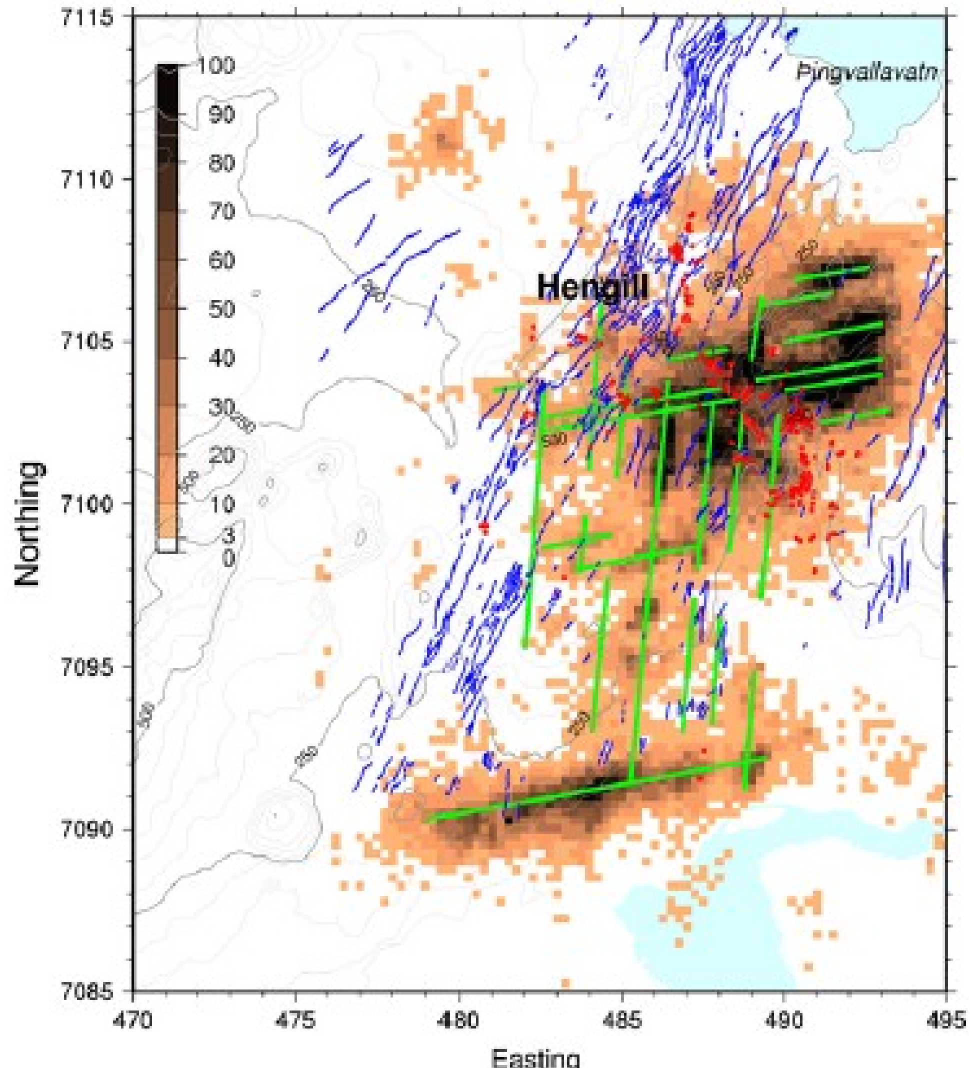

Fig. 3. Density of seismic epicentres (number within 250 m × 250 m bins) from 1991 to 2001 and inferred transform tectonic lineaments (green lines). The lineaments are based on the overall distribution of the seismicity as well as more focused analyses of individual episodes (earthquake swarms). Blue lines: faults and fissures mapped on the surface; red dots: geothermal surface manifestations (Sæmundsson, 1995). Thin black lines: topographic contour lines in m a.s.l. Distances are given in km. Modified from Árnason and Magnússon (2001). (For interpretation of the references to color in this figure legend, the reader is referred to the web version of the article.)

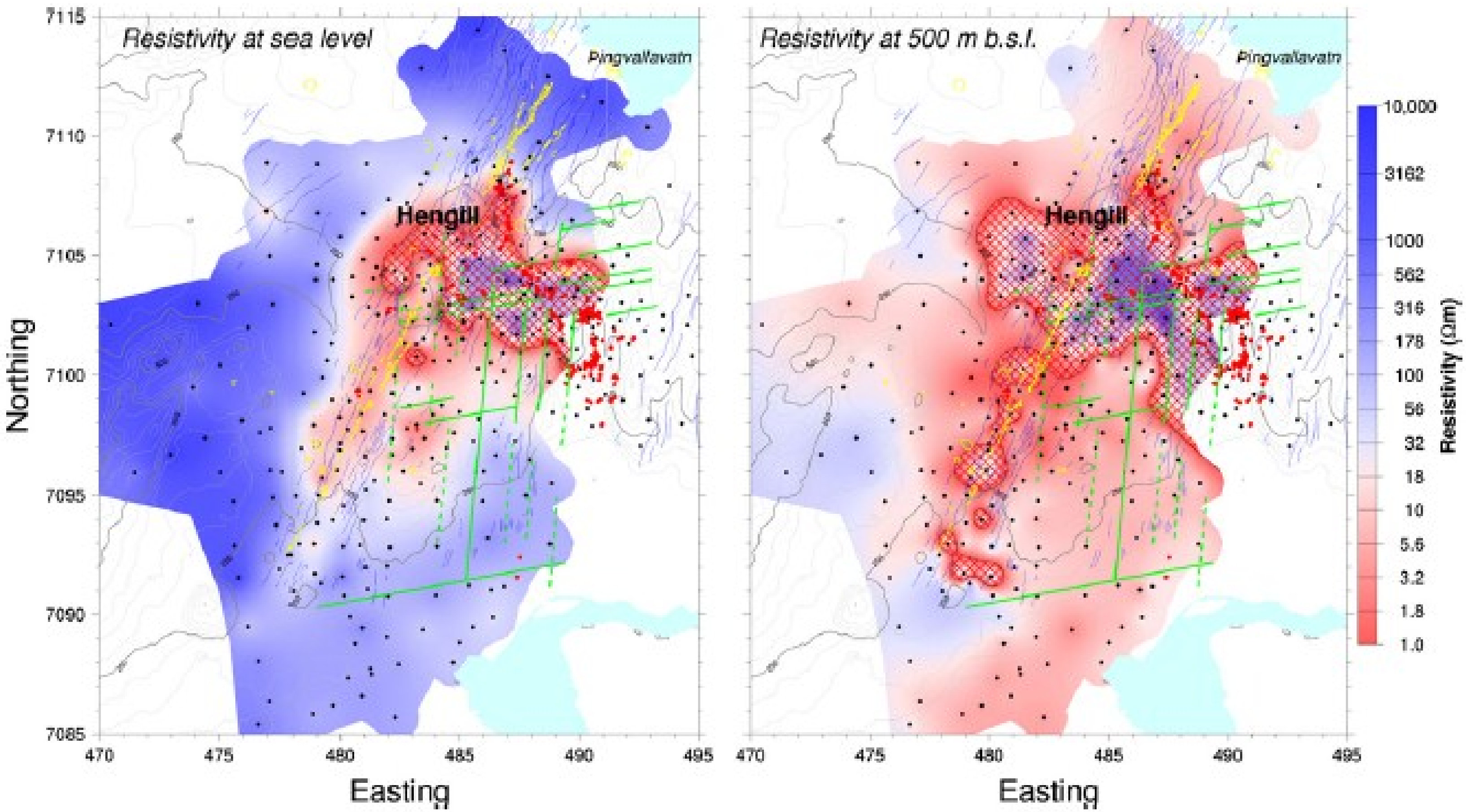
Resistivity at sea level
Resistivity at 500 m b.s.l.
Þingvallavatn
Hengill
Northing
Easting
7115
7110
7105
7100
7095
7090
7085
470
475
480
485
490
495
Resistivity (Ωm)
10,000
3162
1000
562
316
178
100
56
32
18
10
5.6
3.2
1.8
1.0

Supported by INTELLIGENT ENERGY EUROPE

BRGM

MT in tenerife – 500 m a.s.l.

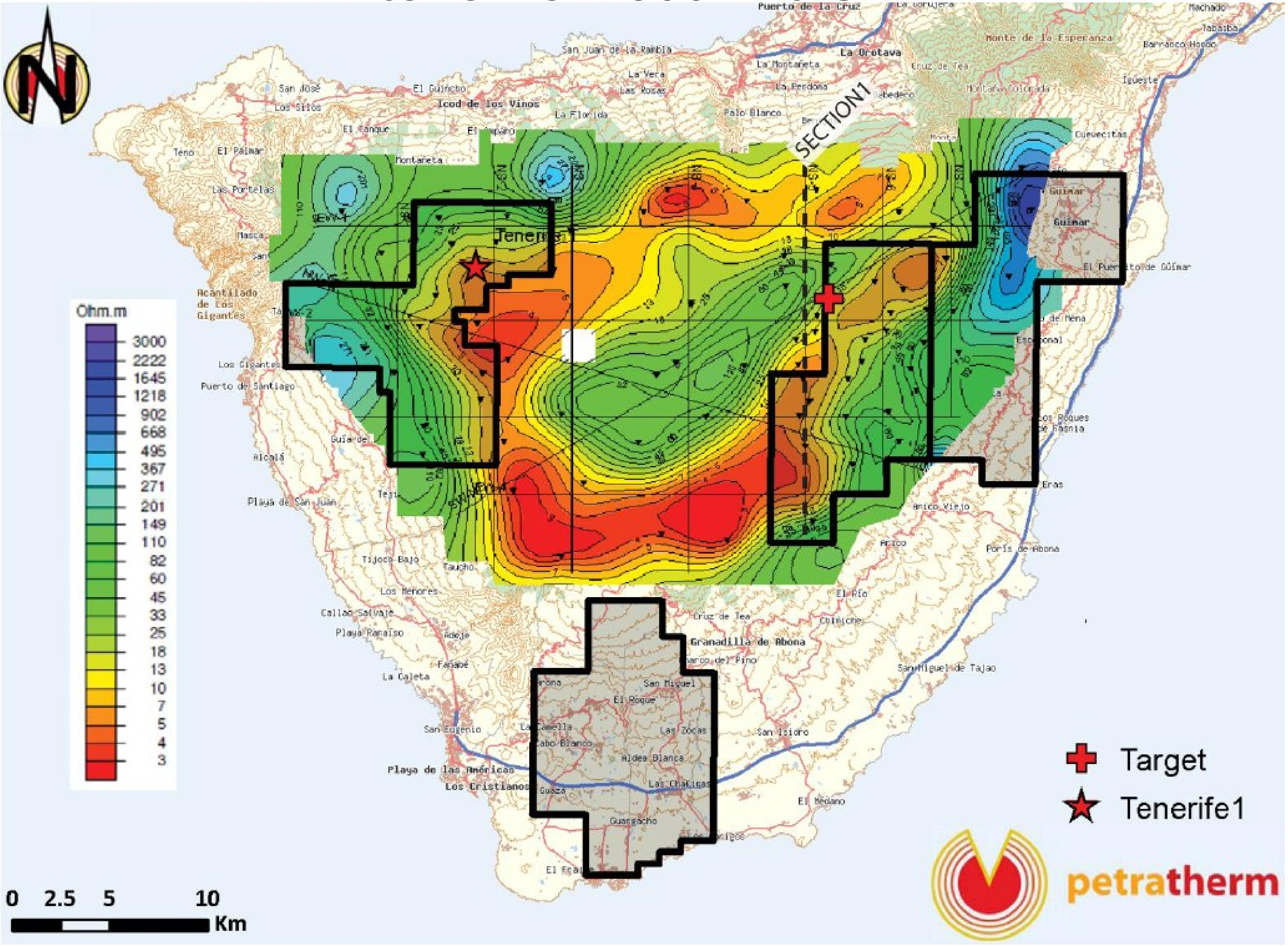

SECTION 1

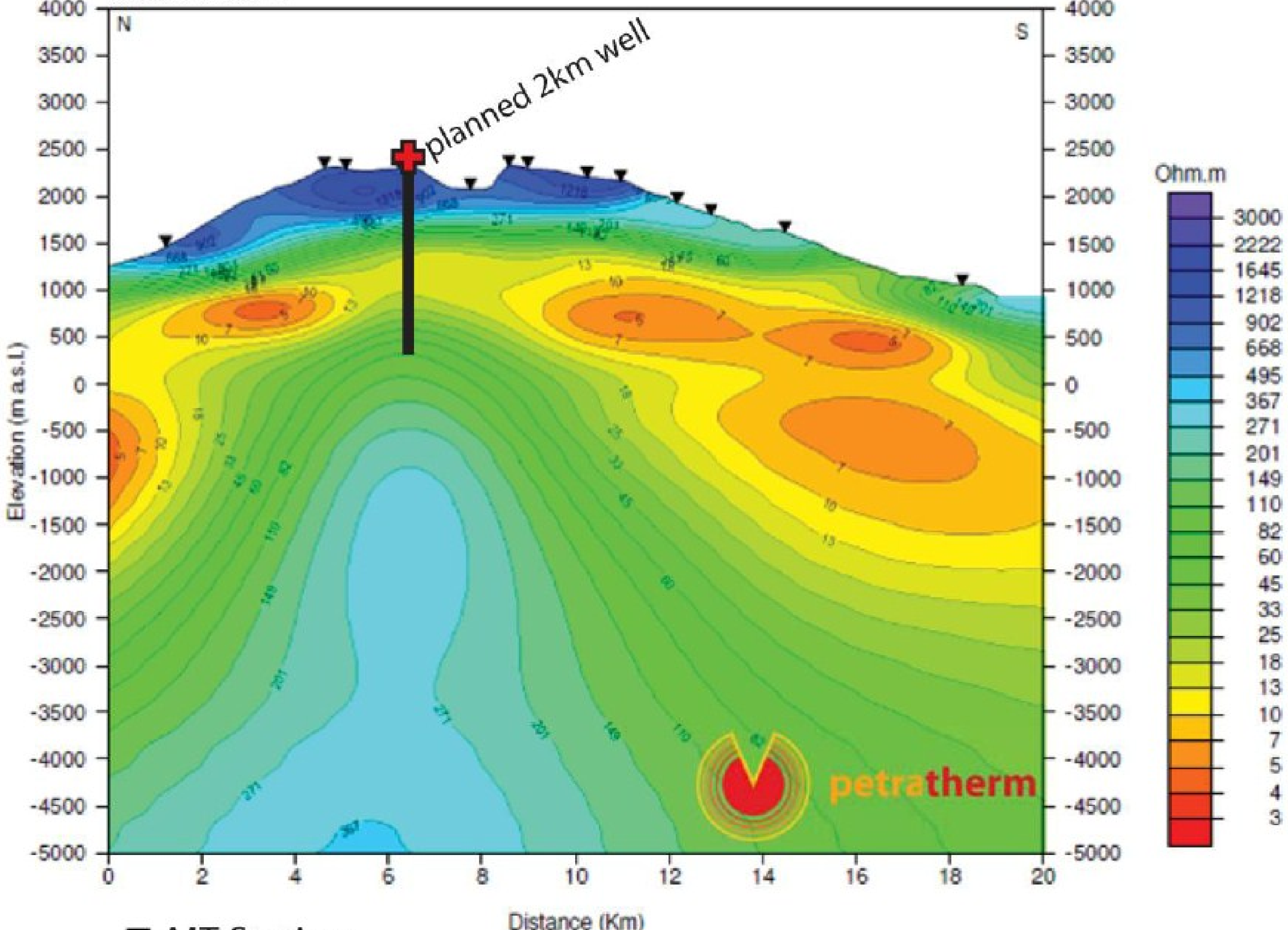

▼ MT Stations

Combination with other techniques

- Seismic structure and velocities
  - Assumption: correlations (e.g. salt high velocity, low resistivity), starting point model boundaries
  - Pitfalls: assumptions (high sensitivity to salt content in pores)
- Gravity
  - Assumptions: Correlations (crustal density, resistive core), flexural isostacy
  - Pitfalls: non-uniqueness
- Microseismicity at above magma chambers
  - Assumptions: occur rheological boundary viscous-brittle)
- Satelite information
  - Vertical movements, temperature

Iceland - Hengill

MT – inversion

(Arnason, 2010)

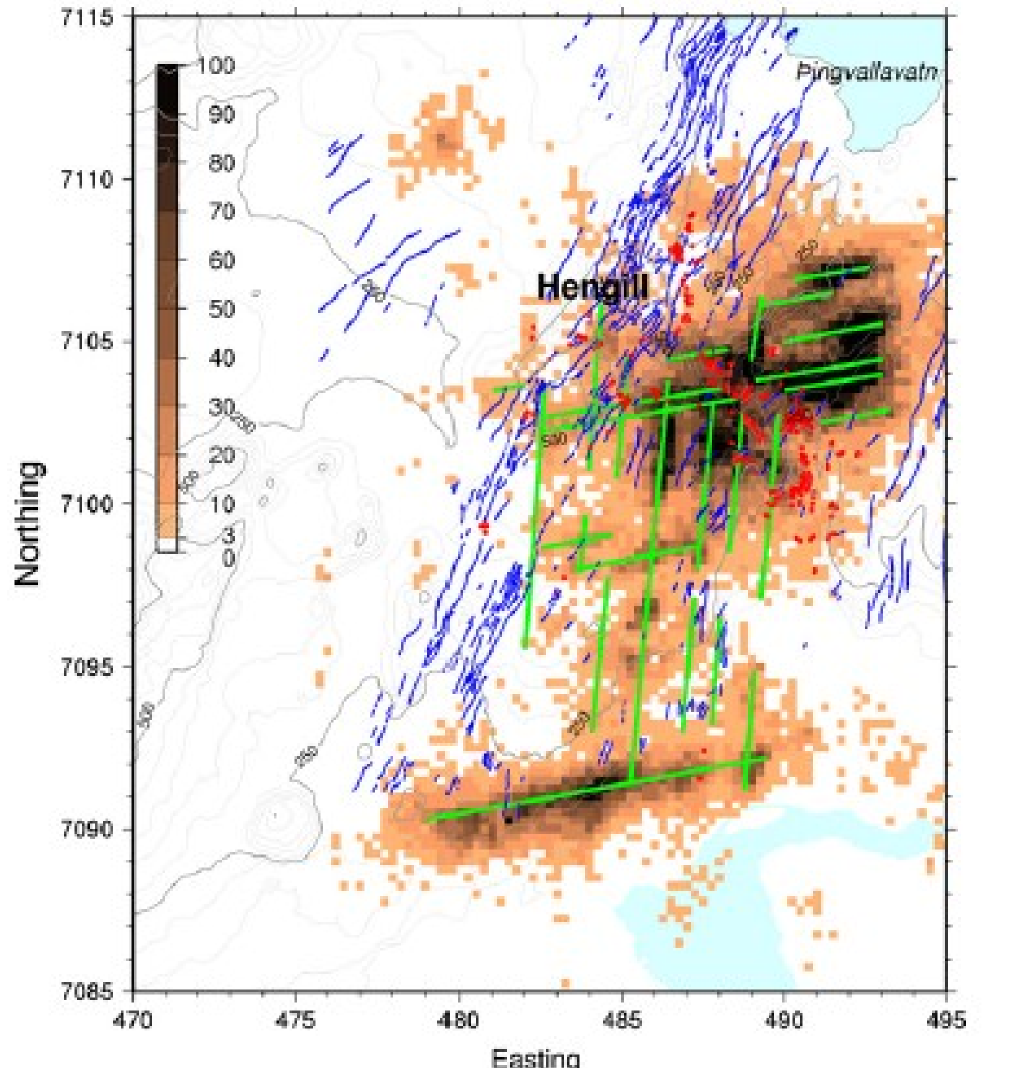

Fig. 3. Density of seismic epicentres (number within 250 m × 250 m bins) from 1991 to 2001 and inferred transform tectonic lineaments (green lines). The lineaments are based on the overall distribution of the seismicity as well as more focused analyses of individual episodes (earthquake swarms). Blue lines: faults and fissures mapped on the surface; red dots: geothermal surface manifestations (Sæmundsson, 1995). Thin black lines: topographic contour lines in m a.s.l. Distances are given in km. Modified from Árnason and Magnússon (2001). (For interpretation of the references to color in this figure legend, the reader is referred to the web version of the article.)

Intra-plate-stresses

World Stress Map project

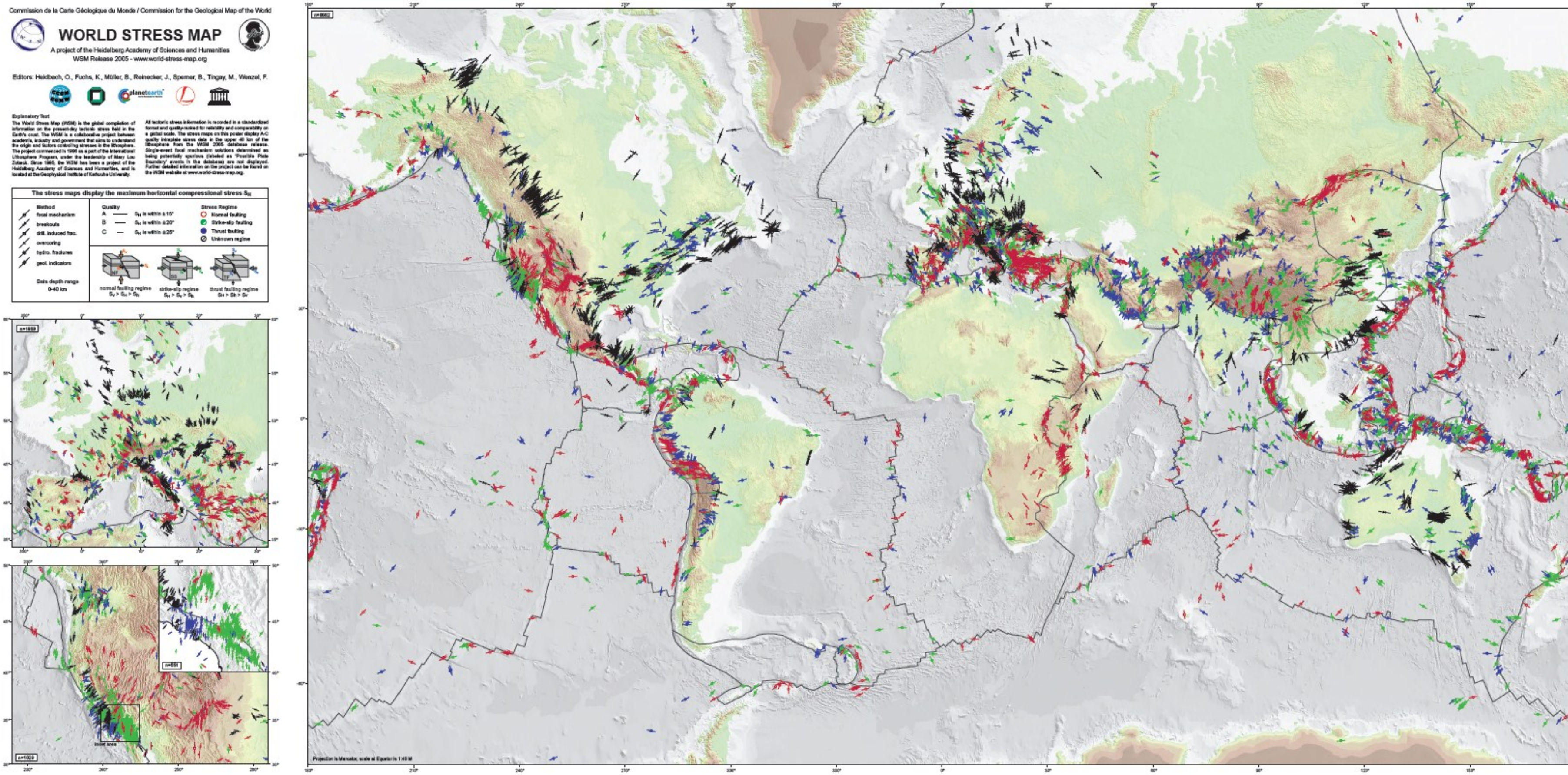

Supported by INTELLIGENT ENERGY EUROPE

BRGM

TNO innovation for life

Enhancing reservoir performance →Stress is critical

Understanding stress

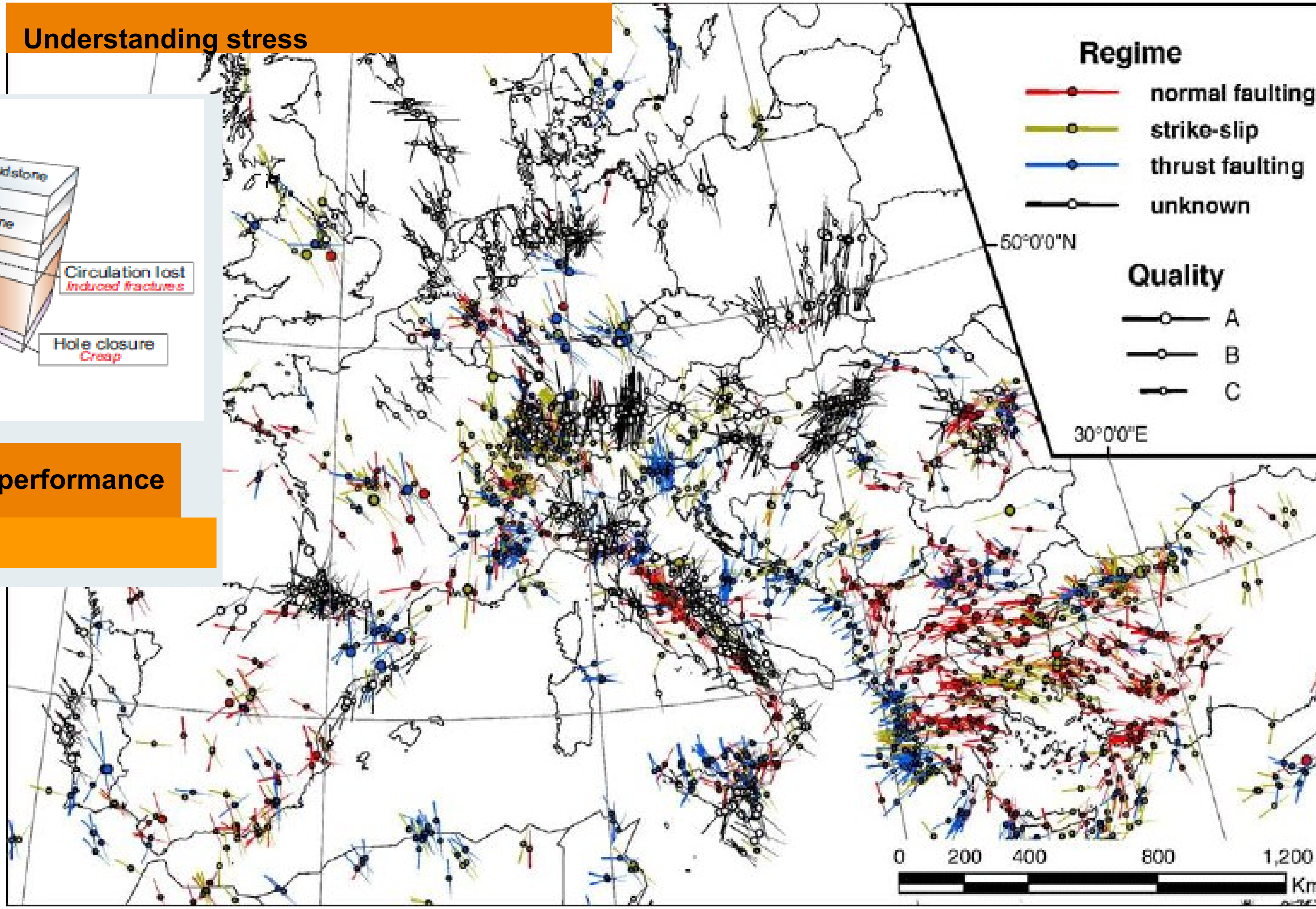

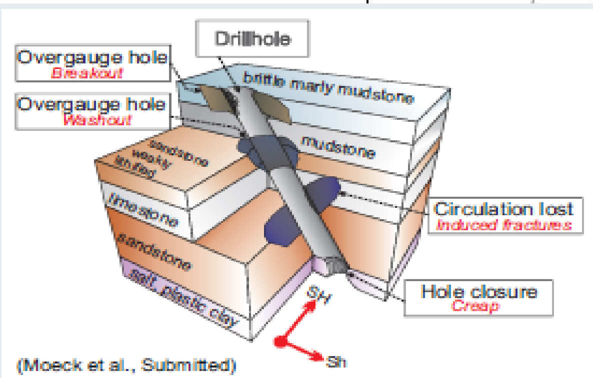

Enhancing reservoir performance

Natural laboratories

Cloetingh et al., 2010

Stress axes and faults

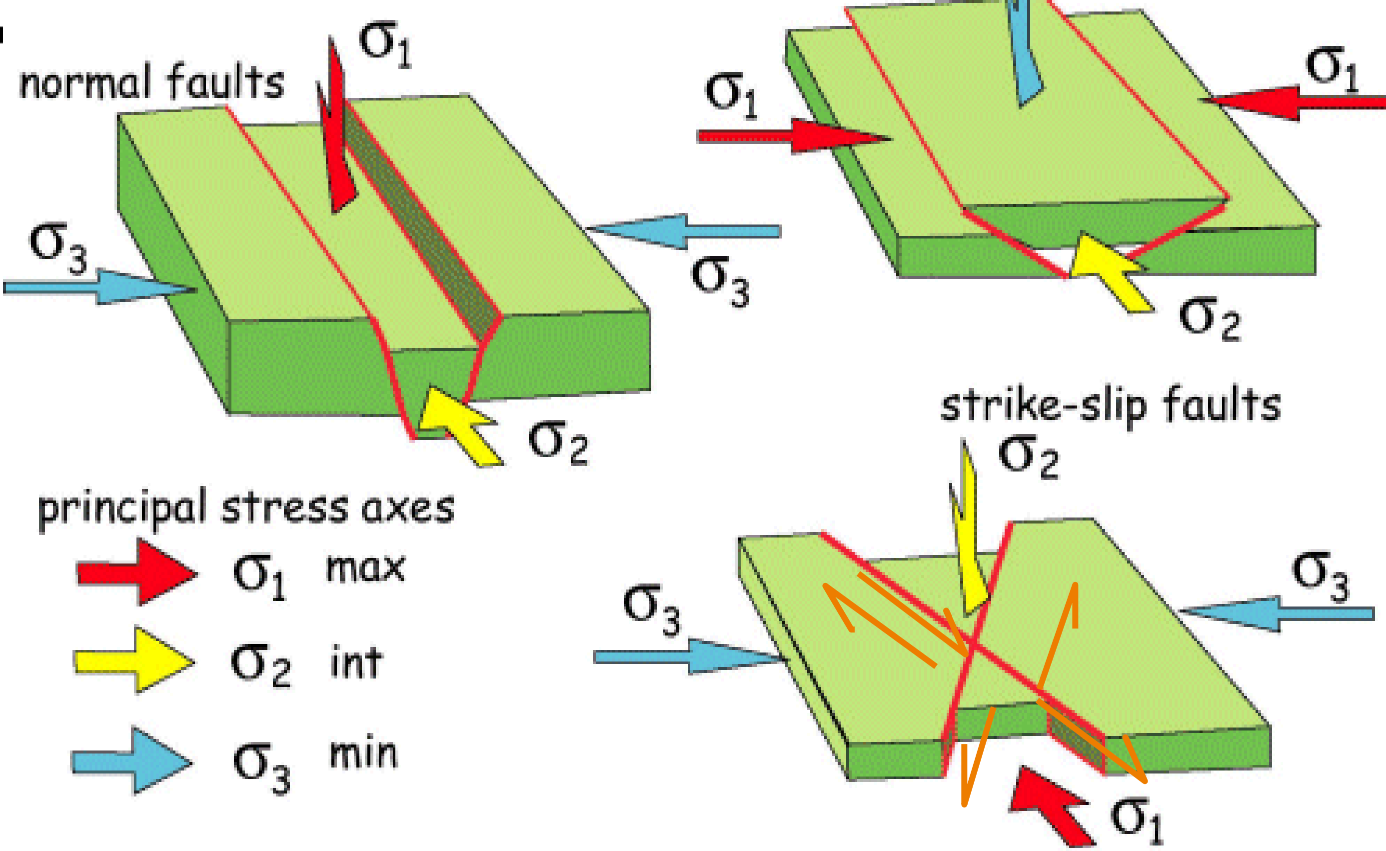

Conjugate faults are excellent indicators of stress directions

FAULT SYSTEMS

The simplest association of faults is formed by conjugate faults

These faults formed during the same deformation event

They

- **have an angle of ~60˚ between each other**
- **the angle is dissected by the maximum compressional stress**

Mohr Coulomb

- Slip along a fault occurs if
  $\sigma_s/\sigma_n > \tan \phi$

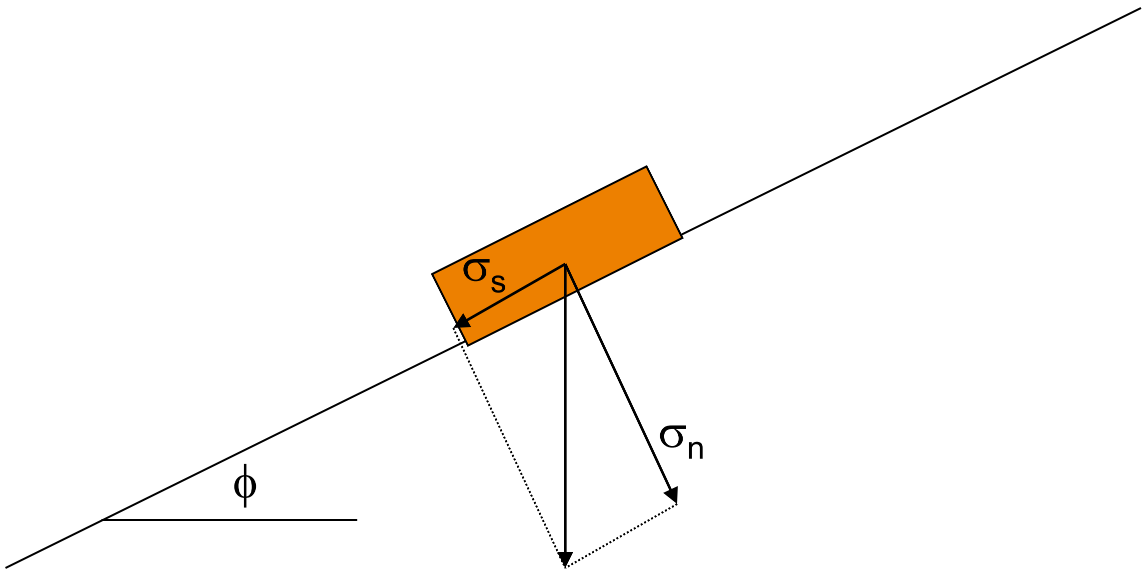

- Slip along a fault plane occurs if

$\sigma_s/\sigma_n \geq \tan \phi$

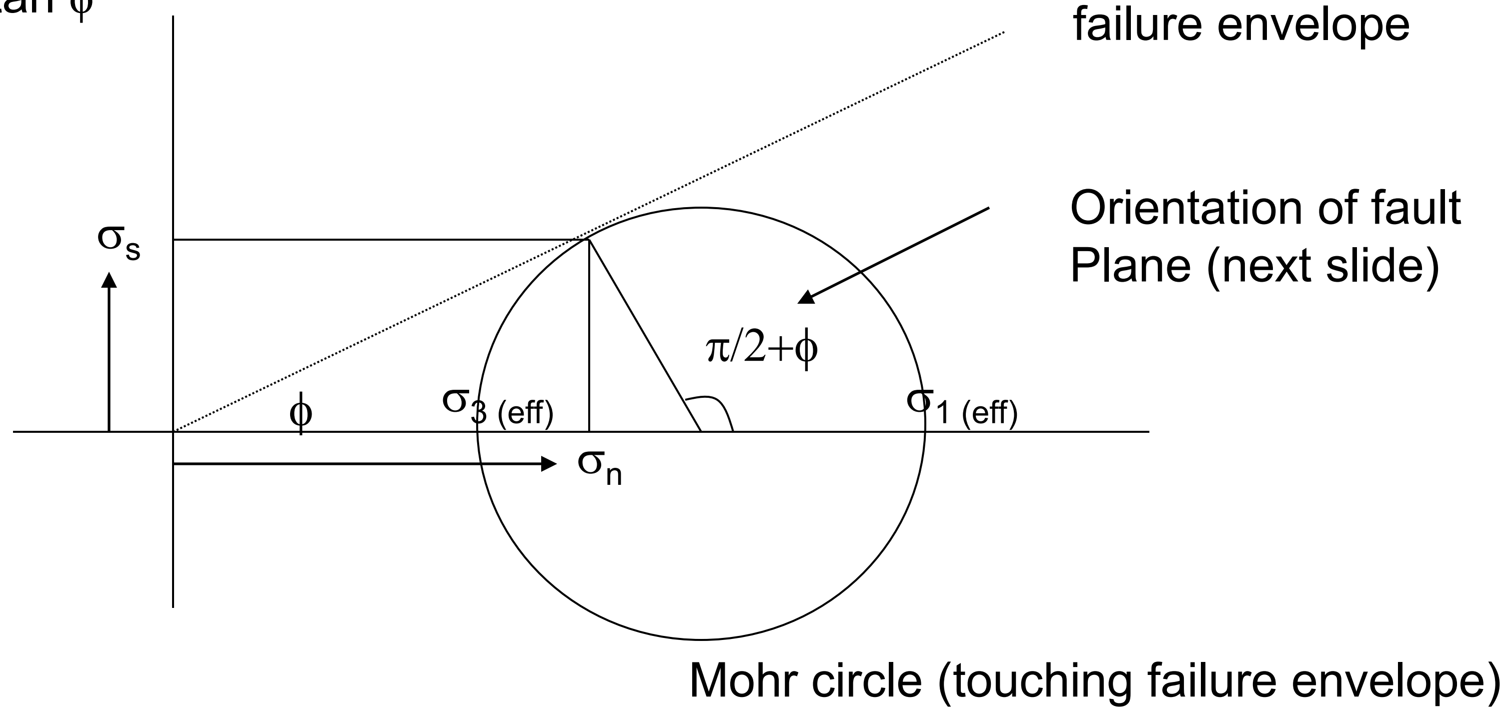

$\sigma_{3\ (eff)}$ = minimum principal effective stress = $\sigma_3 - P_f$

$\sigma_{1\ (eff)}$ = maximum principal effective stress = $\sigma_1 - P_f$

P_f = fluid pressure is typically ρ_w g z (assuming connected pore space) which is ca one third of total vertical stress $\sigma_z = (\rho\ g\ z)$

- Slip along a fault plane occurs if

$\sigma_s/\sigma_n \geq \tan\phi$

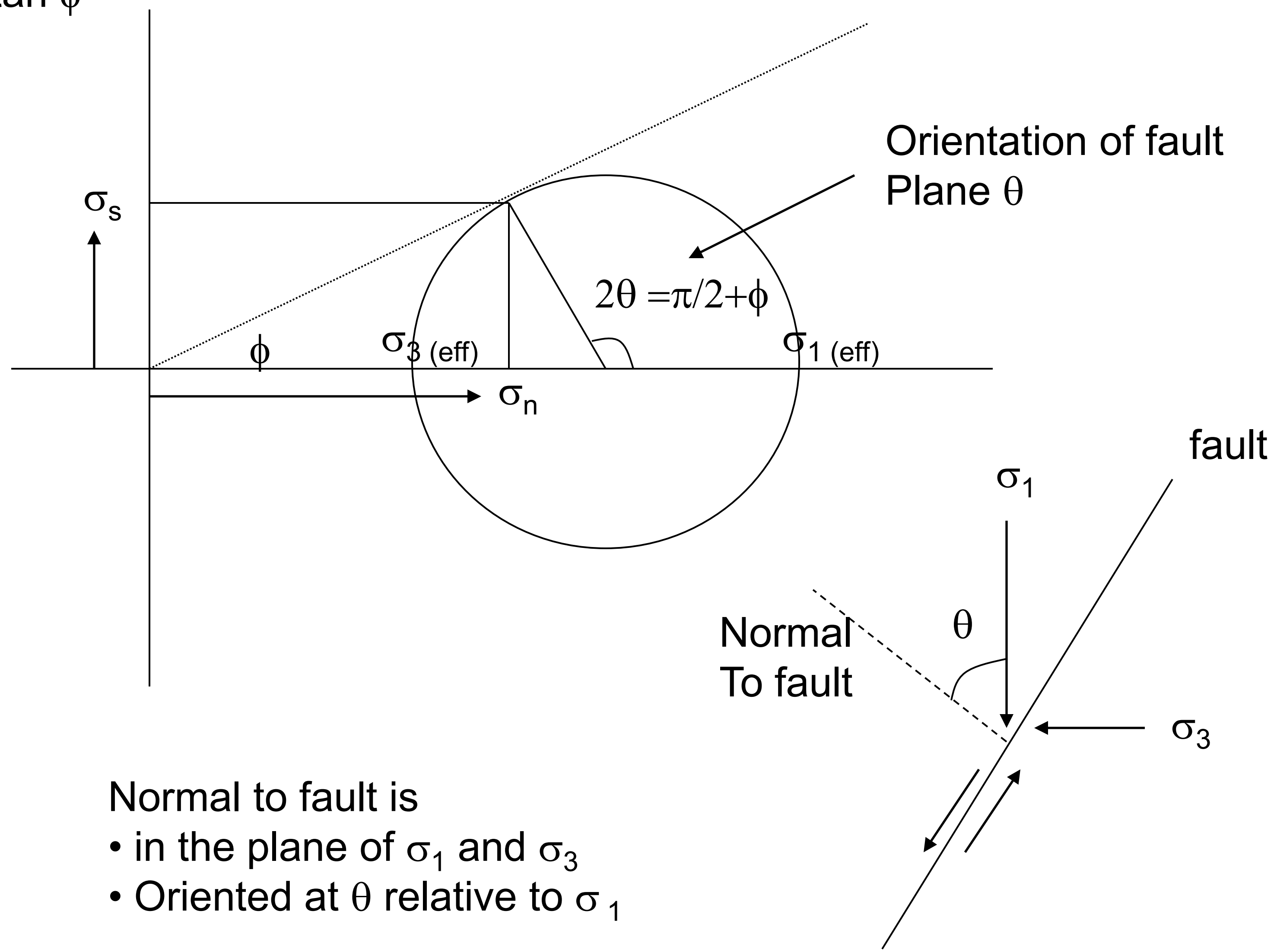

Normal to fault is
- in the plane of σ_1 and σ_3
- Oriented at θ relative to σ_1

Stress axes and faults

BRGM

TNO innovation for life

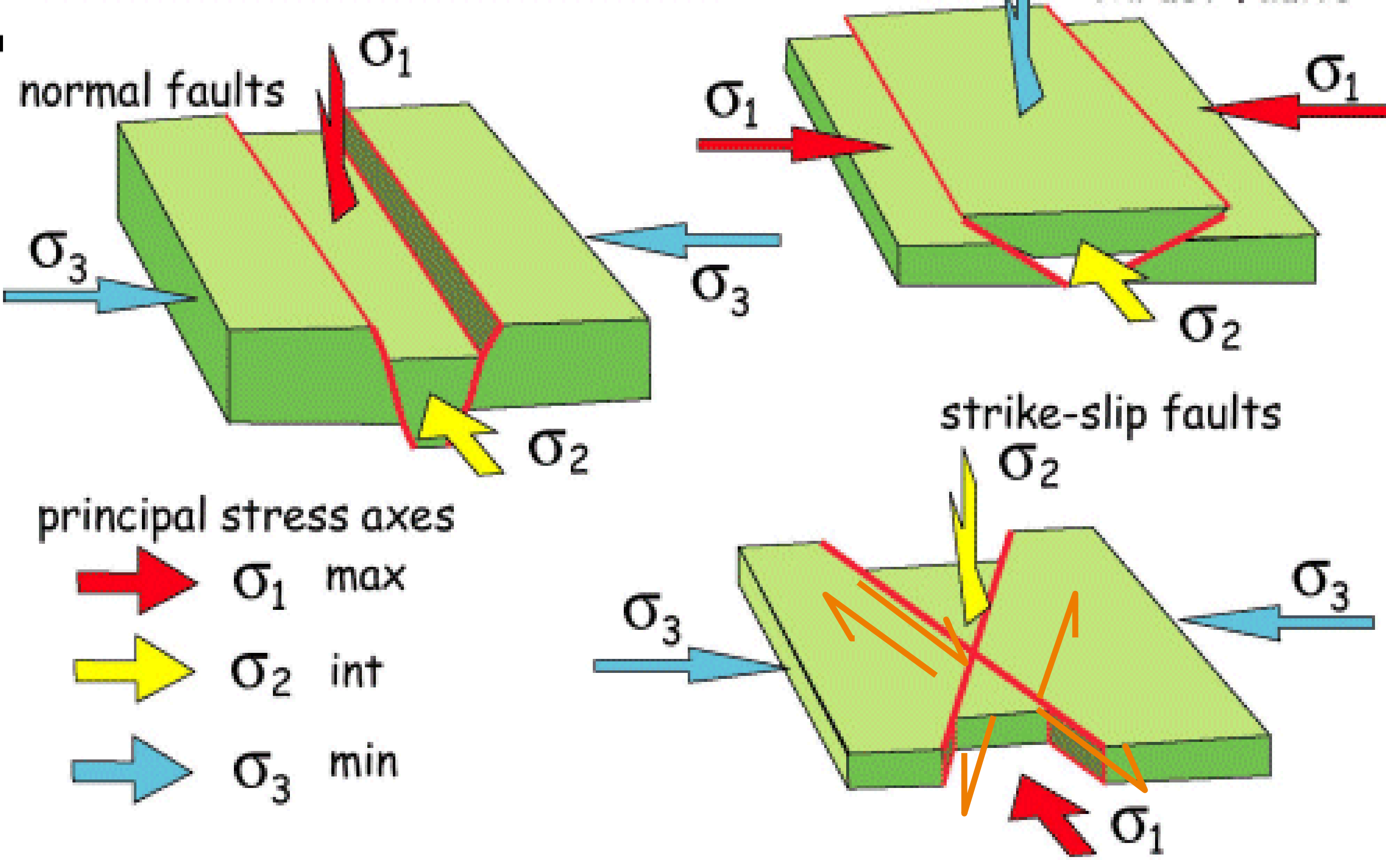

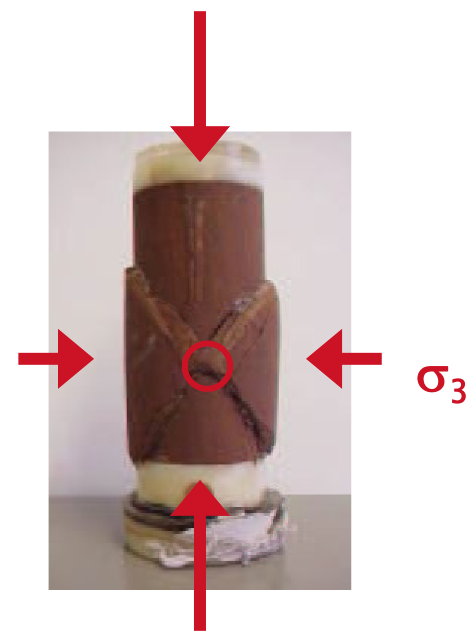

Conjugate faults are excellent indicators of stress directions

FAULT SYSTEMS

The simplest association of faults is formed by conjugate faults

These faults formed during the same deformation event

They

- **have an angle of ~60˚ between each other**
- **the angle is dissected by the maximum compressional stress**

Measurements of stress

- Stress estimation
  - Well data (tommorow)
    - Break-out data
    - LOP
    - Minifrac tests
  - *Earth quakes*
    - *moment tensor*
    - *Maximum depth as indicator for Brittle-ductile transition*
  - *Fault and fracture analysis*
    - *Slip tendency (stress which fits with fractures/faults)*

P-wave first arrivals polarity (up-P, down-T) → beach balls

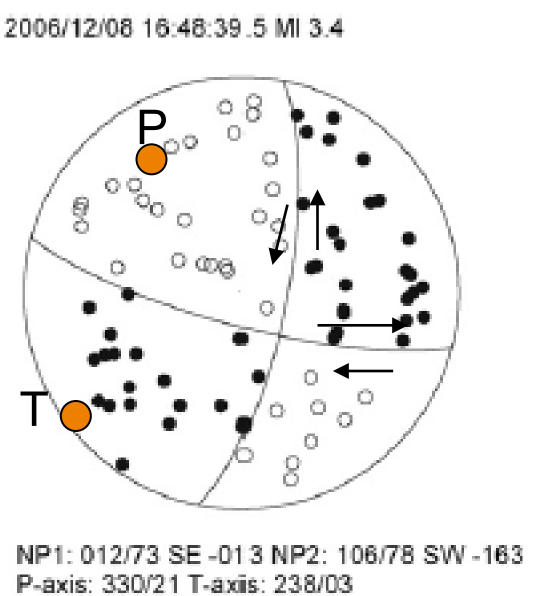

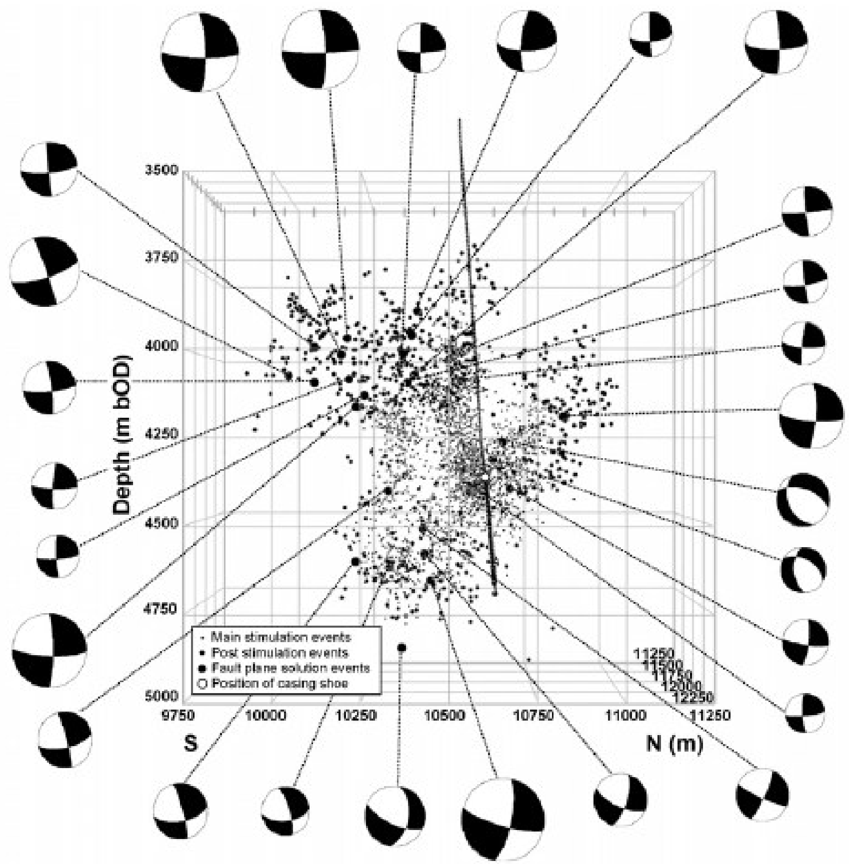

- Compressional arrival (P) → σ1
- Tensional arrival (T) → σ3

Beach balls

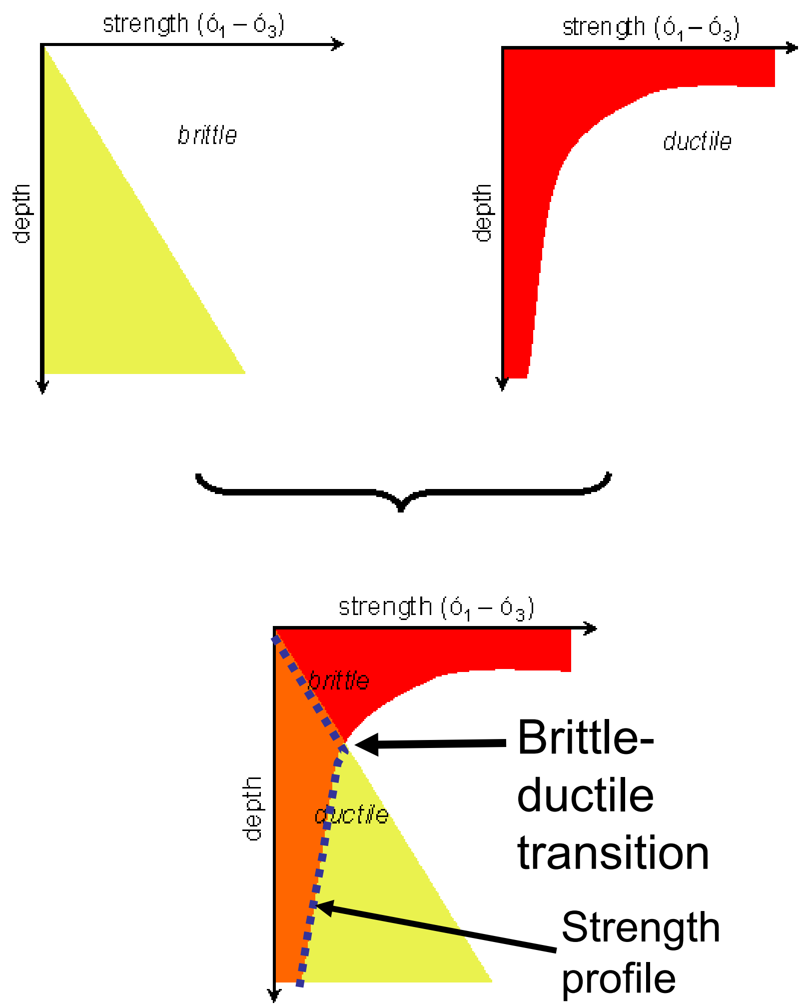

Rheology of the lithosphere → maximum depth of earthquakes

Combining brittle and ductile laws results in a rheological strength profile, showing the change of rock strength as a function of depth.

Data from Krafla where a magma was recently met during drilling

Prior to drilling of the IDDP well:

- The resistivity surveys shows a conductive body mostly staring at 4-5 km depth but with spikes up to 2km depth.
- The micro-earthquake-studies shows that all micro-earthquakes occur above the conductive body indicating more than 700°C

The IDDP well drilled in 2009:

- Drilled close to one of the spikes but was not intended to enter it.
- Acidic magma was found at 2,1 km depth preventing further drilling and underlining the needs for more accurate exploration methods

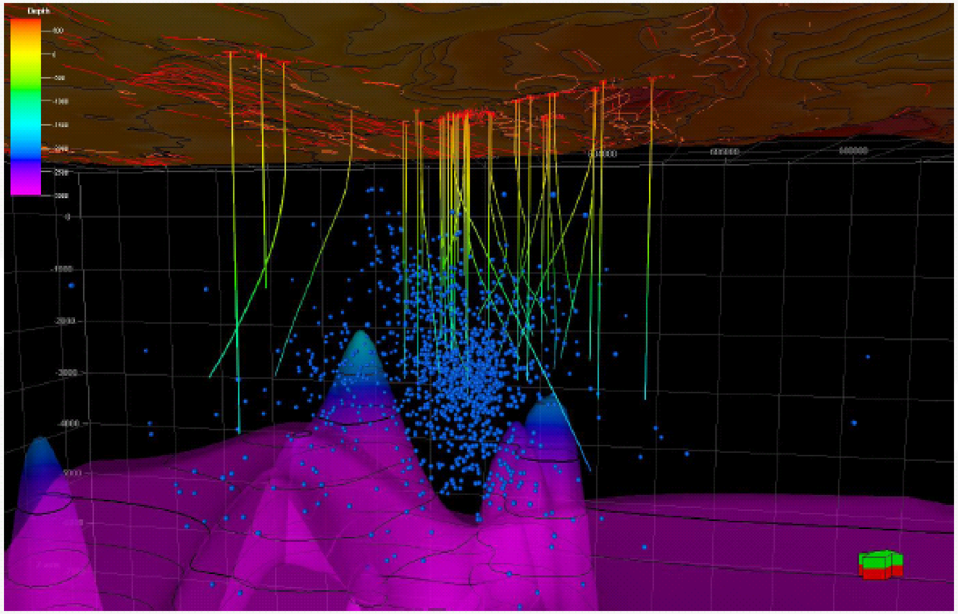

Combined results of resistivity soundings (TEM/MT) and micro-seismicity analysis

BRGM

Slip tendency → criticallity of stress & fluid flow potential

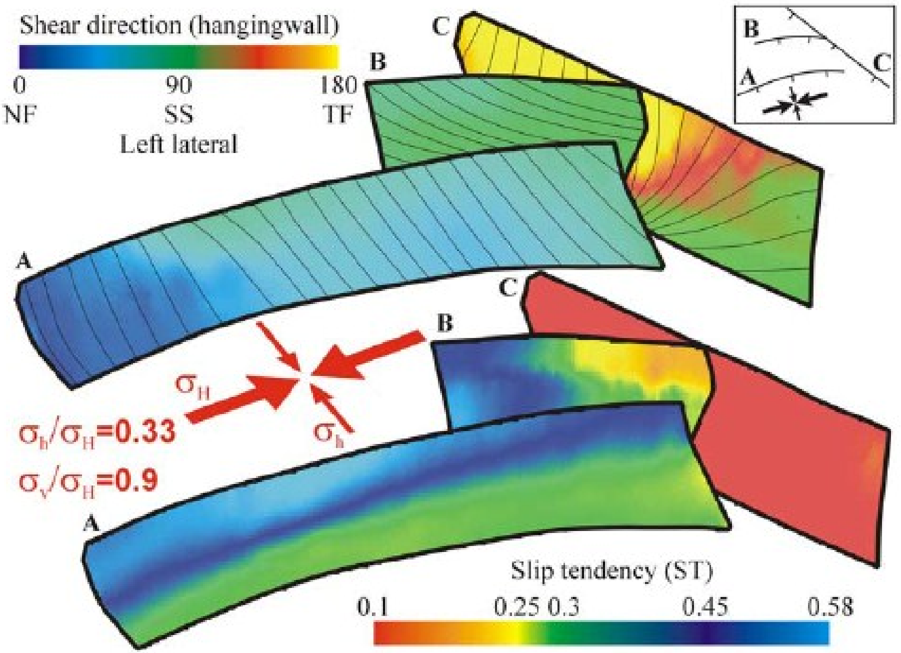

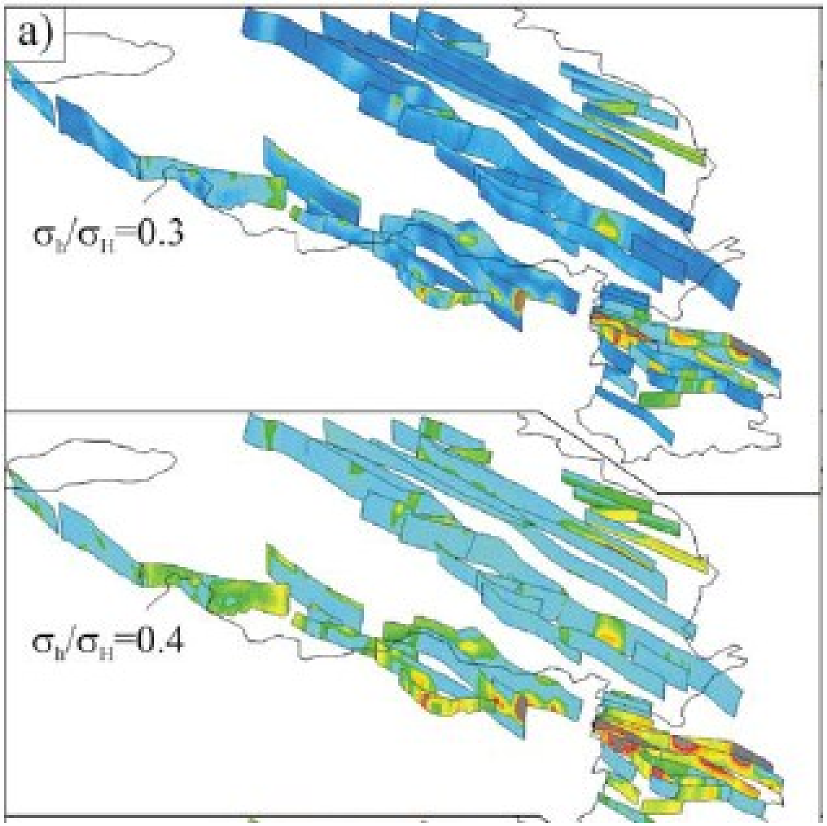

Slip Tendency (Worum et al., 2004)